MSc. Thesis

Modeling long-term beach and dune evolution with interacting longshore and cross-shore processes

Inelotte Krijnen

Technische Universiteit Delft

TU Delft

MSc. Thesis

Modeling long-term beach and dune evolution with interacting longshore and cross-shore processes

by

Inelotte Krijnen

to obtain the degree of Master of Science in Civil Engineering
at the Delft University of Technology,

An electronic version of this thesis is available at http://repository.tudelft.nl/.

TUDelft

Abstract

In future decades, coasts will be exposed to increasing risks because of climate change and sea level rise, which poses an increased threat of coastal inundation, erosion and ecosystem loss. The natural variability of coasts can make it difficult to identify these impacts. Most beaches worldwide show evidence of recent erosion. Sea level rise is currently not necessarily the primary driver, but will become very relevant in the future. Understanding both the short-term and long-term development of a coast is considered essential for coastal managers, in order to maintain safety in the future. For a generic evaluation of the state of the coastal zone, it is also important that not only the coastline changes are examined, but also the behavior of the dunes. The interactions between transport mechanisms should be investigated in order to make a good prediction of the large-scale and long-term development of the coastal zone. Therefore, the adaptation of the dunes and the coastline to interacting cross-shore and longshore sediment transport processes must be studied. To get a comprehensive view on those interactions, a new coupled surfzone-dune model is developed and validated.

This coupled model consists of a combination of coastline model "Unibest-CL+" and coastal profile model "the CS-model". The coupled model has the capability to simulate beach and dune evolution at decadal to centennial timescales including the relevant sediment transport processes that impact the beach and dune evolution: dune erosion and overwash, aeolian dune build-up, beach erosion and accretion due to gradients in longshore sediment transport, adaptation to sea level rise and response to nourishments. The model is tested quantitatively based on the sediment balance, in a very simple and a more complicated academic case focused on the individual effects of all transport mechanisms included in the coupled model. All test cases in the simple case – which consist of the smallest scale situation the coupled model is able to simulate – demonstrate sediment conservation and therewith confirm that the implementation of the different transport equations and their interaction in the coupled model is correct. In the complicated test cases – covering a varying number of cross-shore profiles along a larger stretch of coastline – the accuracy of the predicted sediment fluxes and the subsequent coastline and dune volume changes have been determined. The accuracy of every individual transport mechanism included in the coupled model is found to be sufficient and the different sediment fluxes within the coupled model are balanced.

After model testing, the model is used to hindcast the 22-year long coastal evolution near IJmuiden. The dune evolution in this highly dynamic case is simulated reasonably. Furthermore, the coastline evolution is predicted in accordance with the data. Overall, the coupled model is found to quantitatively and qualitatively perform satisfactory. The model is capable of quantifying the long-term beach and dune evolution with interacting longshore and cross-shore processes. Though coupling the models and therewith simulating the longshore sediment transport gradients instead of deriving them from data induces model uncertainties, the application of the model on the IJmuiden case shows that it is possible to simulate the longshore sediment transport gradients using a schematized wave climate to predict the dune volume evolution sufficiently. Furthermore, the interaction between the cross-shore and longshore sediment transport processes enables the simulation of the redistribution of nourishments, improving the predictive ability of both model components with regard to the coastline evolution as well as the evolution of the dune volume. For future research it is recommended to use the coupled model to look into nourishment strategies and their effectiveness on the long-term, climate change scenarios and their effect on decadal to centennial scale dune and beach evolution and the relative importance of different transport mechanisms on the long-term beach and dune evolution.

Preface

With this thesis I am finishing my masters Hydraulic Engineering at the Delft University of Technology and completes my Master of Science program in Civil Engineering with the specialization 'Hydraulic Engineering'. The research project was carried out at Deltares, an independent institute for applied research in the field of water and subsurface.

This research has been very educational and made me realize that I have a huge passion for coastal morphology. The associated model development was quite challenging, but mostly just a complicated puzzle that had to be solved step by step. I'm proud of the end result and hope you enjoy reading my report.

This graduation research was conducted under the supervision of Deltares and I would like to thank them for the expert support they provided. During my thesis I have been supervised by an inspiring committee which I would like to thank for their supervision and guidance throughout this process. I would first like to thank Ad for chairing the committee and the various (digital) meetings. Your guidance has helped me to remain objective throughout the process. I also want to thank you for the good help when it was urgently needed. Sierd, I want to thank you for your inspiring enthusiasm about all of the coastal dynamics research that led me to do this research. You guided me in the right direction by identifying the key points in my research project. Caroline, thank you for all your helpful and thorough feedback. You helped me a lot in interpreting model results and took the time to think along when something inexplicable happened. Your positivity throughout the process has motivated me many times. Bas, sharing your expertise on Unibest has been invaluable to this thesis. The inimitable speed with which you can write scripts to process data, provide insight into results or change the model is enormously inspiring. I have learned a lot from you and would like to thank you for the time and attention you have devoted to supervise my thesis research.

I wrote most of this thesis during the Corona pandemic. It has been a lonely time, working from home without colleagues. Luckily, Misiu got us to move to the best home office a few months ago and since then I have been able to hear and smell the sea while modeling coastal behavior. Thanks for that!

Inelotte Krijnen
Scheveningen, December 2021

Contents

List of Symbols

α	ratio between seaward and landward deposition of eroded dune volume	$-$
β_F	maximum foreshore slope angle	°
β_L	landward dune slope angle	°
β_S	dune ramp slope angle	°
δ	empirical fetch coefficient	m^{-1}
ΔV_{CL}	volume change in CL-model component	m^3/m
ΔV_{CLCS}	volume change in coupled model	m^3/m
ΔV_{CS}	volume change in CS-model component	m^3/m
κ	von Karman's constant	$-$
ϕ	coastline angle against shore normal	°
ρ_a	air density	kg/m^3
ρ_s	sand density	kg/m^3
θ	wind angle against shore normal	°
a	slope coefficient	$-$
A	empirical overwash coefficient	$-$
A_e	coefficient describing fraction of negative sediment budget deposited on dune crest	$-$
A_q	coefficient describing fraction of longshore and Bruun Rule transport available for aeolian transport	$-$
A_s	coefficient describing fraction of stable sediment budget deposited on dune crest	$-$
A_w	coefficient in critical shear velocity equation	$-$
B	active profile width	m
$B_{Bruun,mod}$	active profile width in modified Bruun rule	m
B_{Bruun}	active profile width in original Bruun rule	m
B_{dry}	dry beach width	m
BSS	Brier Skill Score	$-$
c	computed value	$-$

c_f	empirical friction factor for wave run-up	$-$
C_S	dune erosion impact coefficient	$-$
D_{50}	median grain size	mm
D_{50}^{ref}	reference median grain size	mm
D_C	depth of closure	m
D_F	dune foot height	m
ECA	Equivalent Coastline Accuracy	mm
$ESFA$	Equivalent Sediment Flux Accuracy	$\%$
F	fetch length	m
g	gravitational acceleration	m/s^2
H_{rms}	deep-water root-mean-square wave height	m
h_0	active profile height	m
K_W	empirical equilibrium aeolian transport coefficient	$-$
L	total coastline length	m
L_0	average deep-water wave length	m
m	measured value	$-$
m_{WE}	potential aeolian transport rate	$kg/s/m$
P	porosity	$-$
q_D	transport rate of eroded sediment from the dune	$m^3/m/s$
Q_{in}	longshore sediment transport inflow at upstream boundary	m^3/yr
q_L	transport rate of eroded sediment from the dune front to the landward side of the dune	$m^3/m/s$
q_{LS}	transport due to longshore sediment transport gradients	$m^3/s/m$
Q_{LS}	longshore sediment transport	m^3/s
q_N	transport due to nourishments	$m^3/s/m$
Q_{out}	longshore sediment transport outflow at downstream boundary	m^3/yr
q_S	transport rate of eroded sediment from the dune to the beach	$m^3/m/s$
Q_{sinks}	sediment sinks	m^3/yr
q_{SLR}	transport due to sea level rise	$m^3/s/m$
$Q_{sources}$	sediment sources	m^3/yr

q_W	aeolian transport, onshore directed	$m^3/m/s$
q_{WE}	potential aeolian transport rate	$m^3/s/m$
q_{WF}	potential aeolian transport rate corrected for fetch length	$m^3/s/m$
R	run-up height	m
R'	run-up height corrected for beach friction	m
R^2	coefficient of determination	$-$
R_{Bruun}	shoreline retreat due to sea level rise	m
S	1. sediment transport rate	m^3/s
	2. dune crest height	m
S_{SLR}	height of sea level rise	m
T	1. wave period	s
	2. total simulated time	s
t	time	s
u_*	shear velocity	m/s
u_{*c}	critical shear velocity	m/s
u_z	wind speed at z m elevation	m/s
V_{beach}	beach volume	m^3/m
V_{berm}	subvolume of beach volume; volume of beach above MSL between shoreline and dune foot	m^3/m
V_{dune}	dune volume	m^3/m
V_N	nourished volume	m^3/m
V_{ramp}	dune ramp volume	m^3/m
V_{SLR}	eroded volume due to sea level rise	m^3/m
V_T	sediment budget	m^3/m
V_W	volume of sediment available for aeolian transport	m^3/m
x	alongshore position	m
X_w	x-coordinate of reference coastline point	m
x_t	horizontal travel distance of wave front	m
y	cross-shore position	m
y_G	intersection between beach height and SWL	m

y_L landward dune foot position m

y_L' landward dune crest position m

y_S seaward dune foot positon m

y_S' seaward dune crest position m

Y_w y-coordinate of reference coastline point m

y_R length coordinate of run-up limit m

z wind gauge elevation m

z_b bedlevel above reference depth m

z_0 roughness height m

y_L

y_L'

y_S

Y_w

1

Introduction

1.1. Context

The coastal zone is defined as the transitional zone between terrestrial and marine regions and spans approximately a fifth of the earth's surface. The coastal zone not only fulfills the services of transport, recreation, tourism and biodiversity, but also produces food, fisheries, habitation, industrial goods, oil, gas and minerals. Furthermore, it can function as a safety zone between the built environment and the water, protecting residential areas against the risk of flooding. About 45% of the human population lives in the coastal zone and three quarters of the metropoles with more than 10 million inhabitants is located along the coast (Crossland, Kremer, Lindeboom, Crossland, & Tissier, 2005). The population density in the coastal zone has been growing dramatically since the 20th century and this growth is expected to continue. This puts a large anthropogenic pressure on land use and hydrological changes (Nicholls et al., 2007).

The coastal zone is naturally highly vulnerable to extreme events, such as storms, which threaten coastal properties, infrastructure and people living along the coast. These extreme events impose substantial costs on coastal societies. Annually, around 120 million people are exposed to tropical cyclone hazards (Crossland et al., 2005). This will further increase over time, since approximately 1 billion people will live in the coastal zone by the end of the 21st century (Neumann, Vafeidis, Zimmermann, & Nicholls, 2015).

In future decades, coasts will be exposed to increasing risks because of climate change and sea level rise. This poses an increased threat of coastal inundation, erosion (as shown in Figure 1.1) and ecosystem losses. An accelerated sea level rise, a further rise in sea surface temperatures, an intensification of tropical and extratropical cyclones, larger extreme waves and storm surges, altered precipitation and resulting run-off and ocean acidification are expected to occur (Nicholls et al., 2007). However, no agreement exists on the forecasts.

The natural variability of coasts can make it difficult to identify the impacts of different sediment transport mechanisms. Coastal erosion is observed on many coasts around the world (Luijendijk et al., 2018), but it is often still unclear to what extent these losses are associated with relative sea level rise and to what extent they are dominated by other sediment transport processes. At the Californian coast it was found that, for example, shoreline change is caused by a combination of cross-shore and longshore wave-driven transport mechanisms and sea level rise at a decadal scale. However, at the centennial scale the shoreline change is dominated solely by sea level rise induced recession (Vitousek, Barnard, Limber, Erikson, & Cole, 2017). This emphasizes the difficulty of drawing conclusions on coastal developments.

Figure 1.1: Erosion after hurricane Matthew, 2016 (Image by Paul Brennan from Pixabay)

Understanding both the short-term and long-term development of a coast is considered essential for coastal managers to maintain safety in the distant future. It is also considered relevant to know the future prospects of the coast, to make sure that measures applied at short-term are also contributing to long-term coastal safety. A combination of adaptation mitigation to long-term sea level rise will be needed to maintain coastal safety (Williams, Rangel-Buitrago, Pranzini, & Anfuso, 2018). Adaptation is defined as the ability of a system to evolve, in order to adapt to climate change and to expand the range of variability which it can cope with. However, in practice, the knowledge on the long-term development of the coast is often lacking. This poses a large constraint on successful management of future risks, which means that short-term measures may not turn out to be as efficient on the long-term. Not only the variability of the coastal zone itself, but also human's incomplete understanding of the variability and the governing processes is a major challenge. This means that investments need to be made in new methods to forecast future changes with sufficient certainty.

Given the large timescales that are considered, it will be important to not only study the most active coastal zone with breaking waves (which is commonly done), but also the wider system which includes the dunes. The dunes will react at a much smaller pace than the actual beach and breaker zone, but do affect coastal change substantially at decadal to centennial time scales (Hallin, Larson, & Hanson, 2019). Dunes are an essential part of the coast as they function as a natural barrier between the coast and the hinterland, which protects lower lying areas against flooding caused by storms. Next to the protective function, dunes have a high recreational value which has to be considered (Provincie Noord-Holland, 2012). Furthermore, dunes generate naturally filtered drinking water. Human-build sea dikes accomplish a comparable protective function, but an advantageous feature of dunes is their ability to adapt to the natural occurring processes.

The capacity of dunes to adapt to changes in both cross-shore and longshore forcing conditions has not been tested in the context of long-term and largescale cases. To investigate the interrelations between these forcing mechanisms, the first objective of this thesis is to study the adaptation of the dunes and the coastline to nourishments, sea level rise, aeolian transport, storm impact and longshore sediment transport gradients along the coast. To get a comprehensive view on those interactions, it will be necessary to develop new means of evaluating coastal changes together with dune development. This results in the second objective, which focuses on the validation of a new coupled cross-shore and longshore sediment transport model.

1.2. Problem

The changing climate will require coastal managers to take substantial measures in the coming decades to protect coastal safety and other functions of the coastal system (e.g. nature, recreation, drinking water and living areas). A clear view should be obtained on the effects of climate change on the coast, which requires insight in the driving processes for coastal change and suitable methods for identification and prioritization of coastal adaptation options. Both the definition of the driving processes and methods of coastal adaptation options are, however, not yet sufficiently developed to judge the effectiveness and efficiency of adaptation interventions.

This research focuses on the development of a coupled model, which is essential for long-term predictions. Insight into interacting cross-shore and longshore processes and their effect on the beach and dune evolution are essential for future-proof coastal management. It is relevant to investigate these processes at decadal to centennial time scales in order to develop robust adapation and mitigation strategies, based on the gained insight in the driving processes on these scales.

The coupled model consists of two model components. One simulates the longshore sediment transport rates and their effect on the coastline position and the other simulates the effect of cross-shore processes, such as dune erosion and sea level rise on dune development. The model coupler translates the cross-shore processes into coastline change and longshore sediment transport gradients into sediment availibility for cross-shore processes. This enables the coupled model to simulate long-term beach and dune evolution. By improving human's capability to predict the long-term and large scale transformation of the coastal zone, the best adaptation measures can be taken.

1.3. Outline

The main aim of the thesis is to: "Develop technology needed to quantify the long-term beach and dune evolution with interacting longshore and cross-shore processes". To achieve this goal, the main research question of this thesis is:

MQ - *"What are the forecasting capabilities of the coupled model for decadal to centennial scale coastline and dune evolution?"*

In Chapter 2, the theoretical background of relevant hydrodynamic (Section 2.2) and morphodynamic (Section 2.4) processes governing the evolution of the coastal zone are described. Furthermore, the characteristics of the Dutch coast are discussed. A brief introduction into numerical modeling to simulate coastal evolution is given in Section 2.6. The coupled model is described in Chapter 3. The hydrodynamic and morphodynamic processes described in the Chapter 2 are used to describe their formulation within the model in Section 3.4. Furthermore, the relevance of the coupled model and the coupling of the model components are described in this chapter. During the model testing, which is described in Chapter 4, the sediment conservation within the coupled model is tested. This part is concluded by answering the first sub-question:

SQ1 - *"Does the coupled model simulate the effect of longshore sediment transport, dune erosion, aeolian transport, nourishments and sea level rise on the shoreline and dune volume evolution in accordance with the sediment balance?"*

After testing the model, the model is applied to the IJmuiden case in Chapter 5. The model performance is studied by hindcasting the coastline and dune evolution of the IJmuiden coast and Kennemer dunes. The objective of the model application is to optimize the performance of the model and quantify the predictive skill of the model using a case study. The model calibration is described in Section 5.2, in which the model performance is studied based on the transport processes governing the long-term coastline and dune volume evolution of the IJmuiden coast. A comparison is made of model results with data. The model calibration is followed by the model validation, which is described in Section 5.3. After the model application, the performance of the coupled model is evaluated. This leads to the answer on the following sub-question:

SQ2 - *"How well does the coupled model perform when compared to field data?"*

Subsequently, the discussion of the research can be found in Chapter 6, which consists of the interpretation of the model results and the implications of the model results, the limitations of the coupled model and recommendations on improvements of the coupled model. Thereafter, the conclusion can be found in the last Chapter 7. The conclusion includes the answers on the research questions, a summary and reflection on the research and recommendations n future application and research.

1.4. Scope and limitations

The focus of this thesis is on the development of the coupled Unibest-CL+ and CS-model, which will enable the research on the quantification of the long-term beach and dune evolution. Therefore, the thesis is focused on model development rather than application. The model is tested by means of test cases which include conditions based on the Dutch coast and the model is calibrated and validated using a case study of IJmuiden. During model testing, it is tested whether the sediment fluxes are computed well. Therefore, the model testing is also development-focused. Model application focuses on a hindcast and evaluates if the model is applicable on large temporal and spatial scale coastal evolution cases. Calibration and validation of the model is focused on the IJmuiden case.

2

Theoretical background

In this chapter, the relevant hydrodynamic and morphodynamic processes governing long-term beach, dune and coastline evolution as well as their interrelations are described. This is of high importance to describe the functioning of the model, along with the definition of the test cases. Since the test cases are situated in The Netherlands, knowledge about the Dutch coast is required. Therefore, the hydrodynamic together with the morphodynamic characteristics of the Dutch coast are covered in this chapter. Apart from its relevance for the definition of the test cases, understanding the coastal behaviour of the Netherlands is also important for the calibration and validation of the model. This is done by using a case study located at the Dutch coast of IJmuiden.

2.1. Coastal Zone

The definition of the coast is subjectively defined, depending on the timescale and the objective under consideration. Coasts are, by definition, the transitional zone between the ocean and the continent. Following this definition, the coastal zone is made up of the part of the land affected by the ocean and the part of the ocean affected by land (Bosboom & Stive, 2011).

There are many definitions for the several regions and characteristic depths within the coastal zone. The definitions used in this thesis are listed below and illustrated in Figure 2.1.

- **The coastline** is defined as the boundary between the beach and the shoreface. In this thesis, the coastline corresponds with the intersection of the Mean Sea Level with the bottom profile of the beach. The coastline marks the beginning of the predominantly dry beach.

- **The shoreface** is also known as the littoral zone, in which littoral morphodynamic processes take place. These morphodynamic processes are mainly related to longshore sediment transport and cross-shore sediment transport. The width of the instantaneous littoral zone varies dependent of the wave conditions. The shoreface boundary is located at the **depth of closure**. The depth of closure defines the seaward limit of the active profile. Beyond this depth, there is no significant change in bottom elevation and no significant net sediment exchange between the nearshore and offshore (Kraus, Larson, & Wise, 1998). The landward boundary of the shoreface is the coastline.

- **The beach** is defined to be the part of the coastal zone between the coastline and the dune foot. The dunefoot is a visible break in the slope between beach and dune. In the present thesis, the dune foot is defined as a fixed elevation above mean sea level. This is further explained in Section 3.3 and shown in Figure 3.3.

- **The foredunes** develop landward of the active beach and generally comprise shore-parallel, convex, symmetrical to asymmetrical dune ridges. In the present research, the term **dune** is used to define the first seaward dunes from the seaward to the landward dune toe. The seaward side of the dune is the duneface.
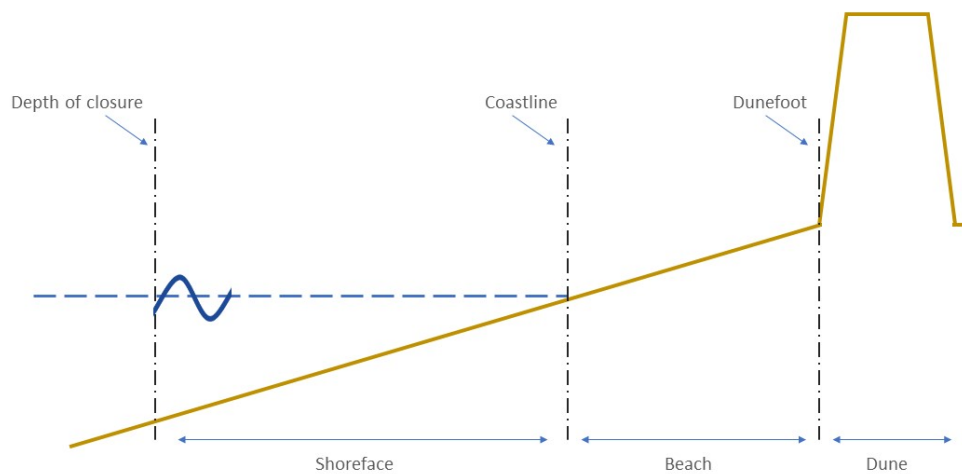
Figure 2.1: Definitions of the coastal zones and terms

2.2. Coastal Hydrodynamics

When waves approach the shore, multiple processes induce wave transformation and this generates net forces acting on the water. These net forces and the currents they induce, result in the sediment transport processes – i.e. morphodynamics – which are studied in this thesis.

This section explains the hydrodynamic processes fundamental to understanding morphodynamic processes. By definition, hydrodynamics are the forces acting on or exerted by the water. The most important hydrodynamic processes in the coastal zone are wind- and tide-induced waves and wind-, tide-, wave- and density-induced currents. These processes force the (in Section 2.4 further elaborated) morphodynamic processes. In the end, this research focuses on the morphodynamics which govern the evolution of the dune, the beach and the coastline.

2.2.1. Wave transformation

Most waves are generated by offshore storms (i.e. swell waves) or the effect of wind (i.e. wind waves). Winds or offshore storms introduce energy to the oceanic water in the form of short waves. When the offshore-generated waves propagate from deep into shallow waters, they transform due to effects of the bottom. Effects of shoaling, refraction , diffraction and reflection will be briefly discussed in this section.

Shoaling causes a distorted wave profile due to the wave asymmetry and skewness it generates. While shoaling, the propagation velocity of the wave decreases because the wave is slowed down due to bed friction and the wavelength shortens correspondingly. Since the tail of the wave-group catches up with the front of it, the wave energy accumulates resulting in increasing wave heights and wave steepness. This increase of wave height and steepness as a result of declining water depth and the resulting reduced propagation velocity is called shoaling. The waves start to transform into a skewed shape, with high short peaks and long shallow troughs. Furthermore, the bottom friction causes the troughs to slow down more than the peaks, resulting in an asymmetric, pitched-forward shape (See Figure 2.2).

Eventually, wave breaking occurs when a certain critical water depth to wave height ratio is exceeded. When the waves are increased in wave height due to shoaling and the water depth decreases, the
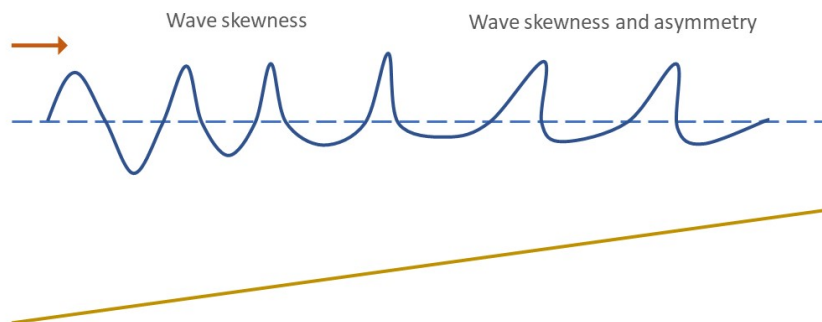
Figure 2.2: Wave transformation: asymmetry and skewness

waves obtain the maximum wave height which is depth-limited. After the wave breaking has occurred, bottom friction causes further energy dissipation and thereby wave height reduction as the water depth becomes more and more shallow.

The waves are not only transformed in the direction they travel. There are also effects along the crest of the wave, induced by the increasing depth. One of these effects is refraction. Waves approaching the shore under an angle tend to shoal faster at that side of the wave ray that is making a smaller angle with the shoreline, i.e. the landward side of the wave crest. Therefore, the waves bend until they are normally-incident waves. This bending is called refraction.

Another effect acting on the wave ray rather than the wave height is diffraction. It occurs when there are sheltering structures such as breakwaters or islands. Diffraction is the process by which energy of a wave is transmitted, dissipated and radiated laterally when reaching an obstacle. The wave propagates into the sheltered region behind the obstacle, showing a bending pattern.

While interacting with a structure or steep coastline, the waves will also partly reflect. This means the wave will bounce back in the opposite direction it came from, with the same angle. Reflection causes the reflected wave to interact with the incoming waves and either strengthen or weaken them.

2.2.2. Wave-induced set-up and currents
The wave transformation described in the previous section results in the propagation of momentum, which is defined to be the product of mass and velocity. Incident waves transport mass flux between the crest and the trough. This flux increases during shoaling. Furthermore, both wave asymmetry and skewness causes a rise in net transport. Eventually the transported mass piles up at the beach forming a water level set-up. The onshore directed mass flux is counteracted with a return current in the lower part of the water column, known as the undertow.

The flow of momentum due to waves and its variability along the coastline and cross-shore results in net wave-induced forces on the water. In the coastal zone, large forces occur due to strong wave transformation as a result of the large gradients in water depth. The shoreface is divided into two zones. The shoaling zone is characterized by shoaling waves until they break at the breakpoint, which marks the beginning of the surfzone. In the shoaling zone, the wave height and hence wave energy increase up to the edge of the surf zone, from where the wave height and energy decreases again.

Because wave height and water level are balanced, described by the momentum balance, the cross-shore change in wave energy due to the changes in wave height results in water level set-down in the shoaling zone and water level set-up in the surf zone. In case the waves approach the shore under an angle, the force in alongshore direction is non-zero in the surfzone, driving an alongshore current.

Due to the irregularity of wave fields and local variations in the bottom profile, the distribution of wave-induced currents and set-up will vary considerably. This variance induces secondary effects e.g., a current from a region with high set-up towards a region with low set-up.

Wave swash is the propagation of the waves onto the beach slope. The swash consists of an onshore phase with decelerating upwards flow (i.e. uprush or swash) and an offshore phase with accelerating downwards flow (i.e. downrush or backwash). Wave run-up is the sum of the wave set-up and the wave swash. The wave run-up is the maximum level the waves reach on the beach relative to the still water level.

2.2.3. Wind-induced set-up and currents

The wind transfers horizontal momentum to the sea by blowing above the sea surface. The momentum transfer results in movement of the water in the direction of the wind. This generates a surface current, depending not only on the direction and the magnitude of the wind but also on the local water depth. When there is a boundary in the downstream direction of the wind-induced current, there will be a water level set-up induced by the wind. The wind-generated currents and set-up have significant effect in shallow waters only (Bosboom & Stive, 2011).

2.2.4. Tidal propagation in coastal waters

Not only wind and waves induce currents in the coastal zone. There is also a tidal-induced current that effects the water movement near the shore. The tidal motion is the rise and fall of sea levels caused by the gravitational forces (Bosboom & Stive, 2011). Although tides are generated in the oceans, they are amplified in shallow waters. Tides can be considered as long waves propagating through the oceanic waters. The previously mentioned phenomena affecting the short waves, transform the tidal waves as well. Due to reflection, refraction, friction and shoaling, the tidal wave transformation depends on the location. This tidal wave transformation results in spatially varying tidal wave asymmetry and variations in the range between the high and low water. The vertical movement of the water level due to the tides are accompanied by a horizontal movement of water, called the tidal current. The differences between ebb and flood tidal currents due to wave transformation induce a net residual current.

Furthermore, the tidal motion influences the wave-induced longshore current in the surf zone. The maximum alongshore flow velocity increases and shifts towards the breaker line if the tidal force is in the same direction as the wave-driven current. But in case the tidal force is in opposite direction, the maximum decreases and shifts towards the coastline (Bosboom & Stive, 2011).

2.3. Dutch hydrodynamic conditions

The hydrodynamic processes described in the previous sections of this chapter vary with geographic location and water properties. For the model tests using academic cases, described in Chapter 4, the hydrodynamic conditions will be based on the environment at the Dutch coast. Furthermore, the IJmuiden case situated at the Dutch coast will be used to calibrate and validate the coupled model, so therefore basic understanding of the hydrodynamics at the dutch coast is required for the present research.

The Dutch coast can be divided in three parts, based on their characteristics: (1) the Delta coast in the south, (2) the Holland coast in the middle and (3) the Wadden coast up north (Figure 2.3). Since the interest of this thesis is the area around IJmuiden, the Holland coast will be the focus of this study.

The Dutch coast is situated at the North Sea, a relatively shallow sea area on the European continental

Figure 2.3: The three subsystems of the Dutch coast

shelf. The North Seas dynamics are dominated by the tidal motion. The tides arise from the tidal wave in the North Atlantic, entering the North Sea via the Channel and via the wide northern entrance.

The North Sea tide is represented by the tidal constituents of the semidiurnal lunar tide and the semid-iurnal solar tide. Both tidal waves travel in counterclockwise direction in the North Sea, which means the tidal wave is directed towards the north during flood at the Dutch coast. The tidal range varies along the Dutch coast. The tidal range at the Holland coast is about 1.6 m, with a maximum of 1.9 m (Wijnberg, 2002). This small tidal range causes the Holland coast to be wave dominated.

The wind climate is dominated by winds from SSW to W and spatial differences in the annual wind climate are insignificant along the Holland coast. The mean annual wind speed at the coast is around 5.5-6 m/s (KNMI, 2021). Waves mainly approach the coast from the SW and NNW directions. The geometry of the North Sea basin is such that swell, generated on the Atlantic Ocean and the north-ern North Sea, will always approach the Holland coast from northerly directions. Therefore, average and extreme wave heights in the North Sea generally decrease southwards. Wijnberg (2002) extracted wave height data from databases managed and updated by Rijkswaterstaat (Dutch Directorate-General for Public Works and Water Management) and presented the mean annual wave height for different directional sections along the Dutch Coast. Given the station of IJmuiden located at approximately the middle of the Holland coast, the mean annual wave height is 1.3 m. Furthermore, the mean wave period is 5-6 s for almost 60% of the time (Van Der Spek & Lodder, 2015).

2.4. Morphodynamic processes

When considering a coastal system, morphological changes such as change of the coastline position, the beach width or the dune profile occur in the case of gradients in the sediment transport rates. Sed-iment transport is the movement of sediment particles, depending on the properties of the sediment material and the flow characteristics (Bosboom & Stive, 2011). Changes in the morphology of the coastal systems depend on the spatial and temporal variations of the sediment transport rates. If the net sediment flux into a certain area is negative, the bottom will supply the sediment deficit by eroding. Because the waves and tidal components on this certain location are depth-dependent, these will re-spond to the bottom change. Therefore morphodynamics are defined to be the mutual adjustment of morphology and hydrodynamic processes involving sediment transport. When studying the morpho-dynamics of a system, the main mechanisms can be explained by using the sediment mass balance (Equation 2.1) in which z_b expresses the bedlevel above a certain reference depth, S expresses the sediment transport rates in both the cross-shore (x) and alongshore (y) direction and V expresses the source or sink term.

$$\frac{\partial z_b}{\partial t} + \frac{\partial S_x}{\partial x} + \frac{\partial S_y}{\partial y} = V \tag{2.1}$$

The interaction between hydrodynamics and morphodynamics is poorly understood due to its complexity and therefore most of the relevant processes are described using empirical relations. In the large spatial and temporal evolution of the coastal zone, the most important morphodynamic processes are the dune erosion, beach-bar migration, aeolian transport, response to sea level rise and coastline evolution due to variations in longshore sediment transport along the coastline (See Figure 2.4). These processes will be explained in more detail in this section. Furthermore, human interferences in the morphodynamics are discussed.
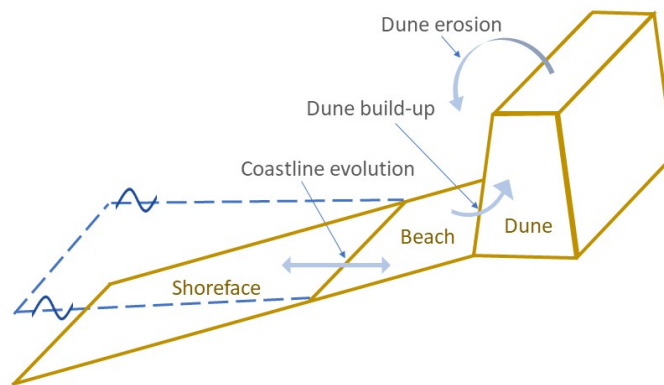
Figure 2.4: Overview of key morphodynamic processes in the coupled model

2.4.1. Dune erosion

At the Dutch coast, dune erosion takes place during storm surges when the mean sea level increases and waves can reach the dune face and impact it. Eroded sand from the dunes is transported offshore by a strong undertow. The high sediment suspensions in front of the dunes result in a large offshore transport capacity. Further seaward, the transport capacity of the flow decreases and the sediment starts to settle. This results in the formation of a new coastal profile that is in better equilibrium with the storm surge conditions. The newly developed beach profile is more efficient in dissipating the energy associated with the incoming waves and consequently dune erosion rates decrease as a storm progresses (van Thiel de Vries, 2009).

After a storm surge the beach width has become substantially wider and the slope more gentle, this is called a mild beach. The coastal profile is not in equilibrium with the post-surge (normal) hydrodynamic conditions. The hydrodynamic processes exerted by the waves, tide and wind reshape the shoreface and the dunes gain part of the eroded sand back. In a situation without longshore sediment transport gradients, the dunes recover to their original volume. However, the time scale of dune recovery is considerably larger than that of erosion.

The impact of waves on dunes is traditionally subdivided in four regimes: the swash, collision, overwash and inundation regime (Sallenger Jr, 2000). The regimes are distinguiged based on the height of the wave run-up with respect to the dune foot or dune crest. In the swash regime, the wave run-up is below the dune toe. Therefore, the waves only erode the foreshore. In the collision regime, the wave run-up is above the dune foot and the waves collide with the dune. In the overwash regime, the wave run-up is above the dune crest, enabling the waves to wash sand over the dunes. During the inundation regime, both the wave run-up and run-down overtop the dune crest, which results in constant inundation of the dune. This causes the dunes to be impacted by processes similar to the processes impacting the surf
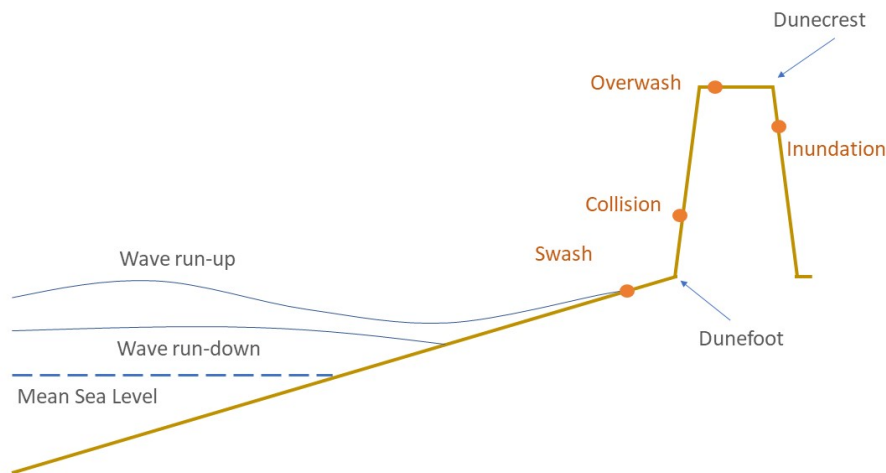
Figure 2.5: Schematic description of Sallenger's (2000) storm-impact model and the four regimes.

zone. The regimes and the boundaries defining them are illustrated in Figure 2.5.

2.4.2. Beach-bar migration

The behaviour of the beach flattening after storm impact followed by dune and beach build-up during the subsequent milder wave conditions is cyclical. The seasonal changing wave climate generates a so-called winter and summer beach profile.

There are six morphodynamic regime destinguished, related to weather conditions on a daily to monthly timescale (Wright & Short, 1984). The regimes rank from dissipative to reflective and four regimes in between. The reflective beach corresponds to a summer beach profile, characterized by a relative steep slope and narrow beach face. This profile is the result of a period of mild wave conditions transporting sediment onshore. On the other side of the spectrum, the dissipative regime corresponding with a winter profile is defined (Wright & Short, 1984). It is characterized by a wide and flat sandy coastal zone. It is the result of high waves that start breaking offshore, typical for a storm wave climate. These storms consisting of high and long waves move sediment offshore, as mentioned in the Section 2.4.1 designated to dune and beach erosion. This sand is deposited in the surfzone, from where it will be picked up and moved onshore during milder wave conditions, rebuilding the summer profile.

This cycle of different beach regimes results in seasonal behavior that resembles a kind of coastline breathing.

2.4.3. Aeolian transport

Dunes grow mainly due to aeolian transport, which is the transport of sediment by the wind. Wind blowing towards the dunes transports sediment from the beach towards the dunes, and thereby builds the dunes up. Aeolian transport can be best understood if it is divided into the process of the transport of sand by wind on one side and the several limiting factors on the other side.

Aeolian transport occurs when the uplifting forces on a grain of sand exceed the force of gravity. There are four different modes in which transport of grains occurs, which are creep, saltation, suspension and reptation (Bagnold, 2012). During creep, the grains roll on the surface. Saltation means the grains jump due to the uplifting forces. Small grains are easily suspended in the wind and transported in suspension. When reptation occurs, the saltating grains set other heavier grains in motion. Fully developed

saltation describes aeolian transport under equilibruim conditions.

Limiting factors

The transport modes described above depend on grain size and wind conditions. However, the aeolian transport is affected by beach slope and width, sediment availability, beach houses and vegetation as well.

The **beach slope** affects aeolian sediment transport, because more wind shear stress is needed to move sediment uphill with respect to moving sediment horizontally.

Beach width determines the fetch of the wind on the beach. The fetch is important for the aeolian transport of sediment, because a critical fetch length is required to reach the transport rates described by the equilibrium equations. The actual fetch length on the beach depends on the dry beach width, which can be defined as the distance from the run-up height to the dune foot, adjusted for the angle of attack of the wind (see Figure 2.6). The aeolian transport is assumed to increase with increasing fetch up to a critical fetch length where the equilibrium transport rate is achieved.
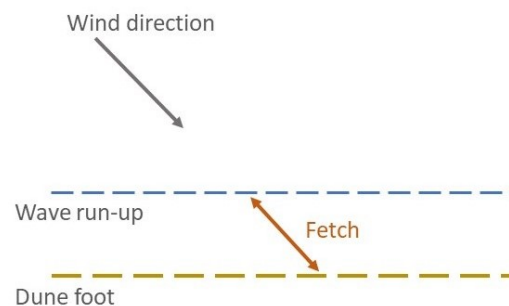
Figure 2.6: Definition of the fetch of the wind

Vegetation is an essential factor for dune growth, since it increases the surface roughness so that the wind speed decreases and sediment deposits more easily.

The beach **sediment budget** affects both the rate of aeolian sediment transport and the dune morphology. The sediment budget can be positive, negative or stable. Based on this sediment budget, four types of dune behaviour are distinguished (Psuty, 1988). The types of dune behaviour are depicted in Figure 2.7.

When the sediment budget is positive and the beach is accreting, dunes will grow fast and create a prograding beach ridge topography, where a new foredune is formed in front of the existing ones. These new foredunes are low with mild slopes (Hesp, 2002; Psuty, 1988), because there is not enough time for them to grow in height before a new foredune is built in front of them. In case the sediment budget and therefore the beach is stable, the dune stays in place and grows higher due to scarping and recover. If the sediment budget is negative, the beach is eroding. Eroding beaches may develop in two different ways, if they are slightly eroding, the dune will maintain or even increase its volume, grow higher, and be displaced inland through scarping in combination with aeolian transport and overwash. If the beach is eroding fast and overwash processes are dominant, the dune will be flattened out and moved landwards.

The aeolian transport is locally blocked when there are **beach houses** located in front of the dunes. Usually, beach houses are seasonal and the aeolian transport is blocked temporarily.
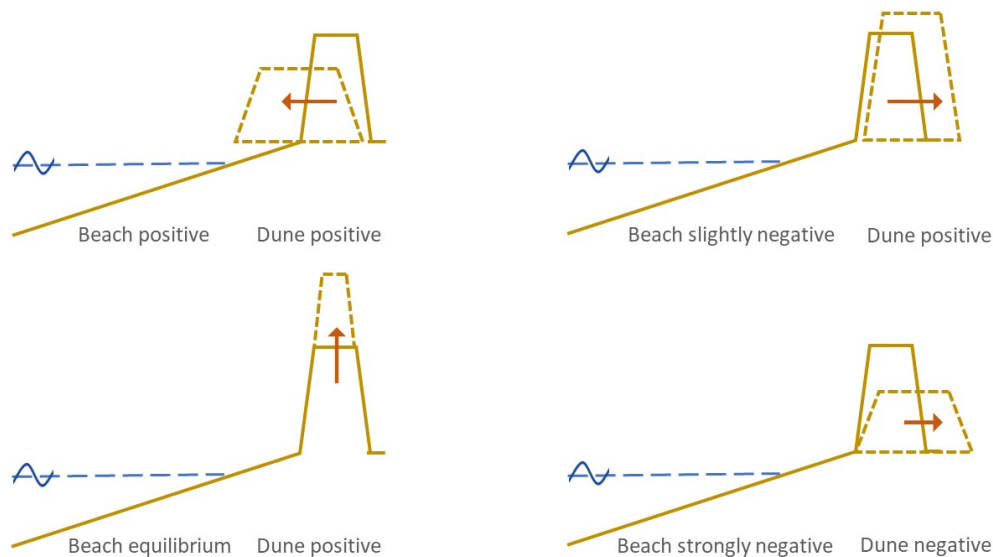
Figure 2.7: Effect of sediment budget on dune growth, based on the theory of Psuty (1988)

2.4.4. Response to sea level rise

On the larger time scale, the morphology of the coastal zone responds to sea level rise. A higher mean sea level enables larger waves to approach the shore, since wave energy dissipation is depth dependent.

The Bruun Rule (Bruun, 1954, 1962) is a formula for estimating the magnitude of the retreat of the shoreline of a sandy shore in response to changes in sea level. It describes the shoreface adaptation to sea level rise based on the concept of an equilibrium profile, assuming a linear relationship between sea level rise and shoreline recession. This rule is based on the assumption that the coastline retreats while adjusting to sea level rise, and therewith creates accomodation space for sediment within the subaqueous part of the active profile. The increase in accomodation space forces the equilibrium profile landward and upward to preserve its shape relative to the new sea level. Consequently, the Bruun rule assumes that the dry part of the beach is eroded as the equilibrium profile moves landward. The eroded volume is deposited offshore, resulting in a seabed rise in the shoreface. The seabed rise combined with the rising sea level results in a constant water depth.

2.4.5. Longshore sediment transport

The longshore current caused by oblique incident waves, generates longshore sediment transport. Since the transport depends on the angle of the waves approaching, different coastline orientations induce different longshore sediment transport rates. When the coastline orientation changes in the alongshore direction, gradients in the longshore sediment transport rates cause erosion or accretion of the coastline.

Dune erosion, beach-bar migration and aeolian transport are morphodynamic processes acting in the cross-shore direction. These transport mechanisms exert changes on the coastal zone morphology on event, seasonal or tidal cycle scale. The beach and dune profile tends to recover after these morphological changes, unless the sediment budget within the considered area is not balance.

The sediment budget is not in balance when there are sinks or sources of sediment such as river outflow or structures blocking the sediment flow. Furthermore, gradients in longshore sediment transport cause imbalance in the sediment budget. These imbalances result in structural change of the coastal zone and are therefore of high importance for the long-term and large scale evolution of the coastal zone this thesis focuses on. The process of longshore sediment transport gradients resulting in coastal erosion or accretion is illustrated in Figure 2.8.
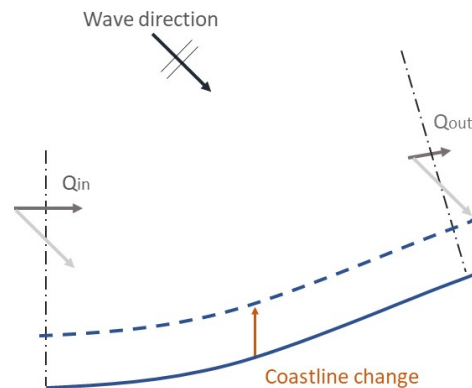
Figure 2.8: Schematic of longshore sediment transport gradients: accretion due to a negative longshore sediment transport gradient

2.4.6. Human interference in the morphodynamics

There are several ways we are able to intervene the natural morphodynamic processes within the coastal zone. Human intervention mostly takes place to counteract erosion of the beach and dunes, and can be subdivided into structures influencing the longshore sediment transport rates, structures providing protection against storm-induced erosion and nourishments (Bosboom & Stive, 2011).

Longshore transport rates are affected by several kinds of structures; jetties or shore-normal breakwaters, (series of) groynes, detached shore parallel offshore breakwaters, piers and trestles. Jetties are structures perpendicular to the coast, used to protect harbours or stabilize the coastline by reducing the wave activity behind them. The jetties block the longshore transport of sand which would otherwise settle into the dredged approach channel of the harbour. Furthermore, jetties stabilize the position of a river mouth or coastal outlet. Two jetties at a river mouth can restrict its width and therewith guarantee a certain flow velocity to prevent sand accumulation and the formation of shoals (which is a major obstacle for shipping). When a jetty is built at the erosive side of the adjacent coast of a tidal inlet, it can prevent the inflow of sediment and therefore prevent coastal erosion and sedimentation of the tidal basin. These effect of a jetty are local, but if one wants to intervene the longshore sediment transport rates on a larger scale, groynes can be used. Groynes are a series of smaller jetties, extending into the surf zone. By keeping the coastal sand trapped between two adjacent groynes, they can stabilize the entire coast along which they are built.

Detached shore parallel offshore breakwaters, either emerged or submerged counteract coastal erosion by reducing the wave activity behind them. This reduces the longshore sediment transport and therewith causes local accretion patterns known as a tombolo or salient. Piers and trestles are not primarily built to change the longshore sediment transport rates, but for recreational purposes or the landing of vessels. However, these structures reduce the local wave height at their lee side and therewith generate local accretion spots.

The structures providing protection against storm-induced erosion are seawalls, revetments and seadikes. These structures provide coastal protection by cutting of the local supply of material.

Nourishments can be subdivided into dune nourishments, beach nourishments and shoreface nour-

ishments. Nourishments can be applied for various reasons; to compensate for losses of sediment as a result of structural erosion, to enhance the safety of the hinterland against flooding and protect the beach and dunes against storm erosion and to broaden a beach or create new beaches. In the case of structural erosion, the nourishment will have to be repeated from time to time, whereas the creation of a new beach and the protection against flooding requires a single measure (Bosboom & Stive, 2011).

2.5. Dutch coastal morphology

The Holland coast consists of 120 kilometres of almost continuous shoreline. The coastline is bounded in the North by the tidal inlet "Marsdiep", connecting the Wadden Sea to the North Sea. The southern boundary of the Holland coast is the long jetty near Hook of Holland, which allow ships to access the Port of Rotterdam. Approximately 290 km of the coast consists of dunes and 60 km is protected by structures such as dikes and dams. It is a closed coastline with two openings in the dune barrier: one near IJmuiden created in the late 19th century to provide shipping access to the city of Amsterdam, and another one at the small harbour entrance at Scheveningen.

The foundation of the Dutch coast consists mainly of sand and is very dynamic in shape. The orientation of the coastline is approximately North–South (10°– 190°) and the coastline has a slightly concave shape, which induces longshore transport gradients. The typical mean grainsize for the shoreface and beach is around 0.2 mm (TAW, 1984). Shoreface slopes range from 1:150 to 1:450 along the Holland coast (Spanhoff & van de Graaff, 2007). The beaches have a width of 100 to 200m from the dune foot to the low water line and have an average slope between 1:35 and 1:60 (Stolk, 1989).

Before 1990, each year approximately 20 ha of dunes disappeared through coastal retreat (De Ruig, 1998). In an analysis of Van Rijn (1997), it is shown that all along the Holland coast, there is structural erosion in the absence of nourishments except at the section of the coast adjacent to the barriers of the Port of IJmuiden. The Dutch coast sediment budget was found to be negative between 1965 and 1995 (Mulder, 2000).

Management of the Dutch coast and mittigation of its structural erosion can be subdivided into several strategies. First, the policy of Dynamic Preservation, introduced in 1991, resulted in yearly nourishment volumes of approximately 5 to 7 Mm^3 in the period between 1991 and 2000. This policy was aimed at keeping the coastline at a fixed position and therefore focused on beach nourishments. In 2000, a new policy targeting the preservation and improvement of the coastal foundation was introduced. The coastal foundation is defined to be the coastal zone including the lower shoreface. Therefore, the preservation of the coastal foundation policy includes shoreface nourishments. Between 1991 and 2012 a total of 207 Mm^3 of sand is supplied to the Dutch coast, half of it being shoreface nourishments (Van Der Spek & Lodder, 2015).

After the introduction of these nourishment strategies, Van Der Spek and Lodder (2015) concluded that the Holland coast was eroding at its northern and southern ends, but the central part was more or less stable. The overall net sediment budget of the Dutch coast is still negative due to erosion of the lower shoreface and the ebb-tidal deltas (Van Der Spek & Lodder, 2015). However, the budget shows that the accretionary status of the upper shoreface, beach and frontal dunes has changed to positive. The sediment budget excluding nourishments is still overall negative with exception of the tidal basins of the Wadden Sea, but with the Dynamic Preservation policy, the coastline retreat has been stopped.

2.6. Numerical modeling to simulate coastal evolution

This section describes the basics of coastal modeling. This thesis focuses on the development of a coupled model in order to numerically model the long-term beach and dune evolution on a large scale, therefore theoretical background regarding numerical modeling of the coastal zone is of fundamental importance.

There are many models describing fundamental processes and predicting their effects in the coastal

zone. Within the modeling of coastal morphology, a simple and clear division can be made between three fundamental sorts of modeling. These are: coastal profile models, coastline models and coastal area models (Roelvink & Reniers, 2011).

A coastal profile model concentrates on the cross-shore processes to predict the cross-shore evolution under different forcing, ignoring the longshore variability of the coastal zone. Coastline models, on the other hand, assume a fixed cross-shore profile which only moves in a seaward or landward direction as an effect of changing longshore conditions. The coastal area models combine effects in both the cross-shore and longshore direction, thus being a 2D model. Coastal area models can be split into two classes, the 2DH models which are depth averaged and the 3D models taking into account the variability of the flow and current velocities over depth.

Furthermore, models can be subdivided into analytical, (semi-)empirical and process-based models. Analytical models are by definition mathematical models that have a closed form solution, i.e. the solution to the equations used to describe changes in a system can be expressed as a mathematical analytic function. An analytical model requires highly schematized geometries, boundary conditions and wave conditions, since it is based on exact solutions of theoretical models.

Numerical models can be subdivided into process-based and (semi-)empirical models. In process-based models, the coastal zones response follows from a balance of forces. They focus on simulating detailed physical processes that explicitly describe system behaviour. Empirical modeling is based on the implicit description of a mechanism. The approach is data-driven and relies on correlative relationships. Empirical models do not fully describe the behaviour of a system and its interaction, but focuses on the equilibrium state depending on certain characteristics of the system.

Every kind of application of a situation asks for a different model. The spatial and temporal scale, the processes of interest and the level of detail of the model determine the choice of the type of model.

3

Model description

This chapter starts with an introduction of the coupled model. Both model components and the processes they simulate are shortly described. Thereafter, a brief introduction into coastal modeling will emphasize the relevance of the coupled model. In the third section, the coastline and cross-shore profile schematization are described. In Section 3.4, the processes governing the evolution of the coastal zone and the way they are described in the coupled model is explained. This chapter is concluded with a description of the model coupler, explaining the way the model components exchange information.

3.1. Model introduction

The coupled model consists of a combination of the coastline model "Unibest-CL+" and the cross-shore (coastal profile) model "the CS-model". It is developed to improve the prediction of the shoreline position in Unibest-CL+ by taking into account dune processes such as dune erosion and aeolian transport and the effects of sea level rise. By including cross-shore processes, the coupled model has a larger application range than coastline-models such as Unibest-CL+. For an overview of the processes included in the coupled model, see Figure 3.1.

The CS-model is a coastal profile model with the capability to simulate beach and dune evolution at decadal to centennial timescales. The CS-model includes the relevant sediment transport processes that impact the beach and dune evolution: dune erosion and overwash, aeolian dune build-up, beach-bar exchange, beach erosion and accretion due to gradients in longshore sediment transport and response to sea level rise.

In the CS-model, the coastal evolution is simulated in single or multiple cross-shore transects, which enables the model to represent coasts in length scales of kilometres. Model output consists of parameters relevant for coastal management such as shoreline change, dune volume, and dune height. Future beach and dune evolution can be investigated through varying input parameters, such as wind speed, wind direction, waves, and water levels. The effect of different nourishment strategies may be investigated through varying the placement, frequency, and volume of nourishments.

The Unibest-CL+ model is a coastline model which consists of the Unibest-LT and the Unibest-CL module. The LT-module is used for computing longshore sediment transport. It is designed to compute tide- and wave-induced longshore currents and sediment transport rates. The tidal current is included as a tidal current velocity at a reference depth. To obtain the longshore sediment transport rates, the model transforms offshore wave data to the coast. During this transformation, the model takes into account the principal processes of wave energy changes due to bottom refraction, shoaling and dissipation by wave breaking and bottom friction, which are described in Chapter 2. The CL-module uses the results from LT-simulations to simulate the development of the coastline under the influence of the computed longshore transport gradients along the considered coast. The transport rates are coupled to the angle of the coastline orientation, which enables the model to efficiently derive the transport rates at every grid cell.

Coupling of these two models enables the CS-model to use the by Unibest-CL+ derived local longshore sediment transport gradients and use these to derive the response of both the beach and the dune volume to these gradients. The effect of cross-shore processes on the local and temporal longshore sediment transport gradient are taken into account by enabling the CS-model to give feedback to Unibest-CL+. The coupled model enables the user to implement time-varying longshore sediment transport gradients in the existing CS-model. This CS-model proved to perform well on predicting the response of the dunes on a large temporal scale, but the model will be able to predict the most relevant effects of climate change within the coastal zone better if it is possible to implement time-varying longshore sediment transport gradients (Hallin, Huisman, Larson, Walstra, & Hanson, 2019). So by coupling these models, a model that can predict both coastline and cross-shore profile evolution at decadal to centennial time scales with short simulation time is supposedly created.
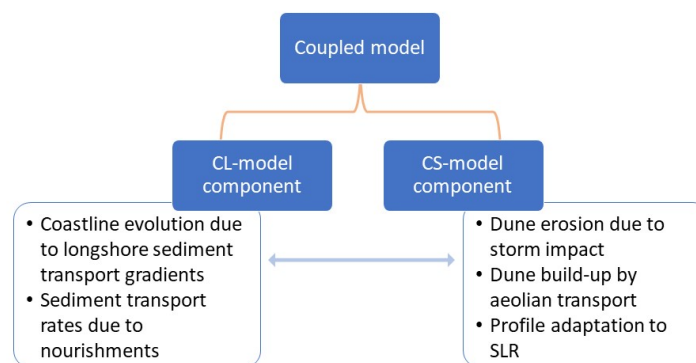
Figure 3.1: Overview of the coupled model and included sediment transport processes

From this point onward, the Unibest-CL+ model as a component of the coupled model is referred to as "the CL-model component" and the CS-model as a component of the coupled model is referred to as "the CS-model component". When Unibest-CL+ or the CS-model is mentioned, the independent model is meant. The coupled model is sometimes briefly addressed as "the model" since it is the subject of this thesis. When "CLCS" is used (e.g. as a subscript of a variable), it refers to the coupled model.

3.2. Relevance of the coupled model

In a previous case study focusing on the IJmuiden case, the gradients in longshore sediment transport were governing the long-term evolution of the dune volume (Hallin, Huisman, et al., 2019). This study was performed using the CS-model independently with implemented longshore sediment transport gradients and it pointed out the need for a more advanced sediment transport schematization within this model. Furthermore, Vitousek et al. (2017) indicated that the established method of modeling shoreline evolution based on longshore sediment transport gradients, as implemented in coastline models such as Unibest-CL+, does not perform sufficient on centennial timescale since it excludes the effects of sea level rise.

Coastal profile models do not take the alongshore variability of the coast into account, which is essential when simulating large scale coastal zone evolution. Coastline models do not include cross-shore processes such as aeolian transport and dune erosion. Furthermore, processes such as sea level rise and the distribution of nourishments affect the cross-shore interaction between beach and dune and

the coastline evolution. Cross-shore processes become more important in the decadal and centennial scale simulation of the coastal zone evolution (Vitousek et al., 2017). So, when simulating large temporal and spatial scale evolution the cross-shore processes should be included. There are several models available making a connection between cross-shore and alongshore processes, but for engineering purposes there is still missing a simple model which is applicable on large temporal and spatial scale and includes alongshore variability of the coastline as well as dune processes (Hallin, Huisman, et al., 2019).

The larger temporal and spatial scale modeling of coastline, beach and dune evolution therefore asks for the coupling between a cross-shore and alongshore oriented sediment transport model, in which the effect of time-varying longshore sediment transport gradients on cross-shore beach and dune evolution is implemented, together with the effect of cross-shore redistribution of sediment on the longshore sediment transport.

3.3. Profile description

The coupled model schematizes the coastal zone, in order to enable the model to predict its evolution. This schematization determines in a high rate the capacity of the model, since it determines the computational effort per time step along with the processes that can be included in the model. Since the coupled model consist of a CL-model and a CS-model component, the coastal zone schematization consists of a coastline and cross-shore profile which consist of several components explained in this section.
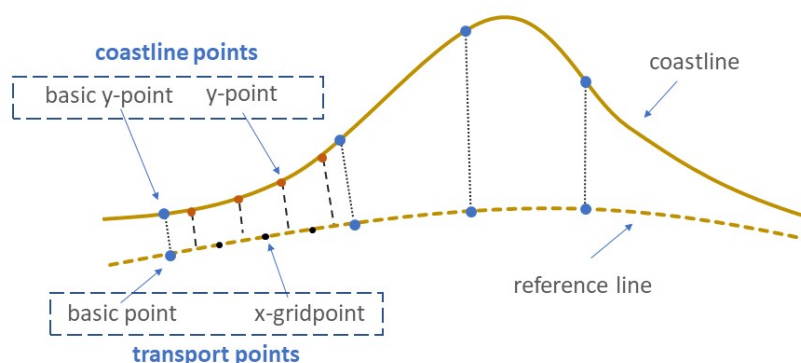
Figure 3.2: Definition of the coastline within Unibest-CL+, the CL-model component of the coupled model

3.3.1. Coastline

The coastline is schematized in the CL-model component. It is schematised by means of a curved reference line through user-defined Basic points in x-direction. The y-direction is defined by the normals perpendicular to the reference line in every Basic point. This curved system can be placed in the "real world" by defining the world coordinates (Xw,Yw) at every Basic point. The user defines the amount of x-points between the Basic points and these x-points and Basic points together form the reference line. The reference line follows the general contours of the coast. The climate of schematized sediment transport rates defined by the LT-module are coupled to locations in the CL-module. In every point

along the reference line, the transport rate is defined by inter- and extrapolating the determined sediment transport rates. This way, the sediment transport rate in every point along the reference line is determined. Furthermore, structures such as groynes, revetments, offshore breakwaters and internal boundaries can be implemented by defining their effect on the local sediment transport rates.

Beside the reference line, a coastline is defined in the model. The initial coastline is defined by the Basic y-points, which are located at a user-defined distance from the Basic points perpedicular to the reference line. After the definition of the x-points, every coastline point is located between two reference line points. The change of the position of a coastline point is determined by the longshore sediment transport gradient of the two adjacent transport points. The profile schematization within the CL-model component is illustrated in Figure 3.2.

For the LT-module, the orientation angle of the coast needs to be specified. This angle is then used to schematize the relation between coast angle and sediment transport, which is the key element of a single-line model such as Unibest-CL+. Furthermore, the active height is defined. The estimation of the active height depends on the wave climate, local bathymetry and time period under considered. The height of the active zone is larger for a continuously eroding coast than for an accreting coast, because sedimentation often (for a large part) takes place in the underwater part of the profile, while erosion also takes place on the dry part of the beach (Deltares, 2011).

3.3.2. Cross-shore profile

Within the CL-model component, the cross-shore profile is defined in the LT-module by a limited number of locations and water depths. The reference coastline defines the location where the water level meets the profile and the dynamic boundary determines the boundary of the dynamic part of the profile. This means that the longshore sediment transport is calculated up to the dynamic boundary. The truncation transport determines a part of the active profile that does not contribute to the total sediment transport, for example due to a rocky bottom. Furthermore, depth-contours are implemented in the cross-shore profile.

The dunes are schematized in one or several cross-shore profiles in the CS-model component, in which the profile is schematized to consist of two main volume entities – the dune and beach volume – that exchange sediment (Figure 3.3). The shape of the beach and dune is resolved through geometrical equations and is updated in every time step.
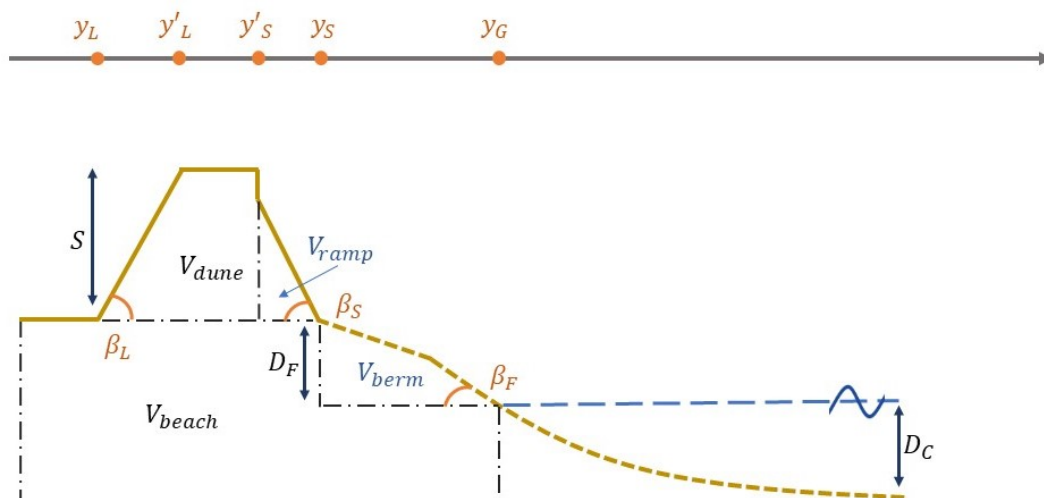
Figure 3.3: Cross-shore profile schematization within the CS-model, the CS-model component of the coupled model

The dune volume, V_{dune}, is defined as the volume of sediment above the dune foot. The dune foot height, D_F, is given relative to a reference still water level, SWL, which can be, e.g., the mean sea level, MSL, or the mean low water level, MLW. V_{dune} has a subvolume V_{ramp}, which is the volume of the dune ramp. The function of the dune ramp is to control the distribution of aeolian transported sediment across the dune. The slope of the dune ramp is defined by a fixed angle, β_S, taken as the angle of repose of dry sand (which is approximately 30-34°). The landward dune slope is defined by the fixed angle β_L, which may be derived from observations.

The shape of the dune is defined through the dune crest height, S, and four horizontal length coordinates given relative to a reference point behind the dune, y_L and y_S are the landward and seaward dune foot position and y'_L and y'_S are the landward and seaward dune crest position.

The beach volume, V_{beach}, is vertically limited by the dune foot height D_F and the depth of closure, D_C and horizontally by a reference point behind the dune and the intersection with the reference SWL, y_G. The depth of closure can be calculated from deepwater wave data (Hallermeier, 1978) or multiple measured profiles. The closure depth is a function of the largest waves of a certain duration during the time period considered, therefore a longer timescale results in a larger value of D_C because the probability of occurrence of more extreme wave events increases with time. Since D_F and D_C are defined relative to the reference SWL, the elevation of the dune foot and the seaward limit of the active profile, are shifted upwards with sea level rise. The beach does not have a specific shape, therefore the beach profile is represented by a dashed line in Figure 3.3. The beach width is described as a function of the volume of the berm, V_{berm}, horizontally limited by y_S and y_G, and vertically by the reference SWL and the dune foot elevation. If a linear relationship is assumed, the beach width is given by Equation 3.1 where a and b are coefficients describing the slope and the intercept with $V_{berm} = 0$, respectively. The rest of the beach volume, $V_{beach} - V_{berm}$ is then described by Equation 3.2.

$$y_G - y_S = a\,V_{berm} + b \tag{3.1}$$

$$V_{beach} - V_{berm} = y_G\,D_C + y_S\,D_F \tag{3.2}$$

The difference between a real cross-shore profile and the schematized cross-shore profile as it is defined in the CS-model component is illustrated in Figure 3.4.
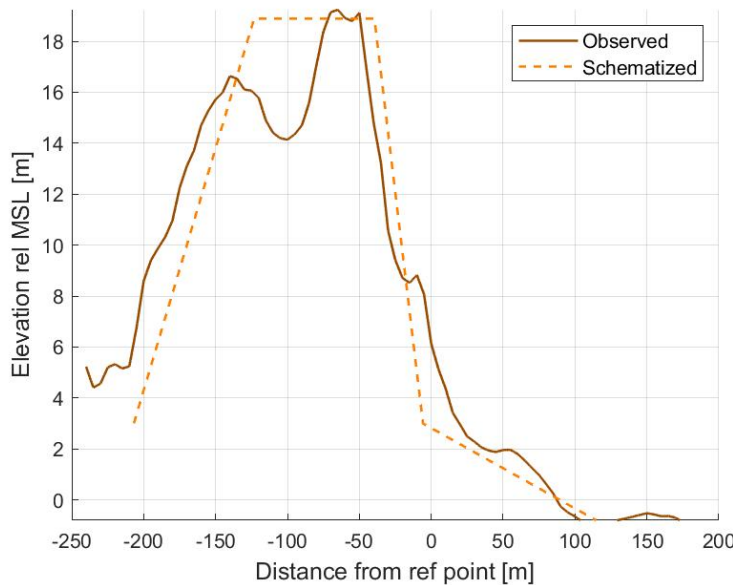
Figure 3.4: Observed and schematized cross-shore profile within the CS-model component of the coupled model, illustrative example based on Profile 9 of the IJmuiden case (See Chapter 5)

3.4. Process formulation

This section describes the chosen schematization of the morphodynamic processes and associated formulas, as applied within the coupled model. The transport mechanisms are depicted in cross-shore direction in Figure 3.5.
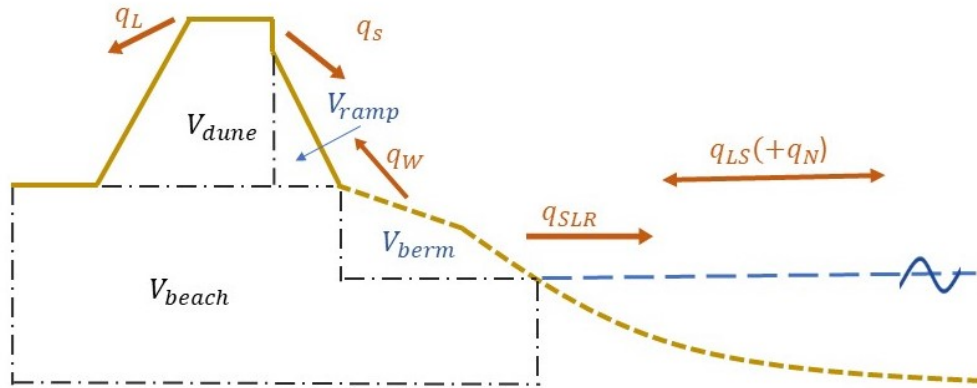
Figure 3.5: Schematization of cross-shore sediment transport mechanisms within the coupled

3.4.1. Dune erosion

There are various analytical and numerical models to simulate dune erosion. Since the CS-model is developed to simulate large scale dune development, analytical models which are easy to use, require a small number of input data and are fast to apply are more suitable. Analytical models can be subdivided into the models based on the equilibrium profile theory and the models based on the wave impact approach. Hallin, Huisman, et al. (2019) pointed out that in real situations, the conditions are time-varying and therefore the equilibrium profile will not be reached. Furthermore, the wave impact approach is more physics based.

The wave impact approach (Overton, Fisher, & Young, 1988) concept is used by Larson, Erikson, and Hanson (2004) to derive an analytical model with dune erosion proportional to the square of the run-up height above the dune foot.

Run-up height (R) is estimated using the formula given in Equation 3.3 (Larson et al., 2004), where H_{rms} is the deep-water root-mean-square wave height, and L_0 is the average deep-water wavelength.

$$R = 0.158\sqrt{H_{rms}\ L_0} \tag{3.3}$$

The run-up height is adjusted for friction over the beach accoring to Equation 3.4 (Hanson, Larson, & Kraus, 2010), where c_f is the empirical friction factor which has typically a value between 0.1 and 0.2, x_t is the travel distance of the wave rushing up, R' is the adjusted run-up height and SWL is the still water level. The travel distance definition is given in Equation 3.5, in which the travel distance is a function of the berm volume because of the undefined shape of the beach.

$$R' = R\ e^{-2\ c_f x_t} + (D_F - SWL)\ (1 - e^{-2\ c_f x_t}) \tag{3.4}$$

$$x_t = \frac{2\ V_{berm}}{D_F}\left(1 - \frac{SWL}{D_F}\right) \tag{3.5}$$

Using the previously given expressions, the dune erosion (q_D) can be determined. Using the in Section 2.4.1 explained regimes of Sallenger, dune erosion is defined for the collision (Equation 3.6a) and the overwash (Equation 3.6b) regime. In these equations, T is the wave period, S is the dune height and

C_S is the dune erosion impact coefficient. A common range for C_S is found to be between the values $1.7 \times 10^{-4} - 1.4 \times 10^{-3}$ when calibrated against data from field and laboratory experiments (Larson et al., 2004).

$$q_D = 4C_S \frac{(R' + SWL - D_F)^2}{T} \qquad \text{if } D_F < R' + SWL < D_F + S \qquad (3.6a)$$

$$q_D = 4C_S \frac{(R' + SWL - D_F)\, S}{T} \qquad \text{if } R' + SWL > D_F + S \qquad (3.6b)$$

In case of the overwash regime, a part of the eroded dune volume is deposited on the landward side of the dune. The eroded sediment q_D is divided into the landward side deposited volume q_L and the seaward deposited volume q_S by ratio α. This ratio is given by Equation 3.7 (Larson, Donnelly, Jiménez, & Hanson, 2009). Using field data, the empirical coefficient A is found to be equal to 3.

$$\alpha = q_L/q_S = \frac{1}{A}(\frac{R' + SWL - D_F}{S} - 1) \qquad (3.7)$$

After erosion, the dune geometry should be updated. First, the volume of the dune ramp (V_{ramp}) will be eroded. This results in a change of dune foot position (y_S) given by Equation 3.8. In this expression $\Delta V = -q_D \Delta t$ is the eroded volume and β_S is the dune ramp slope angle.

$$\Delta y_S = \frac{\sqrt{2}(\sqrt{tan(\beta_S)(V_{ramp} + \Delta V)} - \sqrt{tan(\beta_S)V_{ramp}})}{tan(\beta_S)} \qquad (3.8)$$

After the dune ramp has been eroded completely and the seaward dune crest length coordinate (y_S') coincides with the seaward dune foot length coordinate ($y_S = y_S'$), the seaward dune crest will retreat, given by Equation 3.9 in which ΔV is the eroded volume and S is the dune height.

$$\Delta y_S' = \frac{\Delta V}{S} \qquad (3.9)$$

If the erosion reaches the point where the seaward dune crest length coordinate coincides with the landward dune crest length coordinate ($y_S' = y_L'$), the dune has obtained a triangular shape and further dune erosion leads to change of the landward dune crest length coordinate according to Equation 3.10 and change of the dune height given by Equation 3.11.

$$\Delta y_L' = \frac{\sqrt{\frac{2\Delta V tan(\beta_L)+S^2}{tan(\beta_L)^2}}tan(\beta_L) - S}{tan(\beta_L)} \qquad (3.10)$$

$$\Delta S = \Delta y_L'\, tan(\beta_L) \qquad (3.11)$$

In case of overwash, the landward side deposited volume of eroded sediment causes dune build-up on the landward side of the dune given by Equation 3.12. In this expression, $\Delta V = q_L \Delta t$.

$$\Delta y_L' = \Delta y_L = \frac{\Delta V}{S} \qquad (3.12)$$

3.4.2. Aeolian transport
Aeolian transport is a process subjected to various limiting factors, as described in Section 2.4.3. During the development of the CS-model, a new method to simulate dune build-up is derived. This reduced-complexity method is based on the assumption that the most critical limiting factor is the supply of material of appropriate grain size, when simulating aeolian transport on a decadal timescale. A site-specific fraction of the longshore and cross-shore transported sediment volumes is assumed to be available for dune build-up by aeolian transport. With V_w being the volume of sediment available for aeolian transport, the fraction is computed using a sediment transport balance (Equation 3.13). In this equation, the available volume of sediment depends on the part of the dune erosion deposited on the beach q_S (described in 3.4.1), on the potential aeolian transport rate q_W, on the sediment transport due to sea level rise q_{SLR} described in 3.4.4, on the local gradient in the longshore sediment transport

rate q_{LS} determined by the CL-model component, on the empirical coefficient A_q (with a regular value around 0.6) and on the length of the timestep in the CS-model component Δt. This empirical coefficient describes the site-specific fraction of sediment that is exposed to the wind and has the proper grain size for aeolian transport. The aeolian transport q_W is limited by the sediment available for aeolian transport, $q_W \Delta t \leq V_W$. If there is no sediment available, there is no aeolian transport, (if $V_w = 0$ then $q_W = 0$). The initial sediment availability $V_{W,0}$ is site-specific as well and depends on factors such as prior dune erosion events and nourishments.

$$V_{W,i} = V_{W,i-1} + (q_{S,i-1} - q_{W,i-1} - A_q(q_{SLR,i-1} - q_{LS,i-1}))\Delta t \quad \text{if } V_W \geq 0 \tag{3.13}$$

If there is sediment available for aeolian transport, the potential aeolian transport rate can be calculated with an equilibrium transport formula. In the CS-model component, the formulation of Lettau and Lettau (1978) is used. In this formulation (Equation 3.14), the potential aeolian transport rate m_{WE} depends on the median reference grain size D_{50}^{ref} which has a typical value of 0.25 mm, local median grain size D_{50}, the air density ρ_a, the gravitational acceleraration g, empirical coefficient K_W with a site specific value to be calibrated and the shear velocity and critical shear velocity at the bed u_* and u_{*c} respectively. If the shear velocity at the bed is smaller than the critical shear velocity ($u_* \leq u_*c$), the potential aeolian sediment transport is zero.

$$m_{WE} = K_W \sqrt{\frac{D_{50}}{D_{50}^{ref}}} \rho_a \frac{u_*^2}{g}(u_* - u_{*c}) \quad \text{if } u_* \leq u_*c \tag{3.14}$$

To calculate the shear velocity, the Prandtl equation also known as the law of the wall is used (Prandtl, 1933). In this equation (Equation 3.15), u_z is the wind velocity at z meters above the surface level, z_0 is the aerodynamic roughness height and κ is von Karman's constant (=0.4).

$$\frac{u_z}{u_*} = \frac{1}{\kappa} ln(\frac{z}{z_0}) \tag{3.15}$$

For the wind velocity conditions below the critical velocity for initiation of transport, the roughness height, z_0, is parameterised using Equation 3.16 derived by Zingg (1953). The variable D represents the grain size, for which the D_{50} can be used.

$$z_0 = 0.081 log_{10}(D/0.18) \tag{3.16}$$

The critical shear velocity can be calculated using the Equation 3.17 (Bagnold, 2012). In this expression, A_W is an empirical coefficient with a typical value of 0.1, ρ_S is the density of the sediment and D_{50} is the median grain size of the sediment.

$$u_{*c} = A_W \sqrt{\frac{(\rho_s - \rho_a)}{\rho_a} g D_{50}} \tag{3.17}$$

The volumetric equilibrium transport rate q_{WE} is derived from the potential aeolian sediment transport rate using Equation 3.18, in which ρ_S is the density of sand and P is the porosity.

$$q_{WE} = \frac{m_{WE}}{\rho_S(1 - P)} \tag{3.18}$$

This volumetric equilibrium transport rate is affected by the fetch of the wind and limited by the angle of incidence of the wind. The fetch length F (Equation 3.19a) depends on the dry beach width B_{dry} and the angle of incidence of the wind θ, as depicted in Figure 2.6. The dry beach width is defined to be the horizontal distance between the run-up limit y_R and the seaward dune foot y_S. Assuming a constant beach slope, the run-up limit is given by Equation 3.20a, and the dry beach width by Equation 3.20b,

in which y_G is the intersection between beach height and still water level SWL and R is the in Equation 3.3 determined run-up height.

$$F = \frac{B_{dry}}{cos(\theta)} \qquad\qquad \text{if } 0° \leq \theta \leq 80° \qquad\qquad (3.19a)$$

$$y_R = y_S + \left(1 - \frac{R + SWL}{D_F}\right)(y_G - y_S) \qquad\qquad (3.20a)$$

$$B_{dry} = y_R - y_S = \left(1 - \frac{R + SWL}{D_F}\right)(y_G - y_S) \qquad\qquad (3.20b)$$

The volumetric equilibrium transport rate corrected for effects of the fetch length q_{WF} is given in Equation 3.21a. In this simplified equation based on the work by Sauermann, Kroy, and Herrmann (2001), δ is an empirical coefficient which represents the wind condition with most aeolian transport and has a typical value ranging between 0.1–0.2 m^{-1} and F is the fetch length determined by Equation 3.19a. The equilibrium transport rate is corrected based on the angle of wave incidence θ, to account only for the onshore component of the aeolian transport. Therefore, Equation 3.21b is the final equation for the potential aeolian transport rate q_W.

$$q_{WF} = q_{WE}(1 - exp(-\delta F)) \qquad\qquad (3.21a)$$

$$q_W = q_{WF} cos(\theta) \qquad\qquad (3.21b)$$

Dune evolution

The sediment budget concept by Psuty (1988) (explained in Section 2.4.3) is used to define the different ways dunes evolve when the wind transports sand towards the dunes. The sediment budget is defined to be the change of volume in the beach-dune system ΔV_T over a significant timescale T_{bud}, in the order of years. In Equation 3.22, the expression for the sediment budget is given. In this expression, $n = T_{bud}/\Delta t$ and q_N is the total transport rate due to beach, shoreface and dune nourishments. Furthermore, the sediment budget depends on the transport rate due to longshore sediment transport gradients q_{LS} and the transport rate due to adaptation of the profile to sea level rise q_{SLR}, which will both be further discussed in Section 3.4.3 and 3.4.4. It should be noted that timescale T_{bud} should be long enough to represent long-term trends instead of seasonal variations.

$$\Delta V_T = \frac{1}{n} \sum_{t=i-n}^{t=i} ((-q_{SLR,t} + q_{LS,t} + q_{N,t})\Delta t) \qquad\qquad (3.22)$$

When the sediment budget is positive, the dune ramp is filled until the ramp height equals the dune height. If the dune is trapezoidal shaped, the sediment will thereafter be deposited on top of the dune until the dune height reaches its maximum. If the maximum dune height is reached, the sediment is deposited on the seaward side of the dune. If the dune is triangularly shaped, the dune grows symmetrically upwards.

In case of a stable sediment budget, the dune ramp is filled until the ramp height equals the dune height. After the dune ramp is filled up, the dune evolution depends on the shape of the dune again. If the dune has a trapezoidal shape, a part (A_s) of the sediment will be deposited on the crest of the dune and the rest (1-A_s) will be deposited on the seaward side of the dune. If the dune is triangularly shaped, the dune grows symmetrically upwards.

If there is a negative sediment budget, the ramps is filled until the critical ramp height is reached. This critical ramp height is assumed to be 1 m below the dune crest level (Christiansen & Davidson-Arnott, 2004)), in case local observations do not suggest differently. Thereafter, the dune evolution depends
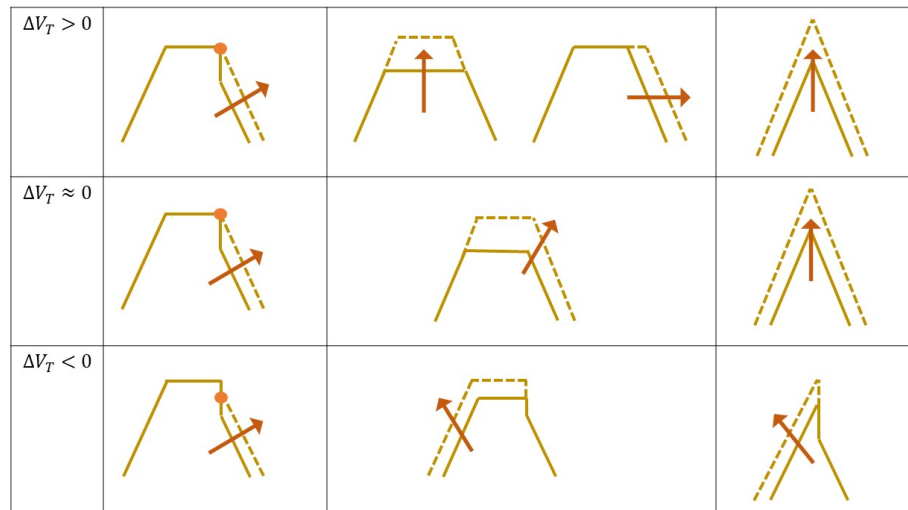
Figure 3.6: Sediment budget and the corresponding stages of dune evolution

on the dune shape again. If the dune has a trapezoidal shape, a part (A_e) of the sediment will be deposited on the crest of the dune and the rest (1-A_e) will be deposited on the landward side of the dune. If the dune is triangurly shaped, the dune grows on its landward side. The various stages of dune evolution are depicted in Figure 3.6.

3.4.3. Longshore sediment transport

In the Unibest-LT module, surf zone dynamics are computed by a built-in random wave propagation and decay model (Battjes & Janssen, 1978). The model transforms offshore wave data to the coast, taking into account the principal processes of wave energy changes due to bottom refraction, shoaling and dissipation by wave breaking and bottom friction. The longshore current distribution across the beach profile is derived from the momentum equation alongshore taking into account bottom friction, the gradient of radiation stress and the tidal surface slope alongshore. A semi-analytical description of the wave-induced, depth-mean longshore current is used, derived through the breaking wave dissipation and using a linearised version of the bottom friction term for wave and current combined (Deltares, 2011).

The longhore sediment transport rates along the coastline and the coastline response due to gradients are calculated within the CL-model component based on the single line theory (Pelnard-Considère, 1957). The basic assumption of the single line theory is that the shape of the cross-shore profile does not change in time and therefore the entire profile moves forward and backwards as the coast erodes or accretes.

Single line models simulate coastal response to longshore transport gradients as a single line, by forcing an equilibrium coastline orientation based on the governing hydrodynamic conditions. Though the cross-shore profile is not assumed to keep a constant shape, the single line theory and the longshore sediment transport relation resulting from it are implemented in the coupled model.

Following the single line theory as shown in Figure 3.7, the volume change within the considered profile ΔV is defined to be the product of the horizontal change of coastline position Δy, the alongshore beach length of the active area Δx and the active height h_0 (Equation 3.23). This profile change is a function of the net inflow of sediment due to a gradient in the local alongshore transport Q_{LS} during a time interval Δt (Equation 3.24).

$$\Delta V = \Delta x \Delta y h_0 \tag{3.23}$$
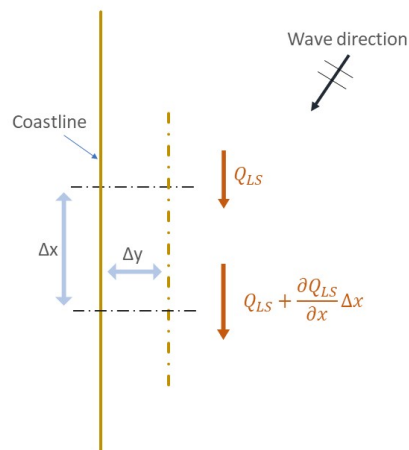
Figure 3.7: Profile change due to longshore sediment transport, according to the Single line theory (Pelnard-Considère, 1957)

$$\Delta V_{LS} = -\frac{\partial Q_{LS}}{\partial x}\Delta x\Delta t \tag{3.24}$$

Combining these two formulae by equating the net sediment inflow and the profile change gives the continuity equation of the single line theory (Equation 3.25).

$$\frac{\partial y}{\partial t} = \frac{1}{h_0}\frac{\partial Q_{LS}}{\partial x} \tag{3.25}$$

$$\frac{\partial y_\phi}{\partial t} = \frac{1}{h_0}\frac{\partial Q_{LS}}{\partial x}\frac{\partial \phi}{\partial x} \tag{3.26}$$

The longshore sediment transport is defined to be a function of the coastline orientation Φ, therefore Equation 3.25 is rewritten into Equation 3.26 in which the sediment transport gradient depends on the coastline orientation.

The relation between the angle of incidence of the incoming waves and the resulting sediment transport for the initial coastline orientation of a certain coastal stretch can be determined by using a sediment transport formula. This relation can be translated into the form of a S-ϕ curve, expressing the relation between the sediment transport rate (S) and the coastline orientation (ϕ) for a certain location and wave-climate. This curve can be used to determine the sediment transport along a temporal and spatial varying coastline and therefore enables the implementation of complex sediment transport formulas in simple models.

The net longshore sediment transport gradient in a certain grid cell is not only a function of the coastline orientation, but is affected by local sinks and sources such as nourishments and dune processes. The local longshore sediment transport gradient causes a positive, negative or stable sediment budget within the cross-shore profile. The local sediment budget affects the dune processes, as described in Section 3.4.2.

Wind driven currents

Wind driven longshore currents can be manually activated in the CL-model component. Using the wind speed, direction and wind drag force, the magnitude of the wind stress at the water surface is determined (Smith & Banke, 1975).

$$\tau_s = C_{drag} * \rho_a * v_{wind} * |v_{wind}| \tag{3.27}$$

In this formula, τ_s is the stress at the free surface, ρ_a is the air density, C_{drag} is the wind drag coefficient and v_{wind} is the wind speed.

Sediment characteristics

An important characteristic of the CL-model component – and therewith the coupled model – is the ability to apply different transport formulae. The choice for a certain transport formula can be based on local characteristics of the conditions or studied situation as well as on the nature of the considered sediment.

The formulations of Bijker (1967, 1971), Van Rijn (1992), Van Rijn (1993) and Soulsby / Van Rijn (1997) are applicable at cases with bed and suspended load of sand. Van Rijn (2004) can be used for bed and suspended load of sand and fine sediment. CERC (1984) provides a simple formula for a sandy beach, with sediment transport by waves only. The Kamphuis (2000) formulation is a bulk equation. The Van der Meer-Pilarczyk (1992) formulation is suitable for cases with gravel beaches with fairly large gravel.

3.4.4. Adaptation to sea leve rise

The effect of sea level rise on the coastal morphology is described by the Bruun Rule, introduced in Section 2.4.4. The Bruun Rule provides a simple method to estimate the shoreline retreat R_{Bruun}, under a slowly rising sea level (Bruun, 1962), given in Equation 3.28. In this equation, S_{SLR} is the sea level rise, B_{Bruun} is the width of the active profile and h_0 is the height of the active profile (Bruun, 1962), which is the sum of the closure depth and the berm height. The width B_{Bruun} is defined to be the distance from the shoreline to the depth of closure.

$$R_{Bruun} = S_{SLR} \frac{B_{Bruun}}{h_0} \tag{3.28}$$
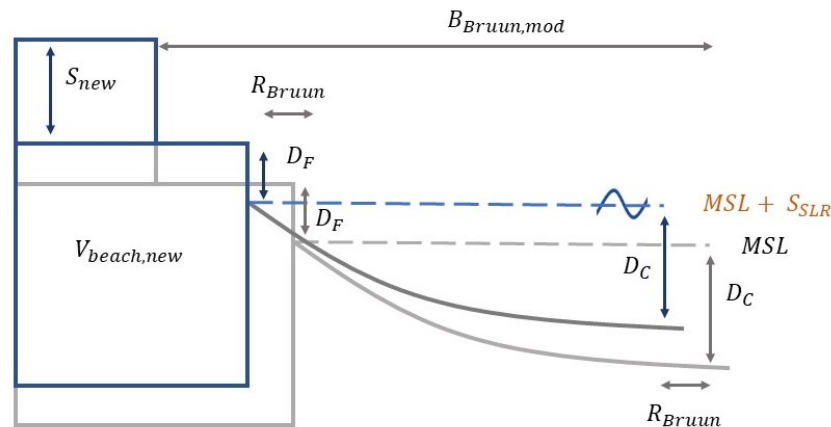
Figure 3.8: Schematic explanation of the Bruun rule concept, the beach and dune volume are rectangular shaped for simplicity

Using the Bruun Rule concept, the sediment transport from the dry beach to the subaqueous part of the active profile – needed to compensate for sea level rise – can be calculated (see Figure 3.8). Furthermore, sediment transport needed for the dry beach elevation is calculated as well. The further developed Bruun rule, with additional landward transport due to wind and overwash is defined by Rosati, Dean, and Walton (2013). In this modified Bruun Rule, the width $B_{Bruun,mod}$ is extended and expresses the horizontal distance between the seaward dune foot and the depth of closure. The depth

of closure and the dune foot height are both kept constant with respect to the mean sea level. The eroded volume V_{SLR} becomes a function of the shoreline retreat and these two characteristic depths as described in Equation 3.29.

$$V_{SLR} = R_{Bruun} \, (D_F + D_C) = S_{SLR} \, B_{Bruun,mod} \tag{3.29}$$

The sediment transport due to sea level rise is the time derivative of the expression for the eroded volume (Equation 3.30).

$$q_{SLR} = \frac{dV_{SLR}}{dt} = \frac{dS_{SLR}}{dt} B_{Bruun,mod} \tag{3.30}$$

In the CS-model component, sea level rise results in a offshore transport q_{SLR}, eroded from the beach volume. Furthermore, the dune volume and height decrease. These changes of the dunes are a function of the sediment transport due to sea level rise and the dune geometry. In the coupled model, the eroded beach volume is implemented as a sediment sink in the longshore sediment transport rate calculated within the CL-model component.

3.4.5. Nourishments
As explained in Section 2.4.6, nourishments can be added to the beach, dune, or shoreface. In the coupled model, the CL-model component covers the implementation of shoreface and beach nourishments. In the case of a beach nourishment, the total volume of sediment is added to a certain part of the considered coastal stretch in a short amount of time (in the order of a few years), and the cross-shore morphology is updated accordingly. To account for shoreface nourishments, a constant amount of sediment is added to the system during a larger period of time. Thus, the transport due to nourishments q_N is a function of the total nourished volume V_N, the alongshore length of the beach that is nourished Δx and the duration of the nourishment Δt, as shown in Equation 3.31.

$$q_N = \frac{\Delta V_N}{\Delta x \Delta t} \tag{3.31}$$

This approach is based on the research of Huisman, Walstra, Radermacher, De Schipper, and Ruessink (2019), implementing their assumption of a linear decay of the volume in the initial nourishment region. The length of the nourishment period depends on the size of the nourishment, the wave characteristics, the local bathymetry and the sediment characteristics. Therefore, it must be determined for every model application individually.

Dune nourishments are implemented in the CS-model component.They are by default added to the front of the dune. First, the dune ramp is filled up according to Equation 3.8 after which the dune grows seaward.

3.4.6. Beach-bar migration
In the CS-model, the bar volume enables the model to simulate the seasonal cyclic behaviour of the beach. In the same way the coastline change is a function of the equilibrium coastline orientation, Larson and Kraus (1989) developed an approach that couples the offshore sediment transport to an equilibrium bar volume which depends on the wave climate characteristics.

Because the coupled model is developed to focus on large scale coastal zone simulation, seasonal cyclic behaviour such as beach-bar migration is less relevant. Beach-bar processes are therefore left out in the coupled model.

3.5. The model coupler

In this section, the interaction between the model components and the model coupler are discussed. In Figure 3.1, an overview of the main processes included in the coupled model is given. These processes and their formulation are covered in the previous sections. In the model coupler, the combined effect of all included processes is simulated using both model components.

The various timesteps of the coupled model are illustrated in Figure 3.9. Initially the CL-model component simulates the coastline change as a result of longshore sediment transport gradients and nourishments. These coastline changes are typically determined at a large amount of grid cells for a limited number of timesteps. In the model coupler the coastline changes are multiplied with the active height to obtain volume changes per meter. Next, the model coupler determines how many timesteps within the CS-model component should be taken to catch up with the CL-model component, since the number of timesteps in the CS-model is typically larger (and the length of the timestep therefore smaller). The model coupler gives the volume change per meter at every cross-shore profile to the CS-model. The total volume change within the cross-shore profile, the sediment availability and the total beach volume is updated, using this volume change due to longshore sediment transport gradients and nourishments. Then, volume changes due to dune erosion, aeolian transport and sea level rise are calculated by the CS-model component for every timestep, until the CS-model component catches up with the CL-model component. Geometrical equations resolve the shape of the cross-shore profile and update the morphology every timestep. The total volume change due to cross-shore transport processes is determined and given to the model coupler. Through dividing the volume changes by the active height of the profile, the total volume change due to cross-shore transport processes are translated to coastline changes. These coastline changes are added to the initially determined coastline changes due longshore sediment transport gradients and nourishments to update the coastline change. Thereafter, the CL-model component determines the coastline change for the next timestep.
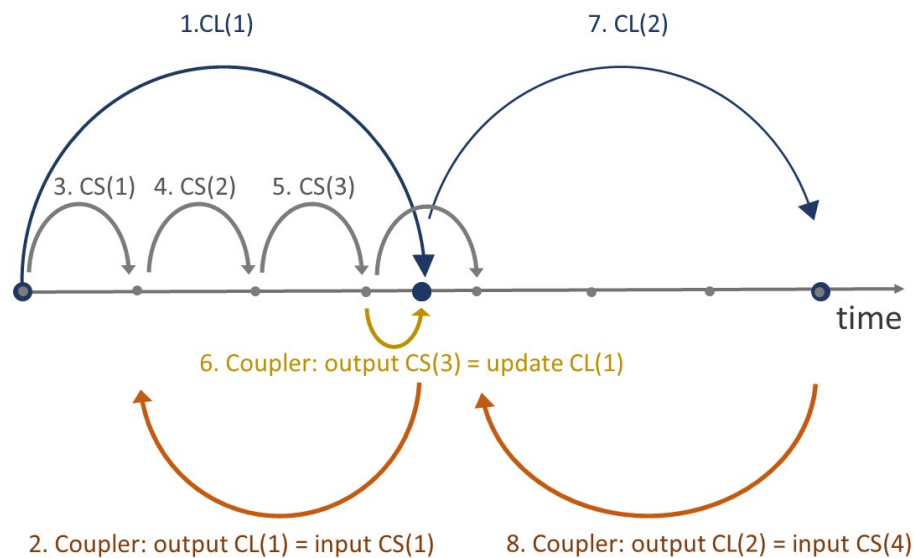
Figure 3.9: A schematic of the model coupling between the CL- and CS-model component

4

Model testing

In this chapter, the testing of the coupled model is described. The model is tested quantitatively based on the sediment balance described in Section 4.1. The sediment conservation within the coupled model is examined in a simple and a more complicated case. For every test case, a particular process within the coupled model and its effect on the sediment conservation within the sediment balance of the coupled model is tested. In Section 4.2 first the simple case with only longshore sediment transport and thus stable dunes is examined. Thereafter processes of dune erosion and dune build-up are simulated by consecutively increasing the still water level and the wind speed. Consequently sediment conservation after implementation of a nourishment or sea level rise is studied. These five different processes are also examined in the cases with multiple cross-shore profiles located along a larger stretch of coastline in Section 4.3. In these cases, the number of defined cross-shore profiles is varied in order to study sediment conservation for different model scales. This chapter is finished with a conclusion drawn from the various model tests in Section 4.4.

4.1. Testing sediment conservation

To test if the model components interact correctly, it is relevant to review the sediment conservation within the coupled model. The sediment balances governing both model components are described in this section. After the sediment fluxes have been described, it is tested for various cases whether sediment is conserved and, if not, to what extent the sediment balance of the coupled model deviates from sediment conservation.

On the scale of a single cross-shore profile, the total volume change within that profile is a summation of the change of the characteristic cross-shore volumes, which are the total beach volume including the berm volume and the dune volume including the ramp volume (see Figure 3.3). This total volume change is equal to the defined three sediment fluxes within the CS-model component, which are:

- longshore sediment transport gradient $\partial Q_{LS}/\partial x$ resulting in a negative or positive sediment transport q_{LS} in the profile defined as $-\partial Q_{LS}/\partial x = q_{LS}$

- positive sediment transport due to a shoreface, beach or dune nourishment q_N

- negative sediment transport due to sea level rise q_{SLR}

In the coupled model, the sediment transport due to shoreface nourishments is calculated in the CL-model component and included in the local longshore sediment transport gradient given to the CS-model component by the model coupler. The sediment balance of the CS-model component on the scale of a single profile is given in Equation 4.1.

$$\frac{dV_{CS}}{dt} = \frac{dV_{dune}}{dt} + \frac{dV_{beach}}{dt}$$
$$= q_{LS} + q_N - q_{SLR}$$

(4.1)

The cross-shore profiles – which are defined in the CS-model component – are located within a certain grid cell of the CL-model component. Within this grid cell, the total volume change is defined to be the sum of the coastline change Δy within that grid cell multiplied by the active height h_0 and the alongshore length of the grid cell Δx. This volume change is equal to the net sediment change resulting from the balance of sediment fluxes within the CL-model component which are:

- longhore sediment transport at the upstream boundary Q_{in}

- longshore sediment transport at the downstream boundary Q_{out}

- sediment sources such as a nourishment or river outflow, including sediment influx due to dune erosion $Q_{sources}$

- sediment sinks such as tidal basins or mining activities, including sediment loss due to dune growth Q_{sinks}

The resulting sediment balance of the CL-model component on grid cell scale is given in Equation 4.2.

$$
\begin{aligned}
\frac{dV_{CL}}{dt} &= \frac{dy}{dt} h_0 \, \Delta x \\
&= Q_{in} - Q_{out} + Q_{sources} - Q_{sinks}
\end{aligned}
\tag{4.2}
$$

The coupled model first gives the local sediment transport gradient determined by the CL-model component to the CS-model component. Then, after one or several timesteps within the CS-model component, the coastline position and sediment budget should be modified based on the change in beach volume due to cross-shore exchange of sediment between the dune and beach volume. For example, the local accretion increases when part of the dune volume is eroded due to a high water level and added to the beach volume. The modified beach volume is given back to the CL-model component, which updates the coastline response due to this change in transport.

As the cross-shore profiles are only defined at fixed points along the coastline, the sediment exchange between the CS- and CL-model component is linearly interpolated between these fixed points to simulate the behaviour of the considered coastal stretch as realistically as possible. For these test cases, the cross-shore profiles are defined as clear as possible; the most upstream located cross-shore profile is called Profile 1 and then the profiles are numbered in downstream direction. The total number of profiles defined within the CS-model component is n. This means that the total sediment balance of the whole coastal stretch under consideration consists of the following elements:

- between the upstream boundary and Profile 1, the volume change of the CS-model component $dV_{CS,1}/dt$ is assumed to be the same to the change in the first profile in every grid cell of the CL-model component

- between the downstream boundary and Profile n, the volume change of the CS-model component $dV_{CS,n}/dt$ is assumed to be the same in every grid cell of the CL-model component

- in between the defined profiles, the volume change of the CS-model component in every grid cell is determined by linear interpolation of the volume change within the profiles.

This results in sediment balance 4.3.

$$
\int_{t=0}^{T}\int_{x=0}^{L} V_{CLCS}\,dx\,dt = \sum_{x=0}^{L}(V_{CL}(x,T) - V_{CL}(x,0)) \quad = \sum_{x=0}^{L}(V_{CS}(x,T) - V_{CS}(x,0))
\tag{4.3}
$$

with

$$
\sum_{x=0}^{L}(V_{CL}(x,T) - V_{CL}(x,0)) = h_0(x)\sum_{x=0}^{L} y(x,T) - y(x,0)
\tag{4.4}
$$

4.2. Simple test cases

In order to test whether the above explained sediment balance is resulting in sediment conservation in the coupled model, some test cases are defined. First, a simplified case study with only two grid cells in the CL-model component and one cross-shore profile in the CS-model component is performed in order to look at the sediment fluxes in detail. The model set-up is shown in Figure 4.1.
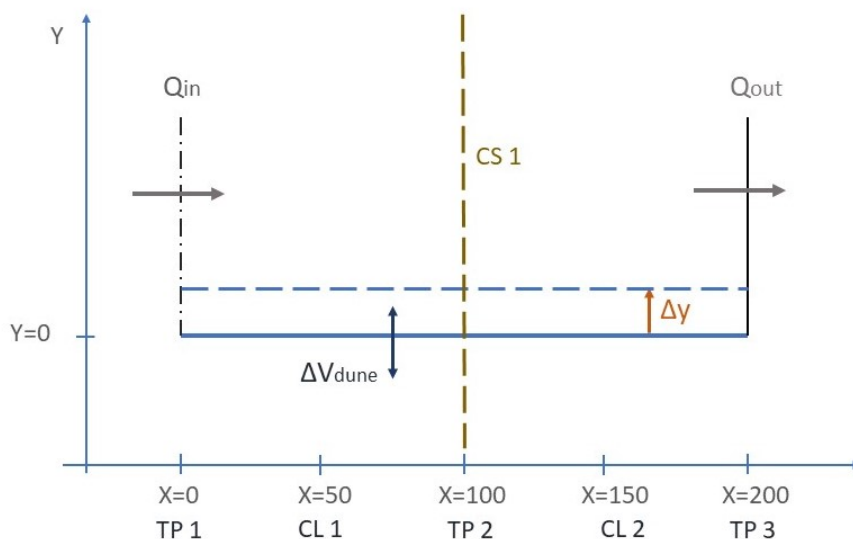
Figure 4.1: Geometry of the simple test cases 1-5; TP are the transport points, CL are the coastline points and CS is the cross-shore profile

General conditions in simple test cases

The CL-model component of all simple cases consists of two grid cells with a length of 100 m each. In the middle of the considered two grid cells is a single cross-shore profile defined within the CS-model component. At the left boundary an inflow Q_{in} of 1000 m^3/yr enters the domain. The right boundary is closed (Q_{out} = 0 m^3/yr). The simulation time is 10 years and the active height is 5 meters in both model components. There is no effect of sea level rise and there are no nourishments. Due to the low waves and water level, there will be no overwash.

Test case 1: Simple case - Stable dunes, longshore sediment transport

In the simple case with stable dunes, there is no change in dune volume due to a low water level and the absence of wind. Therefore, only the longshore sediment transport gradient causes changes. The theoretical sediment fluxes in this case are given in Table 4.1. The volumes are all given in m^3/m, which is defined to be the change in volume along 1 m of coastline.

As shown in Figure 4.2 the coastline change Δy after the simulation time is 10 m. The volume change of both the beach and dune volume are depicted. It is shown that after the simulation time, the beach volume change ΔV_{beach} is 50 m^3/m and the dune volume change ΔV_{dune} equals zero. In the figure showing the total volume change in each model component, the ΔV_{CL} is defined to be the coastline change multiplied by the active height and the ΔV_{CS} is defined to be the summed volume change of both the dune and beach volume. It can be read in the graphs that these total volume changes in both model components are similar and equal to 50 m^3/m.

Simple case - Stable dunes		
Variable	Derivation	Value
ΔV_{CL}	$Q_{in} - Q_{out}$	50 m³/m
ΔV_{CS}	q_{LS}	50 m³/m
ΔV_{dune}		0 m³/m
ΔV_{beach}	$\Delta V_{CS} - \Delta V_{dune}$	50 m³/m
Δy	$\Delta V_{CL}/(h_0)$	10 m

Table 4.1: Theoretical sediment fluxes in test case 1
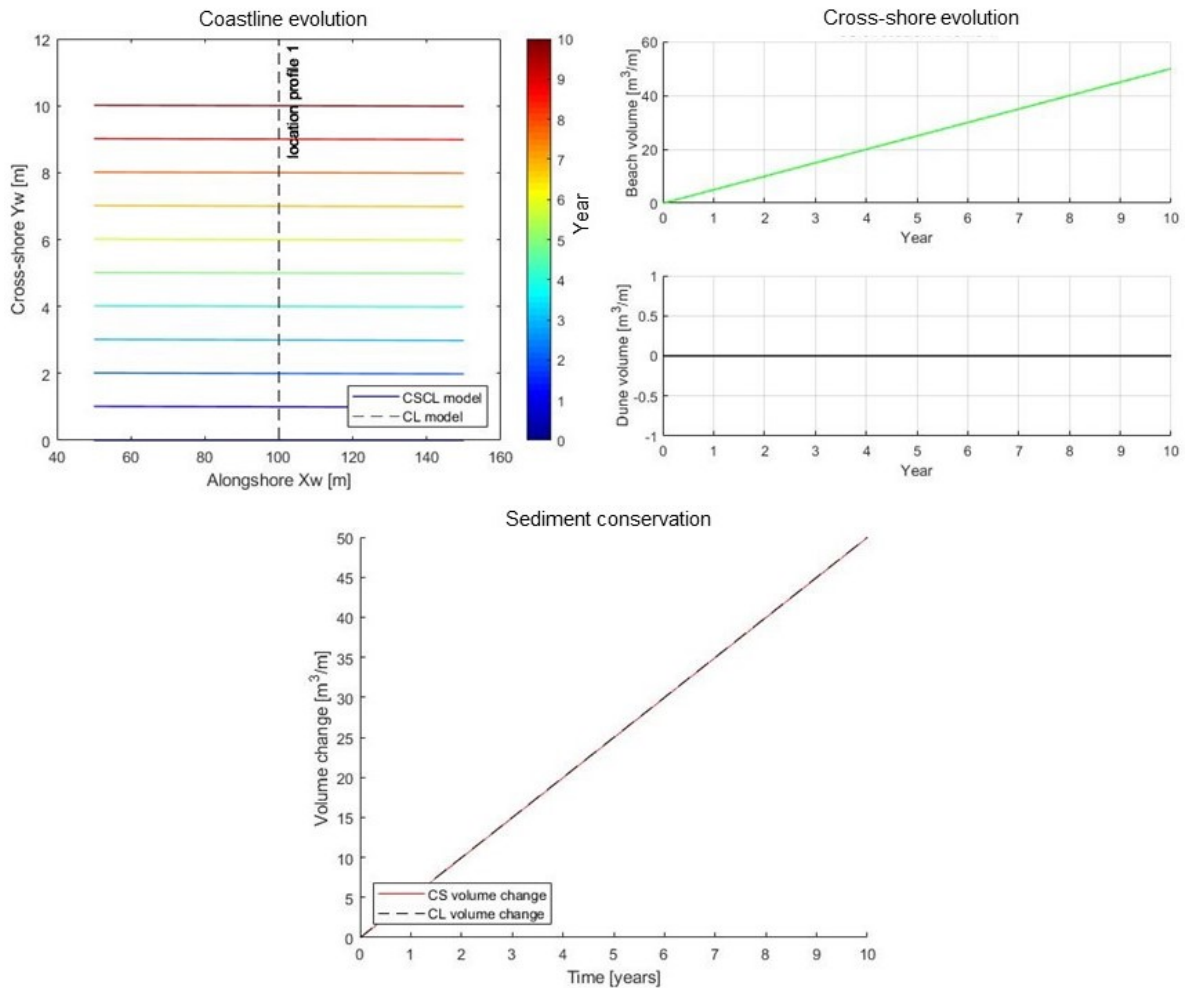
Figure 4.2: Results of test case 1: Coastline change, beach and dune volume change and total volume change in the CS- and CL-model component.

Test case 2: Simple case - Dune erosion

In this simple case with dune erosion, a high water level in the CS-model component causes the dunes to erode. The eroded dune volume is a source for the CL-model component. The theoretical sediment fluxes in this case are given in the Table 4.2.

It is shown in Figure 4.3 that the coastline change Δy after the simulation time is 50 m. The beach volume change ΔV_{beach} is found to be approximately 250 m³/m. In this second test case, the dune volume change ΔV_{dune} is -200 m³/m. The total volume changes ΔV_{CL} and ΔV_{CS} are equal to 250 m³/m and 50 m³/m respectively.

Simple case - Dune erosion		
Variable	Derivation	Value
ΔV_{CL}	$Q_{in} - Q_{out} + Q_{sources}$	250 m³/m
ΔV_{CS}	q_{LS}	50 m³/m
ΔV_{dune}		-200 m³/m
ΔV_{beach}	$\Delta V_{CS} - \Delta V_{dune}$	250 m³/m
Δy	$\Delta V_{CL}/h_0$	50 m

Table 4.2: Theoretical sediment fluxes in test case 2
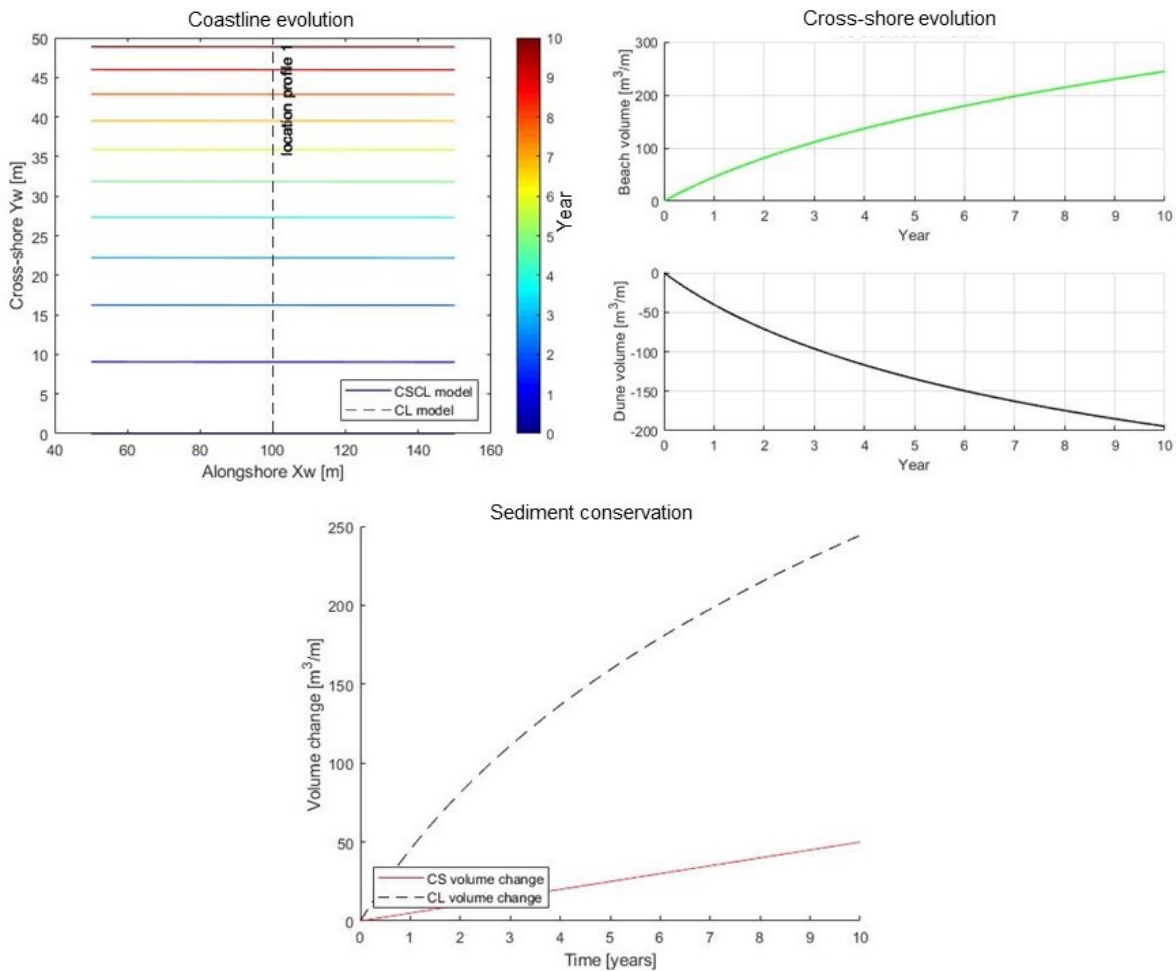
Figure 4.3: Results of test case 2: Coastline change, beach and dune volume change and total volume change in the CS- and CL-model component.

Test case 3: Simple case - Dune build-up

In this third simple case with dune build-up, wind causes the dunes to build up. Therefore, a continuous storm with a wind speed of 26 m/s is added to the simple case. The volume of sand added to the dune volume is eroded from the beach. The added dune volume is a sink for the CL-model component. The theoretical sediment fluxes in this case are given in Table 4.3.

Simple case - Dune build-up		
Variable	Derivation	Value
ΔV_{CL}	$Q_{in} - Q_{out} - Q_{sinks}$	20 m^3/m
ΔV_{CS}	q_{LS}	50 m^3/m
ΔV_{dune}		30 m^3/m
ΔV_{beach}	$\Delta V_{CS} - \Delta V_{dune}$	20 m^3/m
Δy	$\Delta V_{CL}/h_0$	4 m

Table 4.3: Theoretical sediment fluxes in test case 3

The resulting coastline change of the third test case can be found in Figure 4.4. The coastline change Δy after the simulation time is 4 m. The beach volume change ΔV_{beach} is found to be 20 m^3/m and the dune volume change ΔV_{dune} is 30 m^3/m. The total volume change in the CL-model component, ΔV_{CL}, is equal to 20 m^3/m and the volume change in the CS-model component, ΔV_{CS}, is equal to 50 m^3/m.
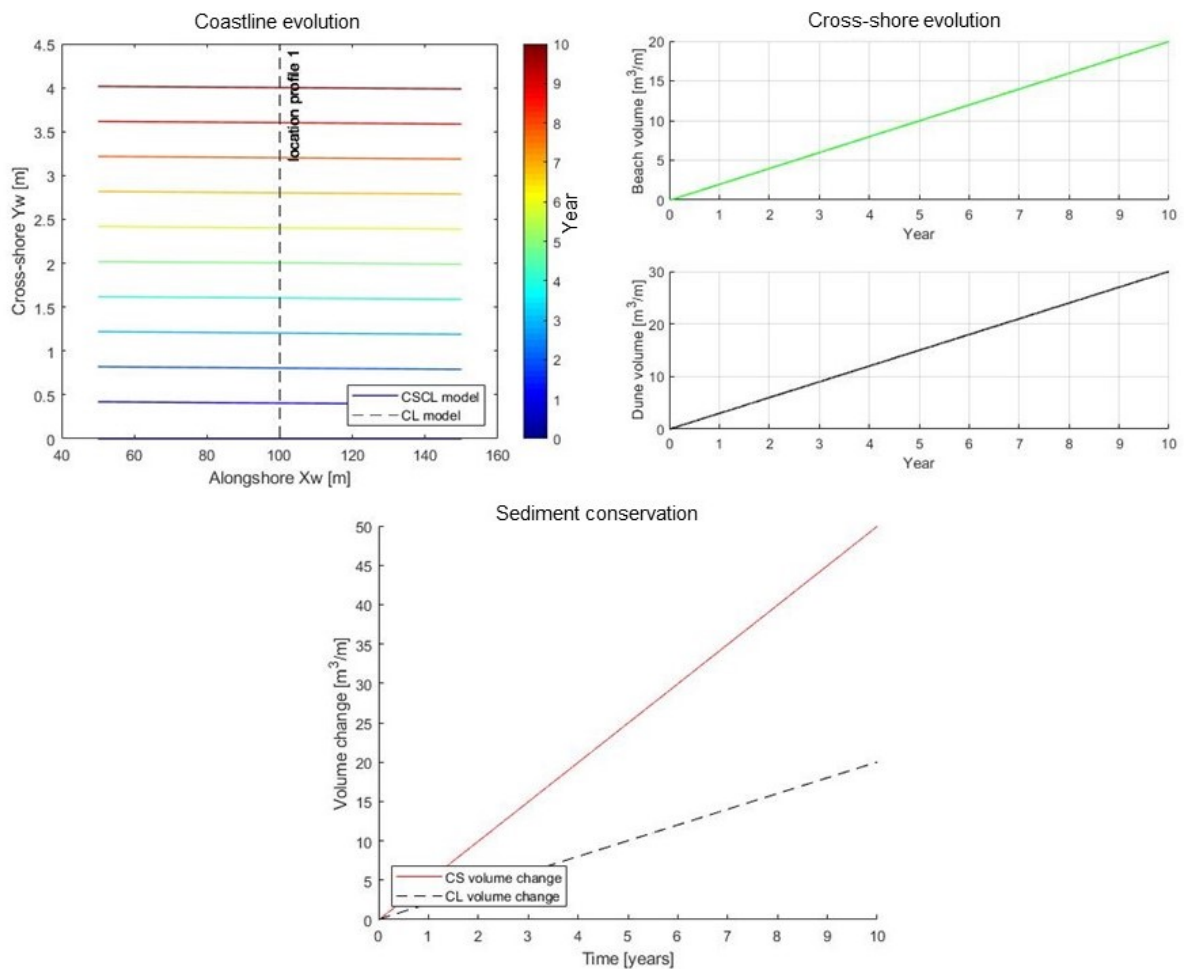
Figure 4.4: Results of test case 3: Coastline change, beach and dune volume change and total volume change in the CS- and CL-model component.

Test case 4: Simple case - Nourishment

In this fourth simple case with nourishment, there is a volume of 500 m^3/yr of sand added to the beach volume. There is no aeolian transport or dune erosion, thus the dunes are stable. The theoretical sediment fluxes in this case are given in Table 4.4.

Simple case - Nourishment		
Variable	Derivation	Value
ΔV_{CL}	$Q_{in} - Q_{out} + Q_{source}$	75 m³/m
ΔV_{CS}	$q_{LS} + q_N$	75 m³/m
ΔV_{dune}		0 m³/m
ΔV_{beach}	$\Delta V_{CS} - \Delta V_{dune}$	75 m³/m
Δy	$\Delta V_{CL}/h_0$	15 m

Table 4.4: Theoretical sediment fluxes in test case 4

The resulting coastline change of the fourth test case can be found in Figure 4.5. The coastline change Δy after the simulation time is 15 m. The beach volume change ΔV_{beach} is found to be 75 m³/m and there is no dune volume change. The total volume change in the CL-model component, ΔV_{CL}, and the volume change in the CS-model component, ΔV_{CS}, are both equal to 75 m³/m.
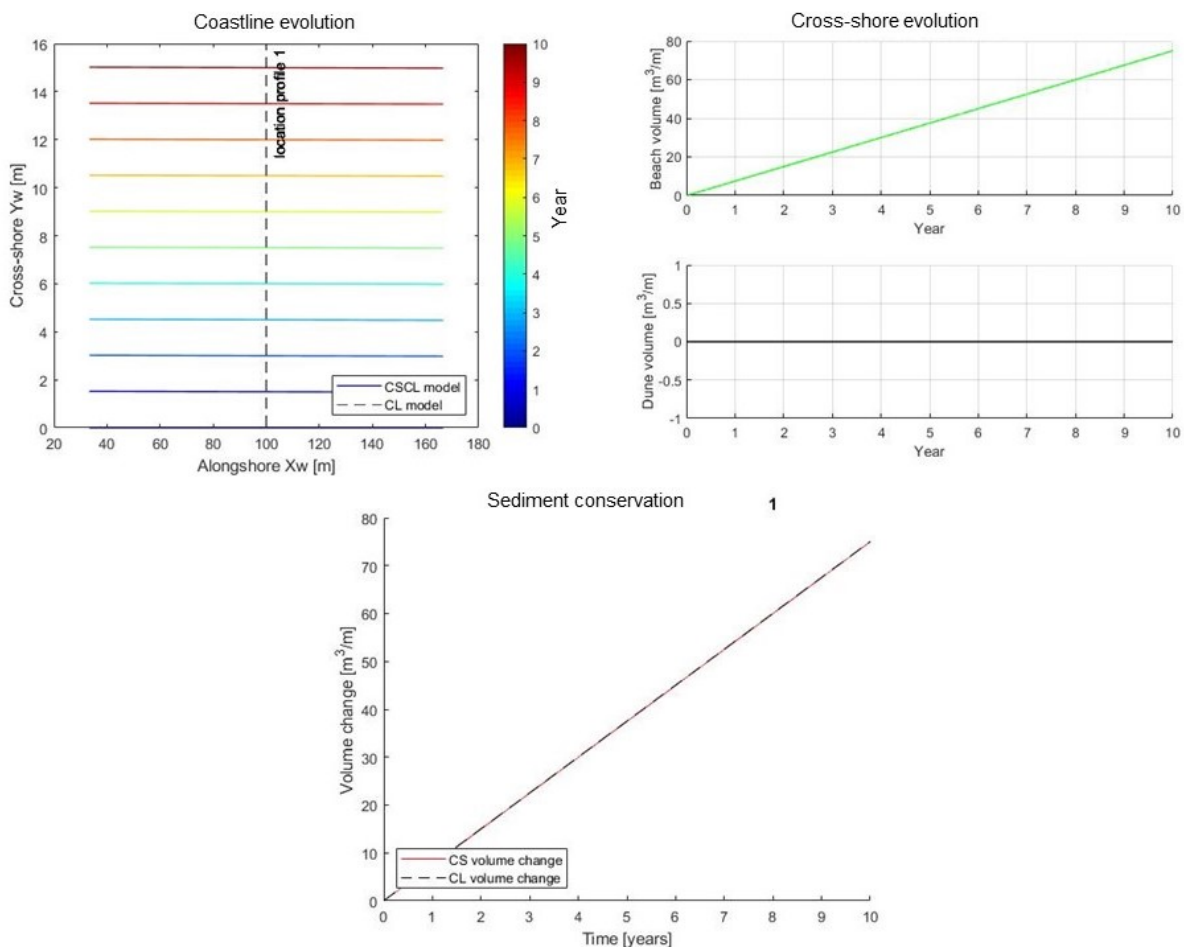
Figure 4.5: Results of test case 4: Coastline change, beach and dune volume change and total volume change in the CS- and CL-model component.

Test case 5: Simple case - Sea level rise

In this last simple case with sea level rise, the sea level rises with 1.2×10^{-10} m/s (equal to 3.78 mm/yr). As described in Section 3.4.4, the sediment transport resulting from sea level rise is a function of the width of the active profile $B_{Bruun,mod}$ (Bruun, 1962). This width is 200 m for this simple case. The theoretical sediment fluxes in this case are given in Table 4.5. The effect of sea level rise is determined by the CS-model component, which updates the sea level rise and corresponding changes to dune and

beach volume once per year to save computation time.

Simple case - Sea level rise		
Variable	Derivation	Value
ΔV_{CL}	$Q_{in} - Q_{out} - Q_{sink}$	42 m³/m
ΔV_{CS}	$q_{LS} - q_{SLR}$	35 m³/m
ΔV_{dune}		-7 m³/m
ΔV_{beach}	$\Delta V_{CS} - \Delta V_{dune}$	42 m³/m
Δy	$\Delta V_{CL}/h_0$	8.4 m

Table 4.5: Theoretical sediment fluxes in test case 5

The resulting coastline change of the fourth test case can be found in Figure 4.6. The coastline change Δy after the simulation time is 8.4 m. The beach volume change ΔV_{beach} is found to be 42 m³/m and there is a volume of 7 m³/m eroded from the dune. The total volume change in the CL-model component, ΔV_{CL}, equals 42 m³/m. The volume change in the CS-model component, ΔV_{CS}, is 35 m³/m.
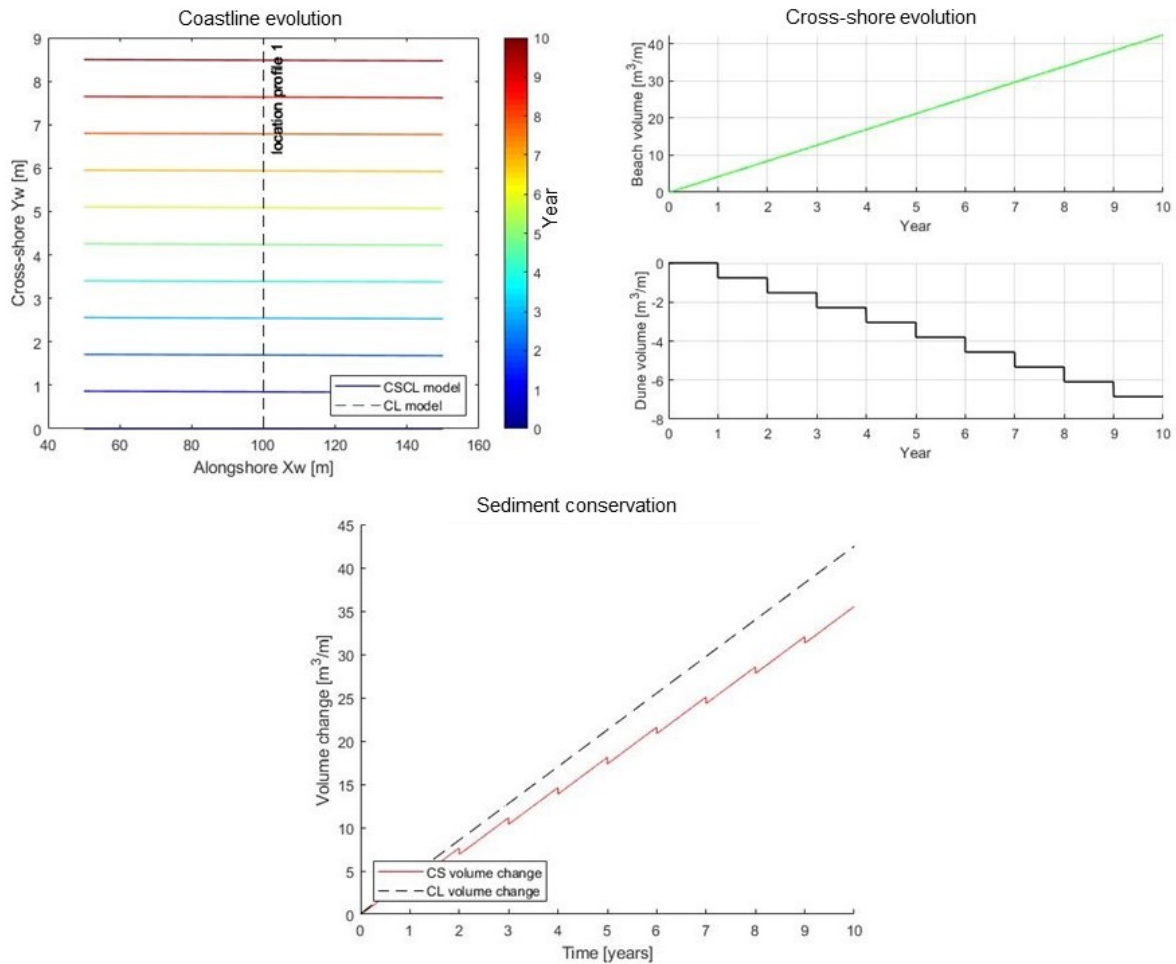
Figure 4.6: Results of test case 5: Coastline change, beach and dune volume change and total volume change in the CS- and CL-model component.

In this case with sea level rise, the dune volume changes in a stepwise pattern due to the fact that the sea level is updated once per year. If the coupled model is applied to a real case, this stepwise pattern will not dominate the dune and beach volume evolution, since other mechanisms such as dune erosion or dune build-up will take place on a smaller timescale. The effect of sea level rise will be further studied

in Section 4.3, in which the sediment conservation within a test case with sea level rise and multiple cross-shore profiles is considered.

4.3. Multiple profile test cases

To check whether the sediment is conserved when multiple cross-shore profiles are defined along the coastline, the coupled model is applied to more complicated test case. The aim of this second part of the model testing is to observe the evolution of the model accuracy for decreasing number of implemented cross-shore profiles. In these test cases, not only sediment conservation within the grid cell at the location of the cross-shore profile along the coastal stretch is checked, but the linear interpolation of the volume changes between the defined cross-shore profiles (as described in Section 3.5) is also investigated. The linear interpolation in case of longshore sediment transport and stable dunes and the difference between total volume change within the CS- and CL-model component is illustrated in Figures 4.7.
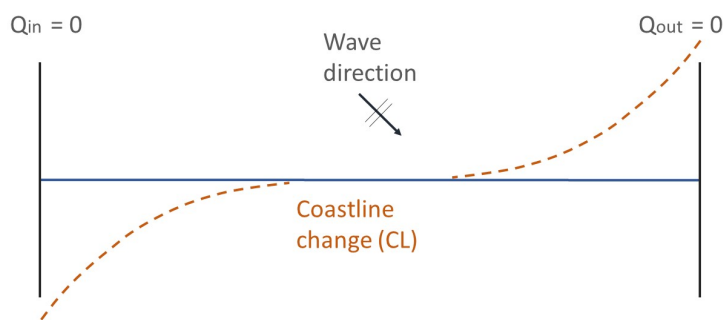
(a) Geometry of multiple profile test cases 6-10
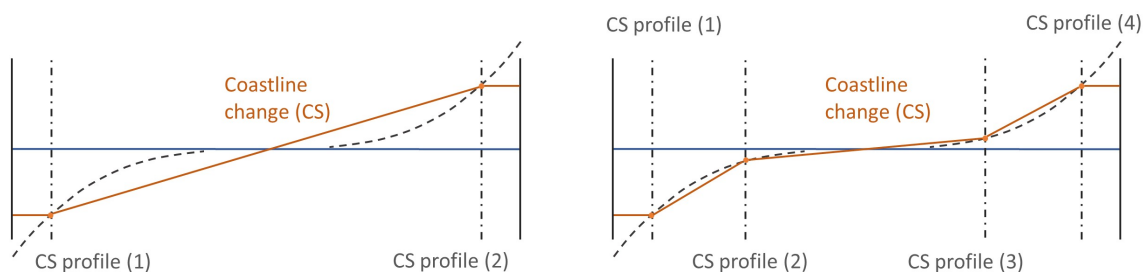
(b) Interpolation of volume change between two cross-shore profiles   (c) Interpolation of volume change between four cross-shore profiles

Figure 4.7: Description of the multiple profile test cases 6-10. The volumes are translated to coastline change for illustration purposes.

The base case for the multiple profile cases consists of two closed boundaries to ensure that sediment is not able to leave the considered coastal stretch at the longitudinal boundaries. The wave climate consists of one oblique incident wave with a wave height of 0.9 m, a period of 5.6 s and a direction of 355°(resulting in 5°obliqueness). Initially, there is no sea level rise or nourishment and the duration of the simulation is 20 years.

In all cases, different numbers of cross-shore profiles are located along the CL-coastline to enable the quantitative determination of the extent to which sediment is conserved within the coupled model. The coastline model consists of 26 grid cells, covering a coastal stretch of 8.4 km. There is a maximum of 26 cross-shore profiles defined in these multiple profile test cases. With 26 cross-shore profiles, there is a profile located in every grid cell along the coastline. This minimizes the deviations from sediment

conservation due to the interpolation between the model components, since the model components interact in every grid cell. However, the definition of a cross-shore profile within every grid cell along the coastal stretch requires a lot of data and computational time during simulation of larger scale problems. Therefore it is interesting to look into the development of the accuracy of the coupled model– defined to be the difference in theoretical and simulated total volume change – for a decreasing number of cross-shore profiles. Consequently, in the various multiple profile test cases the effect of the definition of 26, 14, 8 and 6 cross-shore profiles along the 8.4 km long coastline with 26 grid cells on the extent to which sediment is conserved and there with on the model accuracy is evaluated. The relation between the number of cross-shore profiles and the linear interpolation between these profiles is illustrated in Figure 4.7.

For every case, the sediment conservation within the coupled model is examined by comparing different volume changes. To make the results easier to interpret, the accuracy of the model components is translated to a Equivalent Coastline Accuracy (ECA) in mm and a Equivalent Sediment Flux Accuracy (ESFA) in %. The ECA is determined by dividing the surplus or deficit of sediment by the total coastline length of 8.4 km. The ECA therefore expresses how accurate the coastline evolution is predicted. This accuracy can be put into perspective by considering that the mean beach width along the Dutch coast is approximately 50 meters (Fryslān, Noord-Holland, Zeeland, & Zuid-Holland, 2011), thus an accuracy of the predicted coastline change of 5 mm is equal to a precision of 0.01%. For the ESFA, the surplus or deficit of sediment is divided by the total sediment flux, which is the sum of the absolute beach and absolute dune volume change for all profiles. Consequently, the ESFA expresses the accuracy of the prediction of the sediment fluxes. Since every case focuses on a single process, the ESFA expresses the accuracy of the prediction of a certain sediment transport process within the coupled model. The model accuracies are based on these academic cases and therefore not directly translatable to an accuracy in practical model applications. The ESFA and ECA of Test case 7, 8, 9 and 10 are estimated with respect to the accuracy of the coupled model in case of stable dunes thus only longshore sediment transport (Test case 6).

Test case 6: Multiple profile case - Stable dunes, longshore sediment transport
In this first case with multiple profiles, there is no wind. The mean water level is zero with respect to the dune foot height of 3 m, hence the water is not able to reach the dunes. Therefore, there will be no dune erosion or build-up, so the dunes will be stable. Since there is no beach-dune interaction in this case, the total amount of added and lost sediment within the coastal area should be equal and therefore theoretically there is no net change of total volume in both the CL- and CS-model components. In Table 4.6, the results of this case are shown.

Multiple profile case - Stable dunes				
	Total ΔV_{CS} in m^3	Total ΔV_{CL} in m^3	ESFA (CS) in %	ECA (CS) in mm
in theory / nr of prof.	0	0		
26	-1060	-18.6	-0.15	-25.32
14	-1780	-18.6	-0.25	-42.37
8	-3340	-18.6	-0.47	-79.56
6	-5170	-18.6	-0.73	-123.12

Table 4.6: Sediment fluxes in test case 6; total volume change in the CS-model component, total volume change in the CL-model component, Equivalent Sediment Flux Accuracy and Equivalent Coastline Accuracy

In the first column, the number of cross-shore profiles is given. Total volume changes within the CS- and CL-model component are given in cubic meters. The total volume change within the CL-model component is the summation of the volume change in all grid cells within the CL-model component over the simulation time. The total volume change in the CS-model component is defined to be the total beach and dune volume change over the simulation time, summed over all grid cells after interpolation. The previously described ESFA and ECA are defined for both model components. Because the ESFA and ECA of the CL-model component are stable, they are left out of the table.

Since the volume change in the CL-model component is constant, the ESFA of -0.0026% and the ECA of -0.44 mm of the CL-model component are constant as well. As showns in Table 4.6, the value for the ESFA and ECA of the CS-model component increases with the decreasing number of implemented cross-shore profiles, which means that the accuracy of the simulated volume changes decreases with the number of implemented cross-shore profiles. So the accuracy of the volume exchange between the model components depends on the number of interaction points in the coupled model. However, the sediment deficit in the sediment balance is negliglibly small and should be attributed to roundoff errors caused by the discretization of time and space. In order to confirm this assumption, extra model runs of the stable dune case were executed. Model runs with a doubled and tripled number of grid cells in the CL-model component shows that the ESFA and ECA decreases with more grid cells. In case of 52 grid cells, the total volume change in the CL-model component is 18 cubic meters, which is a small decrease. In case of 78 grid cells, however, the volume change is only 6 cubic meters.

Test case 7: Multiple profile case - Dune build-up
In this second case with multiple profiles, wind is added to the base case with only longshore sediment transport gradients. With a windspeed of 14 m/s, significant dune build-up takes place. As shown in Formula 3.13, the amount of aeolian transport that takes place depends on the amount of sediment available for aeolian transport. Because there is a longshore sediment transport gradient and the left part (0 - 4.2 km) of the coastal stretch under consideration is eroding, aeolian transport only takes place at the right part (4.2 - 8.4 km) of the coast. The wind erodes sediment from the beach and deposits it on the dunes, resulting in a sediment sink in the CL-model component. Therefore, there is sediment loss in the CL-model component. However, the total amount of sediment lost in the CL-model component should equal the amount of volume added to the dunes in the CS-model component. The difference between the total volume change of the dunes and the total volume change within the CL-model component are therefore compared in this case, as shown in Table 4.7.

Multiple profile case - Dune build-up							
	Total ΔV_{dune} in m^3	Total ΔV_{CS} in m^3	Total ΔV_{CL} in m^3	ESFA (CS) in %	ECA (CS) in mm	ESFA (CL) in %	ECA (CL) in mm
in theory / nr of prof.		0	-ΔV_{dune}				
26	121910	-1135	-121920	-0.01	-1.70	0.0012	0.20
14	123100	-1861	-123070	-0.01	-1.94	0.0065	1.16
8	128940	-6752	-128960	-0.46	-81.20	-0.0002	-0.03
6	138910	-17454	-138920	-1.65	-292.46	0.0012	0.20

Table 4.7: Sediment fluxes in test case 7; total dune volume change, total volume change in the CS-model component, total volume change in the CL-model component, Equivalent Sediment Flux Accuracy of the CS-model component, Equivalent Coastline Accuracy of the CS-model component, Equivalent Sediment Flux Accuracy of the CL-model component and the Equivalent Coastline Accuracy of the CL-model component

For the calculation of the ESFA and ECA, the ESFA and ECA of Test case 6 with stable dunes is subtracted. The ESFA and ECA can thus be attributed solely to the dune build-up. The accuracy of the CL-model component is determined by the difference between the by the CS-model component determined accreted dune volume and the loss of sediment in the CL-model component. In this case, the accuracy of the coupled model is determined by the deviations from sediment conservation in both model component. Since the total volume change within the CS-model component should equal 0, all surplus or deficit of sediment in the CS-model component is attributed to the inaccuracy of the coupled model.

The ESFA and ECA of the CS-model component, shown in Table 4.7, are small for the cases with 26 and 14 profiles compared to the ESFA and ECA of the CS-model component in Test case 6 (shown in Table 4.6). So, in these cases the deviation from the sediment balance between the model components due to interpolation of the dune build-up is smaller than the inaccuracy due to interpolation of the erosion and accretion of the beach volume caused by the longshore sediment transport gradient. Furthermore, it is shown in Table 4.7 that the accuracy of the CL-model component does not change significantly with the decreasing number of inserted profiles, and therefore the inaccuracy of the determination of the sediment sink in the CL-model component due to dune build-up in the CS-model component, are expected to be caused by roundoff errors in the discretization of time and space.

Test case 8: Multiple profile case - Dune erosion
In the third case with multiple profiles, dune erosion due to a higher water level and its effect on the sediment conservation within the coupled model is tested. The water level is 1.5 m and the wind speed is zero is this case. When the dunes erode in a collision regime (see Figure 2.5), the eroded sediment is deposited on the beach. Therefore, the eroded volume is a source for the CL-model component. Since the added volume of sediment cannot leave the coastal area under consideration due to the closed boundaries, the total beach volume change and therewith the total sediment source in the CL-model component is equal to the amount of sediment eroded from the dunes. Because there is only an exchange of sediment between the beach and dune volume in this case, the total volume change in CS-model component (that theoretically equals zero) with respect to the total sediment flux expresses the accuracy of the CS-model component. For the CL-model component, the accuracy is defined by the difference between the eroded dune volume in the CS-model component and the volume of sediment added to the CL-model component.

Multiple profile case - Dune erosion					
	Total ΔV_{dune} in m^3	Total ΔV_{CS} in m^3	Total ΔV_{CL} in m^3	ESFA (CS) in %	ECA (CS) in mm
in theory / nr of prof.		0	$-\Delta V_{dune}$		
26	-1018200	-955	1018200	0.00	1.62
14	-1018300	-1674	1018300	0.01	2.52
8	-1018600	-3188	1018600	0.01	3.64
6	-1019000	-5002	1019000	0.01	4.02

Table 4.8: Sediment fluxes in test case 8; total dune volume change, total volume change in the CS-model component, total volume change in the CL-model component, Equivalent Sediment Flux Accuracy of the CS-model component and Equivalent Coastline Accuracy of the CS-model component

The ESFA and ECA of the CS-model component are shown in Table 4.8. These deviations from sediment conservation are small compared to the ESFA and ECA of both previous cases with multiple profiles, the ones with stable dunes and dune build-up shown in Table 4.6 and 4.7. Furthermore, the

accuracy of the coupled model hardly improves with the increasing number of cross-shore profiles. So, dune erosion results in a significantly small deviations from the sediment balance within the coupled model. The ESFA and the ECA is of the CL-model component are both equal to zero. All sediment that is eroded from the dunes is added to the CL-model component as a sediment source.

Test case 9: Multiple profile case - Nourishment

For this fourth case with multiple profiles, a volume of 211750 m^3 of sediment is added as nourishment in the CL-model component. This volume is directly added to the beach volume in the CS-model component, since there is no wind in this case. Therefore, the difference between the volume change in the CL-model component and the CS-model component expresses the accuracy of the response of the coupled model to a nourishment in this case.

Multiple profile case - Nourishment				
	Total ΔV_{CS} in m^3	Total ΔV_{CL} in m^3	ESFA (CS) in %	ECA (CS) in mm
in theory / nr of prof.	$= V_N = 211750$	211750		
26	210660	211740	0.00	-0.64
14	209900	211740	-0.01	-1.68
8	209040	211740	0.09	15.04
6	208750	211740	0.30	51.69

Table 4.9: Sediment fluxes in test case 9; total volume change in the CS-model component, total volume change in the CL-model component, Equivalent Sediment Flux Accuracy of the CS-model component and Equivalent Coastline Accuracy of the CS-model component

The ESFA and ECA shown in Table 4.9 are small for the cases with 26 and 14 profiles. Since the accuracy of the coupled model regarding the simulation of the response to nourishments is determined relative to the model accuracy in case of stable dunes, the ESFA and ECA for these cases is negative. However, the accuracy decreases when a lower number of cross-shore profiles is defined. The deviation from sediment conservation is, however, relatively small compared to the inaccuracy in the simulation of dune build-up. So, the implementation of a nourishment results in small deviations from sediment conservation within the sediment balance of the coupled model.

Test case 10: Multiple profile case - Sea level rise

For the last case with multiple profiles, the effect of sea level rise is taken into account. The sea level rises with a speed of 1.2×10^{-10} m/s (equal to 3.78 mm/yr), which is similar to the sea level rise in test case 5. Since the length of the simulation is 20 years and the width of the active profile as defined by Bruun (see Section 3.4.4) is 700 m, the total volume change along the 8.4 km long coastline theoretically equals 407918 m^3. Sea level rise is covered by the CS-model component and it results in both dune and beach erosion. It is directly translated to a beach and dune erosion within the CS-model component, so therefore only the accuracy of the simulated sediment sink within the CL-model component is examined.

Multiple profile case - Sea level rise				
	Total ΔV_{SLR} in m^3	Total ΔV_{CL} in m^3	ESFA (CL) in %	ECA (CL) in mm
in theory nr of prof.	$= -V_{SLR}$ =-407918	-407918		
26	-407918	-408080	-0.0183	-3.42
14	-407918	-408060	-0.0157	-2.94
8	-407918	-408060	-0.0157	-2.94
6	-407918	-408060	-0.0157	-2.94

Table 4.10: Sediment fluxes in test case 10; total volume change due to sea level rise, total volume change in the CL-model component, Equivalent Sediment Flux Accuracy of the CL-model component and the Equivalent Coastline Accuracy of the CL-model component

The ESFA and ECA of the CL-model component for the cases with 14, 8 and 6 profiles are the same and therefore it is likely that the inaccuracy of the determination of the sediment sink in the CL-model component due to sea level rise is caused by roundoff errors in the discretization of time and space. It is, however, recommended to decrease the interval between the timesteps on which the beach and dune volume changes due to sea level rise are updated within the CS-model component in order to minimize these roundoff errors.

4.4. Conclusions of model testing

The coupled model is tested by analyzing the conservation of sediment within the sediment balance of the coupled model. Every individual sediment transport process included in the model is studied, using academic cases that focus on a single sediment transport process. The sediment balance of the coupled model consists of seven sediment fluxes. In the CS-model component, these fluxes are the sediment transport due to gradients in the longshore sediment transport, sediment transport caused by nourishments and sediment transport as a response to sea level rise. In the CL-model component, there is sediment transport at the upstream and downstream boundary of the considered coastal area, and there are sources and sinks of sediment.

In the previous sections, it was tested whether these sediment fluxes are balanced in the coupled model. This was done by defining five different test cases for two different set-ups. Cases with stable dunes and longshore sediment transport, dune erosion, dune build-up, a nourishment and sea level rise were tested. The first set-up tested if these fluxes result in conservation of sediment in case of the definition of only two grid cells within the CL-model component and a single cross-shore profile in the CS-model component. The second set-up consisted of 26, 14, 8 and 6 cross-shore profiles which were defined along a 8.4 km long coastline divided into 26 grid cells.

In case of one cross-shore profile and two-grid cells, all test cases demonstrate sediment conservation, as shown in the results of the simple test cases in Section 4.2. This means that overall, implementation of the different longshore and cross-shore sediment transport equations and their interaction in the coupled model is done correctly. The different sediment fluxes within the coupled model are balanced and no deviations from sediment conservation occurred in the interaction between the model components.

Overview: ESFA of all transport processes				
	ESFA (CS) min	ESFA (CS) 1 prof./km	ESFA (CL) min	ESFA (CL) 1 prof./km
	in %	in %	in %	in %
longshore sediment transport	0.73	0.47	0.0026	0.0026
dune build-up	1.65	0.46	0.0065	0.0002
dune erosion	0.01	0.01	-	-
nourishments	0.3	0.09	-	-
sea level rise	-	-	0.0183	0.0157

Table 4.11: Simulated Equivalent Sediment Flux Accuracy of all processes included in the coupled model, derived for both model components. Split into the minimum Equivalent Sediment Flux Accuracy and the Equivalent Sediment Flux Accuracy in case one cross-shore profile is defined for every kilometer of coastline that is simulated.

For the more complex cases, with multiple profiles along a 8.4 kilometer long coastline, the results of the model testing are translated into Equivalent Sediment Flux Accuracy (ESFA) and Equivalent Coastline Accuracy (ECA). For every case, the effect of one of the in the coupled model included sediment transport processes on the simulated sediment balance is evaluated. Therefore, the accuracy of all the included transport processes is determined and expressed in the ESFA and ECA value of the transport process. For some processes, both model components impose inaccuracies on the simulated sediment balance. An overview of the ESFA values resulting from the model testing can be found in Table 4.11 and an overview of the ECA values can be found in 4.12.

The results of the test cases 6–10 show that the implementation of multiple cross-shore profiles along the coastline induce inaccuracy in the CL-model component that do not depend on the number and location of the cross-shore profiles. Because of this independence, it is likely that this sediment deficit of 19 m^3 is caused by roundoff errors in the discretization of time and space. The accuracy of the CS-model component increases with the number of implemented cross-shore profiles. Presumably, the difference between the simulated coastline change and beach volume change is related to the linear interpolation of the longshore sediment transport gradients for the grid cells located between the defined profiles. This phenomenon is illustrated in Figure 4.7. Translating the accuracy of the coupled model in case of longshore sediment transport gradients to a minimum Equivalent Sediment Flux Accuracy of 0.73 % and a Equivalent Coastline Accuracy of -12 cm puts these deviations within the sediment balance in perspective. The coastline evolution is theoretically predicted with an accuracy of 8 cm in case of the definition of one cross-shore profile for every kilometer of coastline simulated. Therefore, it can be concluded that the accuracy of the modeled sediment fluxes related to longshore sediment transport gradients in the coupled model is sufficient.

The process of dune build-up as a result of aeolian transport, results in inaccuracies in both model components. The accuracy of both model components increases with the number of implemented cross-shore profiles. The accuracy of the CS-model, which is determined by the difference between the volume of sediment added to the dunes and the volume of sediment eroded from the beach, rises to a minimum of 1.65 % of the sediment flux. Initially, the deviation from the sediment balance in case of aeolian transport and longshore sediment transport was considered to be caused by a time lag of erosion and deposition of the sediment. Therefore, it was decided to let the aeolian transport only occur during the first 10 years of the simulation period of 20 years. The model accuracy did not change significantly. The inaccuracy of the CS-model component in case of aeolian transport is therefore likely related to the linear interpolation of the volume exchange (as illustrated in Figure 4.7) within the coupled model. Since the aeolian transport is depending on sediment availability thus longshore sediment transport gradients and these are not linear along the coast. Consequently, the linear in-

terpolation of volume changes between defined cross-shore profiles causes an extra deviation of the sediment balance in case of aeolian transport. This means, that in case of strong aeolian transport and strong longshore sediment transport gradients, it is recommended to enlarge the number of defined cross-shore profiles per kilometer of coastline. With a theoretical coastline prediction accuracy of 8 cm in case of one profile per kilometer coastline and a minimum Equivalent Sediment Flux Accuracy of 1.65 %, the accuracy of the simulated sediment fluxes related to aeolian transport is concluded to be sufficient.

When sediment is eroded from the dunes and deposited on the beach, there is no difference between the simulated volume changes in the CL- and CS-model component. Thus, there is no deviation in the sediment exchange between the model components. However, there is a small inaccuracy within the CS-model component. The volume of sand eroded from the dunes is not fully added to the beach volume of the CS-model component but it is fully added to the CL-model component as a sediment source. Because there is no difference in simulated volume changes between the model components, the inaccuracy of the CS-model component is fully attributed to the linear interpolation in the integration of the sediment fluxes. With a minimum ESFA of 0.01 % and and minimum ECA of 4 mm, the sediment fluxes related to dune erosion are considered to be modeled in accordance with the sediment balance.

A nourishment implemented in the CL-model component results in a small difference between the volume of sand added to the CL-model component and the volume of sand added to the CS-model component. Again, with a decreasing number of cross-shore profiles defined along the coastline, the difference between the linear interpolated volume changes at the points between the cross-shore profiles and the actual volume change increases. The minimum Equivalent Sediment Flux Accuracy is 0.3% and the minimum Equivalent Coastline Accuracy is 5 cm. These accuracies increase with the number of defined cross-shore profiles along the coast. It is concluded that the sediment fluxes are simulated sufficiently accurate, with an ESFA of 0.09 % and an ECA of 2 cm in case of the definition of one cross-shore profile along every kilometer of coastline, though it is recommended to define a large number of cross-shore profiles at potentially dynamic locations along the coastline.

Overview: ECA of all transport processes				
	ECA (CS) min in mm	ECA (CS) 1 prof./km in mm	ECA (CL) min in mm	ECA (CL) 1 prof./km in mm
longshore sediment transport	123.12	79.56	0.44	0.44
dune build-up	292.46	81.20	1.16	0.03
dune erosion	4.02	3.64	-	-
nourishments	51.69	15.04	-	-
sea level rise	-	-	3.42	2.94

Table 4.12: Simulated Equivalent Coastline Accuracy of all processes included in the coupled model, derived for both model components. Split into the minimum Equivalent Coastline Accuracy and the Equivalent Coastline Accuracy in case one cross-shore profile is defined for every kilometer of coastline that is simulated.

Finally, sea level rise and the sediment transport that results from it, are considered in the last test case. Because the ECA and the ESFA of the CL-model component are small, it is concluded that there is no significant sediment deficit between the model components. With an ESFA of -0.02 % and and ECA of 3 mm in case of one cross-shore profile for every kilometer of coastline, the sediment fluxes related to sea level rise are considered to be modeled in accordance with the sediment balance.

Therewith, all sediment fluxes included in the coupled model are considered to be modeled in accordance with the sediment balance. The minimum Equivalent Sediment Flux Accuracy is found to be 1.65 % , the minimum Equivalent Coastline Accuracy is 29 cm and for these model accuracies the simulation of the effect dune build-up is normative. Improvement of the precision of the model should be aimed at the number format within the coupled model and clear guidelines in the number of cross-shore profiles to be defined. In case one cross-shore profile is defined along every kilometer of coastline, the Equivalent Sediment Flux Accuracy increases to 0.47% and the Equivalent Coastline Accuracy to 8 cm.

At last, it is important to take into account that these simplified academic cases designed to test sediment conservation within the coupled model, do not represent reality. If the coupled model is applied to simulate coastal behaviour of a real case, model accuracy is highly dependent on the input data and consequently the precision of the determination of the coastline position or sediment fluxes mentioned in this section are not normative.

<div style="text-align: right;">

5

</div>

Model application

This chapter describes the model application. The coupled model is used to hindcast the dune and coastline evolution along the IJmuiden coast. The specifics of the case are described in Section 5.1. Then the model calibration is discussed in Section 5.2. The results of the IJmuiden hindcast are described and depicted in Section 5.2.7. After this, the model is validated in Section 5.3. Conclusions on the model performances on the IJmuiden case is described in Section 5.4.

5.1. IJmuiden case

The North Sea Canal is a ship canal from Amsterdam to the North Sea, constructed between 1865 and 1876 to enable seafaring vessels to reach the port of Amsterdam. A small set of locks were built at the mouth of the North Sea Canal and at that location, the new town of IJmuiden formed (Figure 5.1). IJmuiden Harbour is located in the middle of the Holland coast and the Kennemer dunes are located south of IJmuiden Harbour. In 1965, the northern jetty of the harbour was extended to a length of 2 km and the southern jetty to 2.5 km (Luijendijk, De Vroeg, Swinkels, & Walstra, 2011). These extensions induce significant accretion at the southern jetty resulting in erosion of the adjacent coast further south (Van Rijn, 1997). Because of this erosion, several nourishment projects have taken place at this part of the coast.

Figure 5.1: Aerial photograph of IJmuiden Harbour, picture by Rob van Zeist

The evolution of the Kennemer dunes and beaches have previously been studied using the CS-model

(Hallin, Huisman, et al., 2019). For this study, a 22-year long data set, from 1994 to 2016, with topographic and bathymetric data from JARKUS (Rijkswaterstaat, 2017), in combination with wind, water level, and deep-water wave observations were available. The dataset and therefore the simulation consists of 26 cross-shore profiles along 2 km of the coastline south of the Port of IJmuiden. The results of this previous study demonstrated that longshore transport gradients are a crucial factor for long-term dune evolution at the Kennemer Dunes (Hallin, Huisman, et al., 2019). In beach profiles with long-term erosion, nourishments were found to have a significant impact on dune evolution through supplying sediment for aeolian transport. The aeolian transport increased after the nourishments, both in simulations and observations, which is in agreement with previous observations along the Dutch coast (Bakker, van Heteren, Vonhögen, van der Spek, & Van der Valk, 2012). Because of the importance of the longshore transport gradients, the present simulation and case study of the IJmuiden coast is performed using the coupled model. The simulation will be compared with both the previous simulations and the available bathymetric data. The coupled model is able to include the temporal and spatial varying longshore sediment transport rates instead of a fixed prescribed longshore sediment transport gradients at every profile as is the case in the CS-model component.

Because the coupled model consists of two model components that both attribute to uncertainties and errors in the predicted coastline and coastal profile evolution, it is expected that the coupled model will predict the volumetric evolution of beaches and dunes less accurate than the CS-model. However, the coupled model enables the prediction of the decadal to centenial scale evolution of the coastal zone with the need of less input data when compared to the CS-model. Furthermore, it includes the longshore spreading of nourishments, which is expected to have a positive effect on the model performance. For the present study, the same JARKUS-dataset in combination with wind, water level, and deep-water wave observations is used, because it improves the comparability of the studies. Additionally, the prediction of the simulated coastline position is studied, since the CL-model component enables the prediction of the large-scale coastline evolution. It is expected that the coupled model will predict the coastline evolution more accurate than the CL-model, because of the positive effect of the inclusion of cross-shore sediment transport processes on the simulated coastline evolution. In order to evaluate the predicted coastline evolution, the simulations are compared with MKL-data. The MKL, which is a Dutch abbreviation for the *momentane kustlijn*, is a common definition of the coastline position and can be translated to the instantaneous coastline. The instantaneous coastline depends on both the horizontal and vertical position of the mean low water level and dunefoot height and is determined annually.
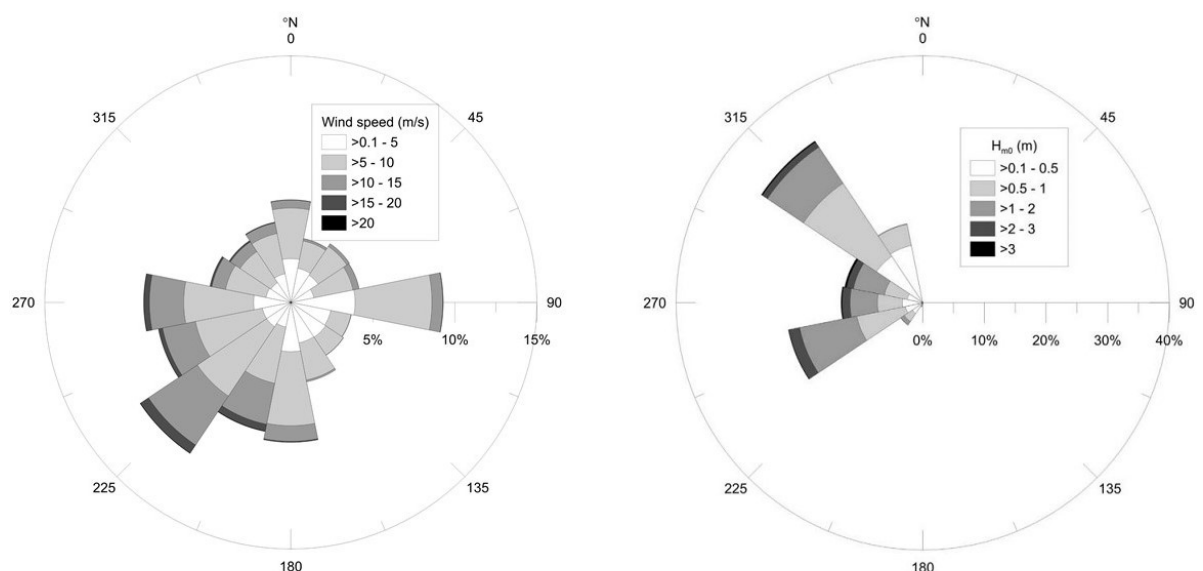
Figure 5.2: Wind and wave climate of the IJmuiden case: Left the wind rose from IJmuiden harbour at 52.462°N, 4.555°E and right the wave rose of the hindcasted significant wave height at 8m depth at the IJmuiden coast (Hallin, Huisman, Larson, Walstra, & Hanson, 2019)

5.1.1. Characteristics of the IJmuiden coast

As previously described in Section 2.3, the average tidal range is about 1.6 m with a maximum of 1.9 m (Wijnberg, 2002). The mean low water level is abstracted from the dataset and found to be -0.8 m relative to MSL. Storm surges occur during the winter and the corresponding highest observed still water level (SWL) within the time series was +3.06 m relative to MSL at 11/9/2007. The wind climate is dominated by winds from SSW to W. The wind data, deep-water significant wave height, wave period and wave direction were used to simulate the nearshore wave climate at 8 m depth using the SWAN wave model (Booij, Ris, & Holthuijsen, 1999). The simulated wave climate is dominated by waves from WSW to WNW, as shown in Figure 5.2. The average wave height during the simulation period is 0.8 m and the maximum wave height is 3.3 m. The average peak wave period is 4.6 s and the peak period is 14 s.

Along the IJmuiden coast, there are temporary buildings (i.e. beach houses) that are placed during summer and removed during winter time. These buildings can be found in the profiles 1–3, 13–15, and 18–26 where they limit dune accretion during summer time. After the winter, the foredunes in these profiles are moulded into terraces before placement of multiple rows of beach houses.
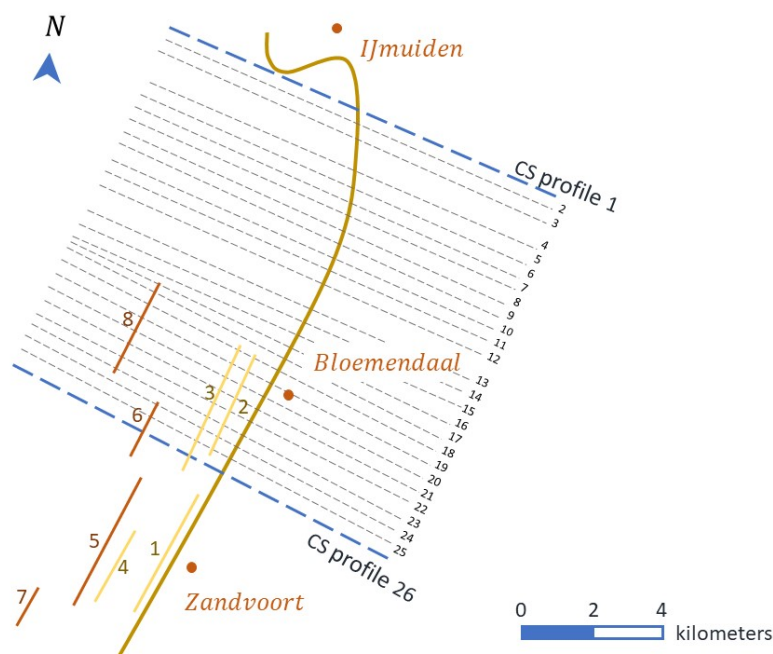
Figure 5.3: IJmuiden case overview, including the location of cross-shore profiles and nourishments.

The dune shape and beach width vary significantly alongshore. Beach widths are largest in the northern profiles and decrease in the southward direction. The wider beaches in the northern profiles are the result of the blockage of longshore sediment transport by the jetties of the Port of IJmuiden. The southern profiles (18–26) have a negative sediment budget excluding nourishments and would therefore be eroding. However, due to the nourishments these profiles are stable.

The nourishments along the IJmuiden coast are described in Table in 5.1. The volume of sediment added to the beach during beach nourishments is directly translated to a sediment source at the beach. The sediment transport rates due to the shoreface nourishments are mainly based on the transport rates found for these particular nourishments by Huisman et al. (2019). For the nourishments not studied in this research, the average decay rate of 34 m^3/m/yr is applied to the shoreface nourishments (Huisman et al., 2019). This results in the duration of the nourishments shown in Table 5.1. The location of these nourishments are depicted in Figure 5.3.

nr.	Location	Date	Total volume in Mm^3	Type of nourishment	Duration in years
		IJmuiden case - Nourishments			
1.	Zandvoort	May '94	0.334	Beach	-
2.	Bloemendaal / Zandvoort	Sep '98	0.193	Beach	-
3.	Bloemendaal	May '01	0.604	Beach	-
4.	Zandvoort	May '01	0.248	Beach	-
5.	Zandvoort-Zuid	Oct '04	1.001	Shoreface	14.72
6.	Zandvoort-Noord	Nov '04	1.202	Shoreface	11.78
7.	Zandvoort-Zuid	Jun '08	0.510	Shoreface	9.11
8.	Bloemendaal	Jun '08	1.003	Shoreface	11.27

Table 5.1: Characteristics of nourishment at the IJmuiden coast between 1994 and 2016 (van Verkeer en Waterstaat, 2021), the number given to the nourishments is used to depict the nourishment location in Figure 5.3.

The measured volume changes of the beaches and dunes are derived from the JARKUS-data and can be found in Figure A.1 in the Appendix. The dunes in the northernmost profiles closest to the harbour jetty are low (with a height of 4 meters) and grow significantly in height during the study period. These dunes are part of a new dune row formed in front of the recreational lake Kennemermeer, which is created after excavations for the construction of a row of dunes along the high tide line to protect the nature reserve. The other profiles are part of one coherent dune landscape with an elevation of about 20 m above MSL. Profiles 4–-12, which do not have temporary buildings in front of them, show fast accretion rates in the foredunes. Profiles 4, 5 and 6 grow at slightly lower rates than the adjacent profiles, which could be related to an opening in the dunes between profiles 3 and 4 functioning as a sediment sink.

The observed coastline evolution is derived from the MKL-data. The coastline evolution is shown in Figure A.3 and the coastline evolution at the location of every cross-shore profile along the IJmuiden coastline is depicted in Figure A.2. As shown in these observations, the northernmost three profiles 1 – 3 located close to the harbour jetties, show almost linear coastline accretion. In profile 4 and 5, the coastline initially erodes and and after 1996 it starts accreting. The coastline first accretes fast in profiles 6 – 11, after which is shows some slower accretion. In the southern profiles 12–26, the coastline evolution shows alternating periods of accretion and erosion.

During the previous study of the IJmuiden case, the yearly fluctuations of the MLW position are found to be greater than the variations of the dune foot position, due to cyclic evolution of the sub-tidal sandbars (Hallin, Larson, & Hanson, 2019). Furthermore, a 4-year periodic cycle in the beach volume evolution is observed. This inter-annual pattern of beach volume erosion and accretion is caused by exchange of sediment between the beach and the bar as a result of the wave forcing. This cycle is strongest for the period before 2004, presumably because after 2004 the exchange of sediment between the dry beach and the subaqueous part of the profile is interrupted by the onshore migration of shoreface nourishments which are placed between profiles 16–26 (See Figures 5.4, 5.5 and Appendix A.3).

The measured dune volume evolution (See Figures 5.4, 5.5 and Appendix A.3) does not show any response to both these cyclic variations. The previous results of the simulation of the IJmuiden case by the CS-model shows the yearly fluctuations in beach volume evolution. These fluctuations are wave-driven and the process of beach-bar exchange included in the CS-model simulates this behaviour accurate. However, the 4-year periodic exchange of sediment between the bar and the beach has been found to be independent of variations in the wave forcing at this site (Wijnberg, 2002) and is therefore not found in the results of the CS-model simulation. In the coupled model, both the yearly fluctuations and the 4-year periodic exchange of sediment cannot be simulated due to the fact that the process of beach-bar exchange is excluded from the coupled model, as described in Section 3.4.3. However, the previous CS-model simulation of the IJmuiden case excluding beach-bar exchange confirmed the

findings of Guillén, Stive, and Capobianco (1999) stating that the bar cycling process does not affect the decadal-scale dune evolution in the study area.
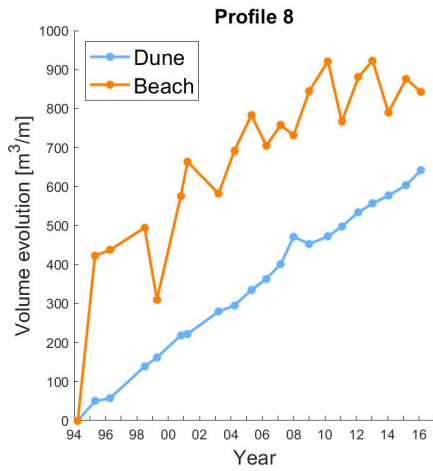
Figure 5.4: Observed beach and dune volume change between 1994 and 2010 in cross-shore profile 8
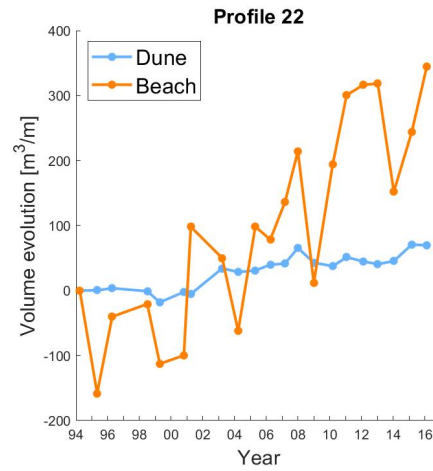
Figure 5.5: Observed beach and dune volume change between 1994 and 2010 in cross-shore profile 22

Because the coupled model is unable to simulate both these cyclic variations that dominate the observed beach volume evolution, the focus of the model results and the evaluation of the model performance is focused on the prediction of the dune volume evolution and the coastline evolution.

5.2. Model calibration

The behaviour of the IJmuiden coast is simulated and calibrated for the period 03/29/1994 – 03/11/2010. During the calibration of the coupled model, several different studies are being conducted. Wave climate schematization and implementation, effects of tide and wind, cross-shore processes, the calibration of empirical coefficients and the effect of the longshore sediment transport gradients are discussed in this section. Thereafter, the results of the model calibration and the hindcast of the IJmuiden case are presented.

5.2.1. Wave characteristics

The CL-model component requires the user to define the wave characterics, which can be implemented as a static wave climate or a time-varying series of wave conditions. Therefore, it is possible to implement static or time-varying forcing within the coastline model.

The waves are measured at regular intervals of 3 hours, resulting in a 22-year long dataset of 63960 wave conditions. In case of the implementation of a wave climate, the variability of the full set of wave-data is schematized in approximately 100 characteristic wave conditions. These wave conditions are different for every one of the 26 profiles where the wave climate is defined. The conditions are put into the LT-model (the part of the CL-model component determining the longshore sediment transport characteristics), which generates a single S-phi curve for every profile along the coast. If the full dataset is used as the input for the LT-model, it generates 63960 S-phi curves for every profile, one for every three hours of the simulation.

Based on the local wave climate a wave data time series and static wave climate is generated and implemented in the CL-model component of the coupled model, in order to determine the effect of the wave forcing on the prediction of the dune and beach volume evolution. A selection of the results of both simulations is shown in Figure 5.6, the rest of the results can be found in Appendix A.5.

Though the temporal variation in the forcing is shown in the beach volume evolution, the effect on the dune volume evolution is small. The temporal varying forcing results in a better dune volume evolution prediction in profile 1–3. For other profiles 4–26, there are no large differences between the predicted dune and beach volume change in both cases.

The applicability of the coupled model is significantly larger if the model is able to perform sufficiently with a minimum amount of input. Furthermore, implementing a wave climate instead of a timeseries of wave data limits the computational time significantly. Because the performance of the model does not improve substantially with the increased precision of the wave input, it is recommended to work with a static wave climate instead of the whole time series of wave data.
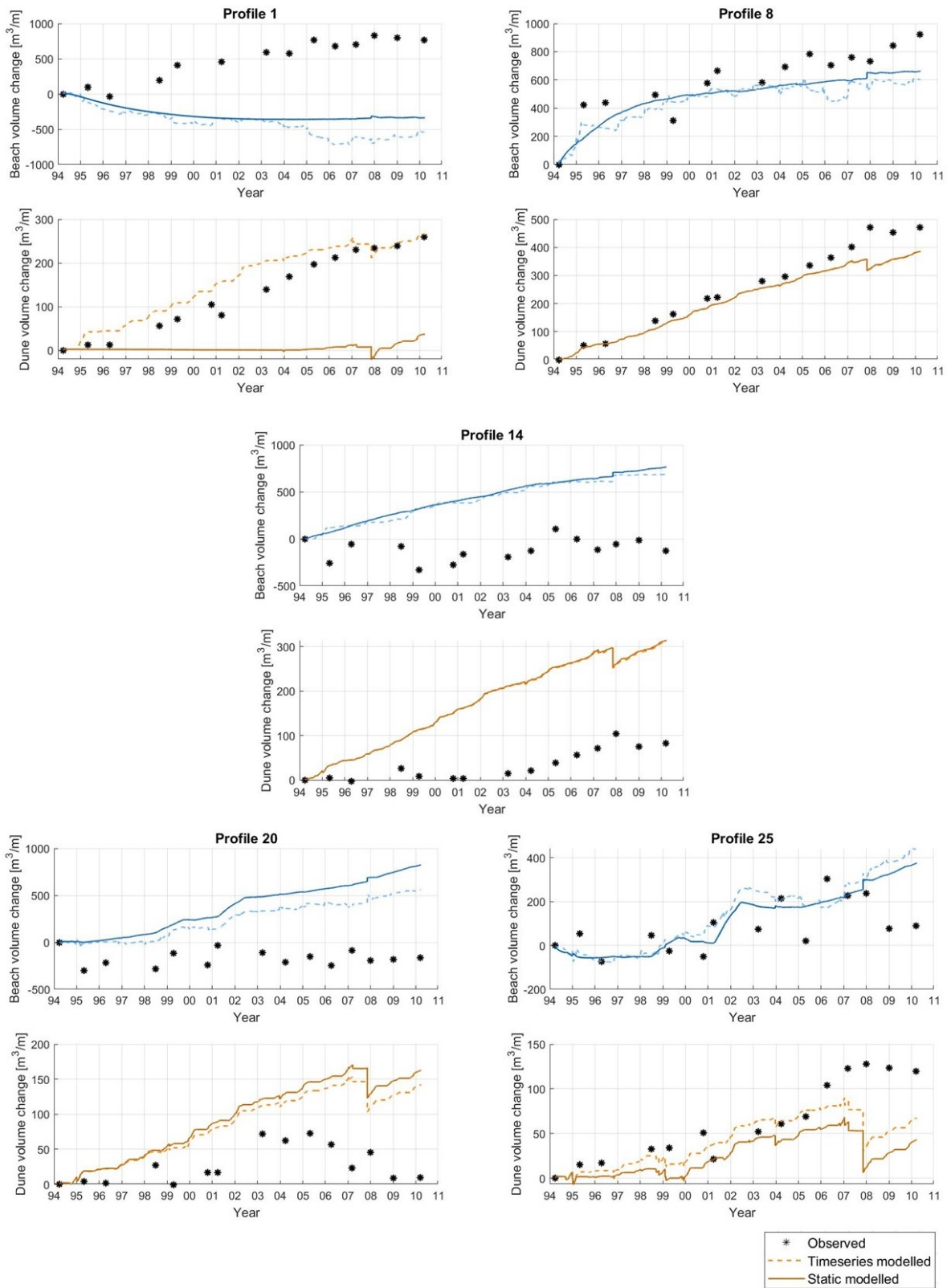
Figure 5.6: Coupled model simulation of beach and dune volume evolution in cross-shore profiles 1, 8, 14, 20 and 25 between 1994 and 2010, using a timeseries of wave data versus a static wave climate as wave input for the CL-model component

5.2.2. Effects of tide and wind

In this section, the effect of tidal- and wind-induced currents on the simulated coastline evolution is discussed. Studying the significance of tidal- and wind-induced currents is relevant, since the Holland Coast is wave-dominated and focusing on wave forcing only would be a logical choice. The CL-model component is able to include the effects of tide and wind. In order to determine whether it is relevant to include these mechanisms, four cases are defined.
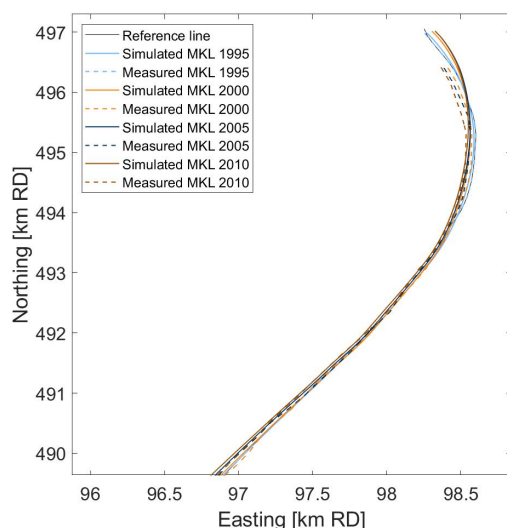
Figure 5.7: Coastline evolution during calibration period (1994–2010) as a result of the effect of only wave-driven longshore sediment transport versus the measured coastline evolution (van Verkeer en Waterstaat, 2021).
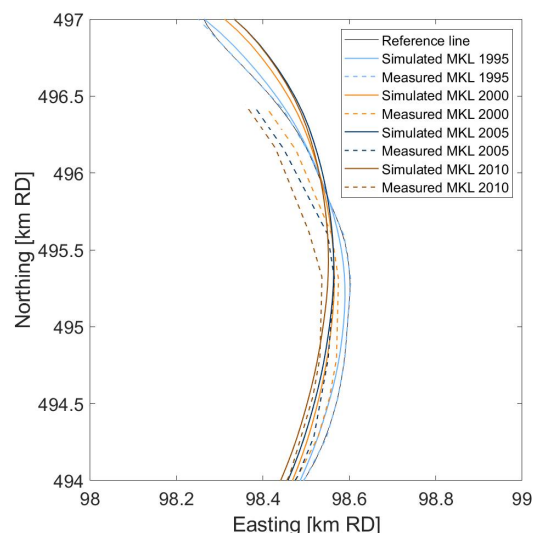
Figure 5.8: Detail of coastline evolution during calibration period (1994–2010) as a result of the effect of only wave-driven longshore sediment transport versus the measured coastline evolution (van Verkeer en Waterstaat, 2021).

First, the coastline evolution forced by wave-induced longshore sediment transport gradients only is simulated (See Figure 5.7) . After this, the cases with wind or tide-induced longshore sediment transport combined with the base case of wave-induced longshore sediment transport are performed. Finally, the combination of all three processes is implemented in the model.

The simulated coastline evolution from 1994 – 2010 forced by wave-induced longshore sediment transport gradients overestimates the accretion in the southern part of the considered coastal stretch, and underestimates the accretion in the northern region in proximity of the harbour jetties (See Figure 5.7 and 5.8). Combined, these two effects cause the simulated coastline to curve too mild when compared to data.

As shown in Appendix A.4, Figure A.5 the wind-induced current stimulates the curvature of the coastline strongly. The simulated coastline evolution forced by wave- and tidal-induced longshore sediment transport, shown in Figure A.6, also shows a stronger curvature compared to the coastline change forced by the wave-driven longshore sediment transport gradients only, though the effect of the additional tide-induced sediment transport gradients and the resulting effect on the curvature of the coastline is smaller than the effect of the wind-induced sediment transport. The combined effect of tidal- and wind-induced longshore sediment transport together with the wave-induced longshore sediment transport has the largest positive effect on the curvature of the coastline. The inclusion of all three of the processes results in the best fit with the data, as shown in Figure 5.9 and 5.10.
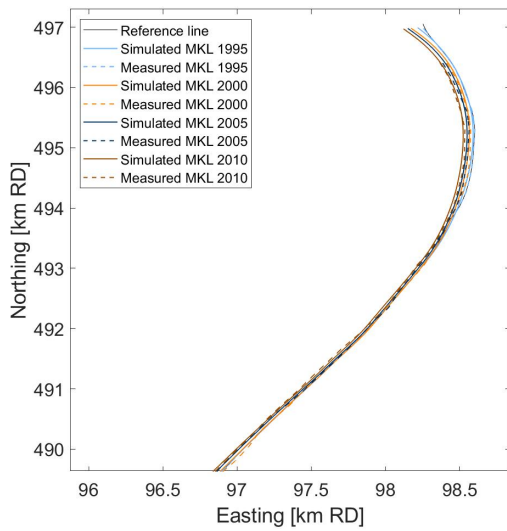
Figure 5.9: Coastline evolution during calibration period (1994–2010) as a result of the combined effect of wave-, wind- and tide-driven longshore sediment transport versus the measured coastline evolution (van Verkeer en Waterstaat, 2021).
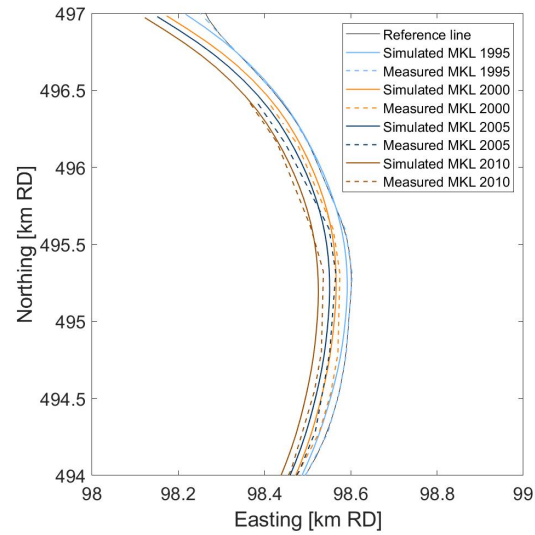
Figure 5.10: Detail of coastline evolution during calibration period (1994–2010) as a result of the combined effect of wave-, wind- and tide-driven longshore sediment transport versus the measured coastline evolution (van Verkeer en Waterstaat, 2021).
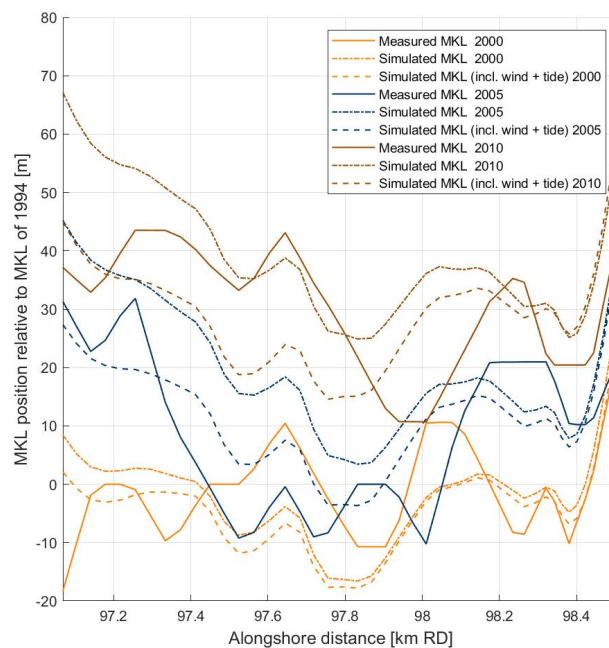
Figure 5.11: Simulated and observed coastline change between 1994 and 2010 along the IJmuiden coast for the area between the cross-shore profiles.

Apart from visual interpretation of the coastline evolution and curvature representation resulting from the different simulations, the absolute coastline changes are evaluated. This enables the quantitative evaluation of the cases. As shown in Figure 5.11, coastline evolution is best simulated when effects of tide and wind are included in the coupled model. It is important to note that the curved coastline is also enhanced by locally tuning the transport rays during model calibration.

5.2.3. Effect of cross-shore processes

The coupled model enables the simulation of coastline evolution as a result of both cross-shore and longshore sediment transport processes. Because the coupling between the cross-shore and along-shore processes is the key of the model, it is relevant to investigate how strong these processes affect each other. In this section, the coastline change simulated with the coupled model is compared with the coastline change the CL-model simulated separately. The results of these simulations are shown in Figure 5.12, in which CLCS is the coupled model.

The simulated coastline evolution from 1994 – 2010 overestimates the accretion in the southern part of the considered coastal stretch, and underestimates the accretion in the northern region in proximity of the harbour jetties. Combined, these two effects cause the simulated coastline to curve too mild when compared to data (As described in Section 5.2.2).

In Figure 5.12 it is shown that the CL-model simulates more accretion then the coupled model in general. This can be explained by the fact that the considered coastline is accreting between 1994 and 2010 at all locations. When the coast is accreting, the coupled model will enable cross-shore spreading of the accreted volume of sand over beach and dune whereas the CL-model will simulate coastline change only. Since the wave-, wind- and tidal forcing in both models is the same, the longshore sediment transport gradients are about the same and therefore the size of the sediment source within every gridcell is the same. Therefore, the CL-model will show stronger accretion by definition.
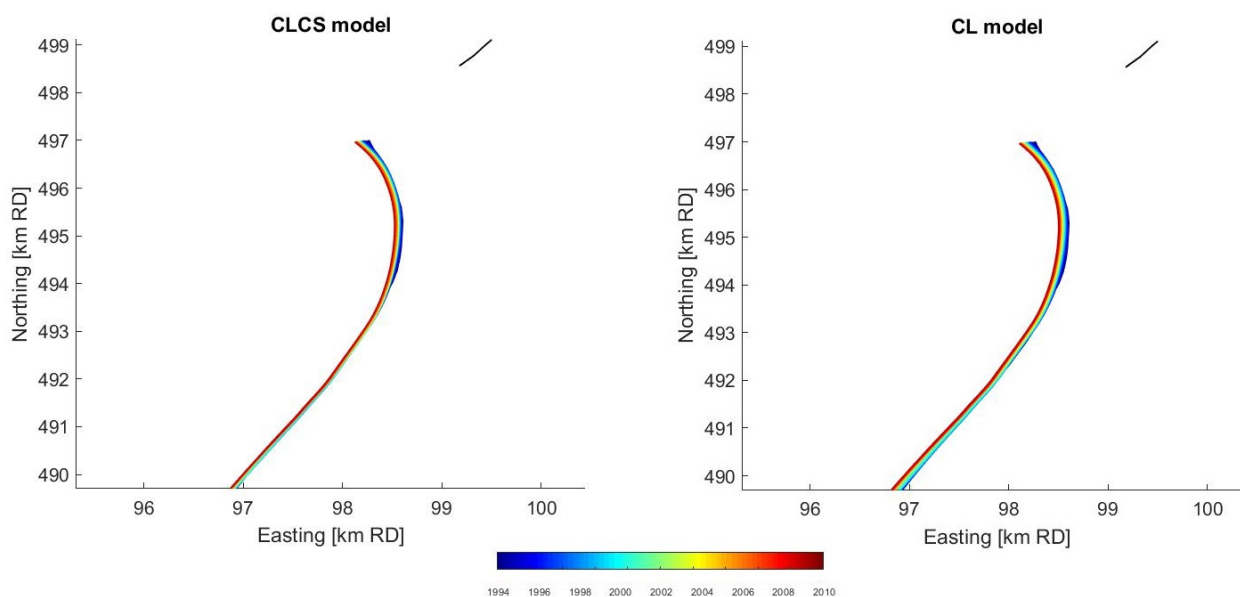
Figure 5.12: Coastline evolution between 1994 and 2010, simulated by the coupled model (CLCS) and by the CL-model (CL).

The coastline change in the area between the first and last cross-shore profile is studied in more detail in Figure 5.13. Studying these simulated coastline changes shows that the difference between the accretion simulated with both models in is considerably larger in the southern part of the considered area. This way, the coupled model corrects the overestimation of the coastline accretion in the soutern part, which is larger in case the coastline evolution is simulated with the CL-model.

In the southern part of the coast, nourishments takes place in the case of IJmuiden (See Figure 5.3 and Table 5.1). The fact that the coastline predicted by the coupled model deviates more strongly in the south from the coastline simulated by the CL-model than these deviate from each other in the northern part of the coast can be attributed to the fact that the accretions in the CL-model are spread

only in longshore direction, while in the coupled model they are also spread in the cross-shore direction.

Overall, the coupled model enhances the curvature of the coastline with respect to coastline predicted by the CL-model and therefore it can be concluded that the interaction of cross-shore and longshore sediment transport processes has a positive effect on the predictive skill of the coupled model with respect to the coastline evolution in the IJmuiden case.
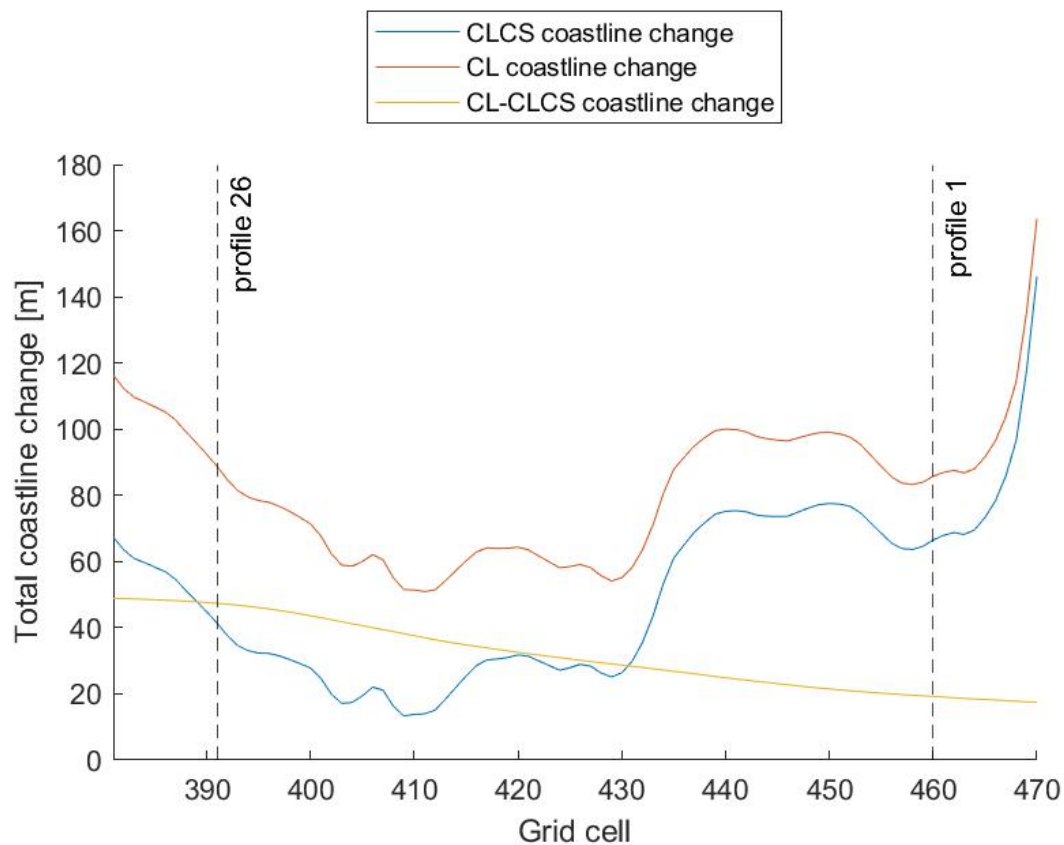
Figure 5.13: Coastline change between 1994 and 2010 simulated by the coupled model (CLCS) and the CL-model, for the area between the cross-shore profiles. The difference between these simulated coastline changes expresses the amount of sediment stored in the dunes of the CS-model component

5.2.4. Nourishments
When the beach and dune evolution of the IJmuiden coast is simulated with the CS-model, there is an underestimation of the accretion in cross-shore profiles 16 and 17. In these profiles, the longshore sediment transport gradients of 0.3 and 0.8 m^3/m/yr are small (See Table A.1). When the longshore transport gradients derived from observations are implemented into the CS-model, the dune volume change (depicted in Figure 5.14 and 5.15) is approximately zero in these profiles until 2008. After 2008, the accretion starts due to shoreface nourishment 8 (See Figure 5.3).

Because the CS-model does not include longshore interaction between the cross-shore profiles and therefore no longshore redistribution of nourishments, it is assumed that the underestimation of the dune volume evolution in cross-shore profiles 16 and 17 is caused by the lack of longshore spreading of the nourishments that took place in profiles 18 – 26 from 1998 till 2001 (nourishments 2 and 3 in Table 5.1 and Figure 5.3). These nourishments presumably result in accretion of the profiles 16 and 17 in reality, but the CS-model cannot predict this behaviour.
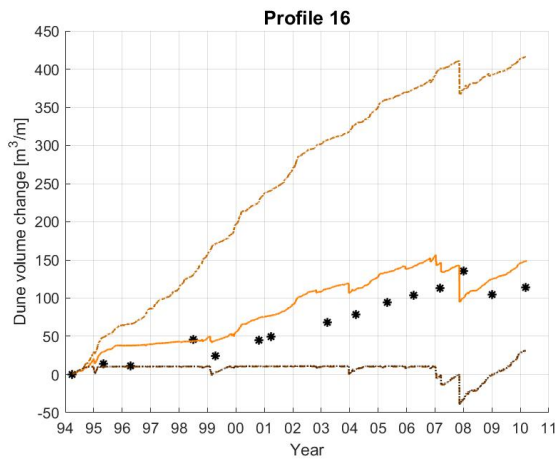
Figure 5.14: Dune volume evolution of cross-shore profile 16, simulated with the calibrated coupled model, observed dune volume evolution and three reference simulations of dune volume evolution performed with the CS-model; a simulation without longshore sediment transport gradients, a simulation with a constant longshore sediment gradient of 1×10^{-5} in all cross-shore profiles and a simulation with the observed transport rates in every profile.
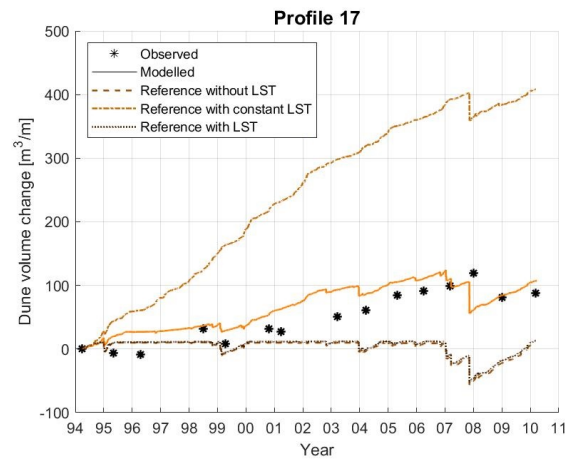
Figure 5.15: Dune volume evolution of cross-shore profile 17, simulated with the calibrated coupled model, observed dune volume evolution and three reference simulations of dune volume evolution performed with the CS-model; a simulation without longshore sediment transport gradients, a simulation with a constant longshore sediment gradient of 1×10^{-5} in all cross-shore profiles and a simulation with the observed transport rates in every profile.

As shown in Figure 5.14 and 5.15, the dune volume accretion within cross-shore profiles 16 and 17 is no longer underestimated when the dune and coastline evolution of the IJmuiden coast is simulated with the coupled model. Due to the interacting longshore and cross-shore sediment transport processes included in the coupled model, the model can simulate the spread of nourishments along the coast.

Furthermore, it can be concluded from the simulated effect of nourishments that the distribution of the nourished volume of sand in both longshore and cross-shore direction ensures that the coastline prediction is more accurate (See Section 5.2.3 on the effect of cross-shore processes). This means that nourishments are simulated better in the coupled model than in both the CS-model and the CL-model.

5.2.5. Calibration of empirical coefficients

The two empirical variables in the CS-model component that needed to be calibrated are dune erosion impact coefficient C_s (Formula 3.6a and 3.6b) and the empirical coefficient in the aeolian transport formula K_w (Formula 3.14).

Since a previous study of the IJmuiden case showed that the CS-model component was most sensitive to changes in the dune erosion impact coefficient, calibration of this parameter is important Hallin, Huisman, et al., 2019. To calibrate the dune erosion impact coefficient, site specific water level data and morphological observations are necessary. When calibrated against field data and laboratory experiments, C_S was found to be typically ranging between 7×10^{-4} and 1.4×10^{-3} Larson et al., 2004.

For the present calibration of C_s, the dune volume evolution was simulated multiple times with the coupled model and results were compared with the data. For every profile, the model performance was evaluated, particularly looking at the simulation of erosion during storm events. After many different simulations, with values of C_S ranging between 7×10^{-4} and 1.4×10^{-3} with steps of 1×10^{-4}, the calibrated value for C_S is 9×10^{-4}.

Because the empirical coefficient in the aeolian transport formula depends on the roughness height parameterisation, there is no ambiguity about the value of K_w within different studies. The calibration of this coefficient is therefore a process of trial and error. Looking at the beach and dune evolution for every profile along the IJmuiden coast, the overall under- or overestimation of the accretion was

considered. Whether the transport from the beach towards the dunes should be increased, decreased or left untouched is evaluated for every model run. With a lot of different tries with values ranging 0 and 15, the calibrated value for K_w is found to be 1.8.

The values of both empirical coeffients are defined to be the same for all profiles. Effect of heterogeneous sediment characteristics along the coast (e.g. due to wind sheltering) are therefore not included in the present IJmuiden model.

5.2.6. Effects of longshore sediment transport gradients

In previous case studies of the IJmuiden dune and coastline evolution, in which the evolution was hindcasted with the CS-model alone, a constant longshore sediment transport gradient was derived from data for each cross-shore profile along the coast (Hallin, Huisman, et al., 2019). The values of these gradients can be found in Appendix A.1 and in Figure 5.16. After this case study, it was concluded that at the scale for which the CS-model was developed – the decadal to centennial time scale – the longshore sediment transport gradients govern the dune evolution. The relevance of the longshore sediment transport gradients is one of the reasons for the coupling of the CS- and CL- model components. In this section the mean longshore sediment transport gradients simulated with the coupled model are compared with the longshore sediment transport gradients imposed in the CS-model in the previous case study. Comparing these transport gradients allows us to better understand how the model performance of the coupled model is constructed. It is also important to look at the differences in order to subsequently be able to analyze whether the differences have an effect on the simulated beach and dune volume evolutions.
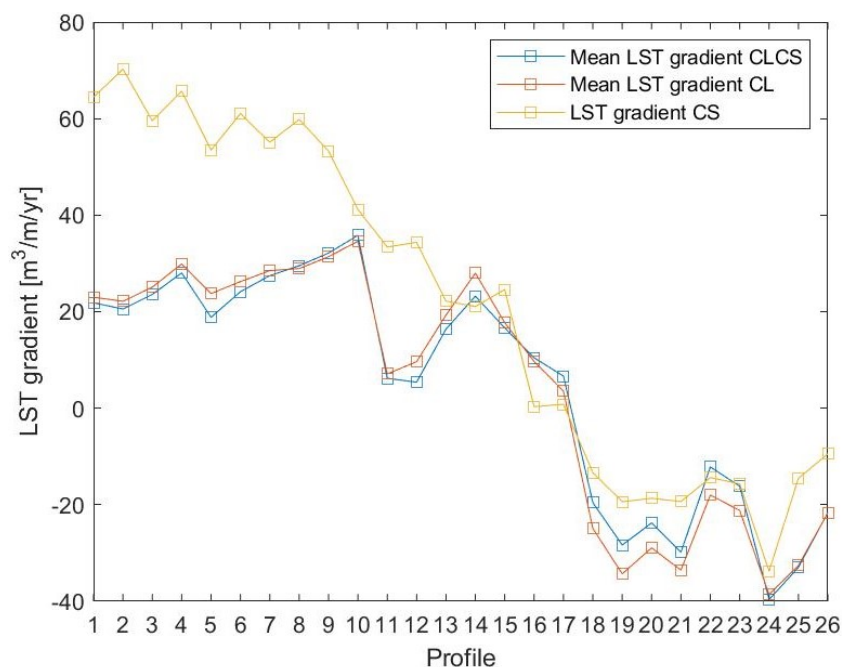
Figure 5.16: Modeled and observed longshore sediment transport gradients in all cross-shore profiles (1–26) in m^3/m/yr

In Appendix A.6 the calibrated model results of the coupled model are depicted in the same figure with the measurements, and the results of the CS-model without longshore sediment transport gradients, with a longshore sediment transport gradient of 1×10^{-5} m^3/s/m at every cross-shore profile and with the longshore sediment transport gradients derived from observations (Hallin, Huisman, et al., 2019).

The mean longshore sediment transport gradient within the coupled model (referred to as the CLCS-

model) differs significantly from the gradients implemented in the CS-model, as shown in Figure 5.16. Overall, the gradients are larger in the CS-model. Especially in the northernmost profiles, the gradients derived from observations are considerably higher. Studying the longshore sediment transport gradients the coupled model simulated for the part of the coast south of the area between the cross-shore profiles (See Figure 5.17), it is important to note that the sediment transport gradients derived from data are within the range of longshore sediment transport gradients simulated along the coastline.
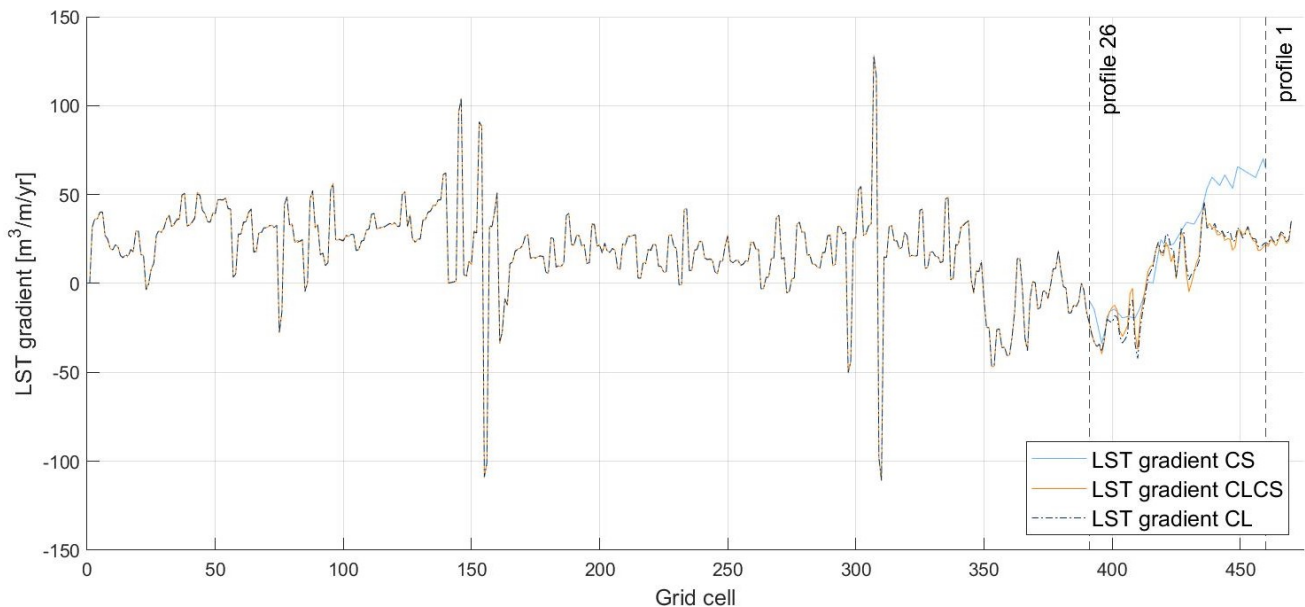
Figure 5.17: Simulated longshore sediment transport gradients along the coast versus the longshore sediment transport gradients derived from data in m^3/m/yr

Because the coupled model uses the CL-model component to simulate the longshore sediment transport rates, the local sediment transport gradients are harder to tune. If locally the sediment transport gradient differs significantly from the mean, it affects the sediment transport rates in the adjacent regions. Large variations in the local sediment transport rates are flattened out by the coupled model due to alonghore processes. The effect of cross-shore processes on the local sediment transport gradient is illustrated in Figure 5.16 by the difference between the longshore sediment transport gradient in the CL-model component with respect to the coupled model as mentioned in Section 5.2.3. This difference is relatively small compared to the difference between the observed longshore sediment transport gradients and the modeled ones.

Considering the dune volume evolution (see Appendix A.6) which is depicted for a selection of the profiles in Figure 5.18, it is shown that the dune volume of profiles 1–6 is best simulated by the coupled model. For profiles 7–10 the dune volume evolution is best simulated by the CS-model with the observed longshore sediment transport gradients. The dune volume evolution in profile 11–13 and 19–20 is best simulated by the CS-model with the observed longshore sediment transport gradients and in profile 14–18 and 21–26 the coupled model performs most adequate. So, the dune volume evolution is simulated better by the coupled model when compared with the CS-model with various settings for the longshore sediment transport gradients.
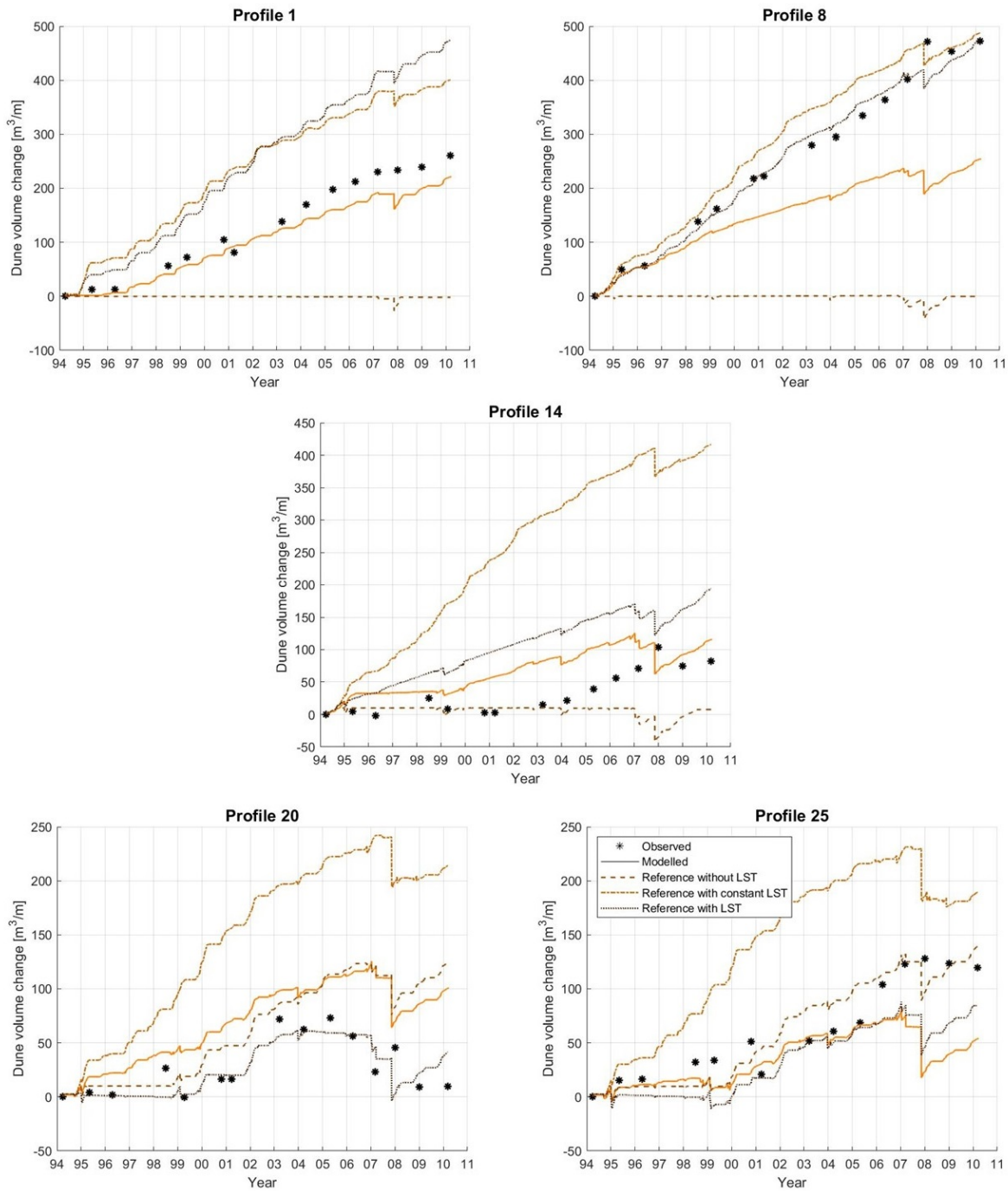
Figure 5.18: Simulated and observed volume evolution of selected cross-shore profiles 1, 8, 14, 20 and 25 simulated with the calibrated coupled model, versus three reference simulations of the CS-model; a simulation without longshore sediment transport gradients, a simulation with a constant longshore sediment gradient of 1×10^{-5} in all cross-shore profiles and a simulation with the transport rates derived from data in every profile.

It is concluded that modeling the longshore sediment transport results in relatively smaller longshore sediment transport gradients than the gradients derived from observations, as used for the previous study of the IJmuiden case performed with the CS-model. The difference in longshore sediment transport gradients between the different cases has a small effect on the simulation of the behaviour of the dunes. Furthermore it can be concluded that the dune processes do affect the modeled longshore sediment transport rates, but the effect is relatively small (see Figure 5.16).

5.2.7. Results of the model calibration

Figure 5.19 shows the by the coupled model simulated dune evolution, the measured dune volume evolution derived from the JARKUS-data and the dune evolution simulated by the CS-model component. There are no longshore sediment transport gradients in the reference simulation performed with the CS-model. Generally, the coupled model simulations show a sufficiently good agreement for most of the profiles. Although the extent of the dune evolution varies greatly along the coast of IJmuiden (with differences up to a factor of ten), the simulated volume evolutions show reasonable agreement with the measurements.

The northern profiles 1–12 are nearly linearly accreting. The model predicts this behaviour well. However, the model overestimates the dunegrowth in profile 4. It is assumed that this overestimation is due to a sediment sink between profiles 3 and 4 (Hallin, Huisman, et al., 2019). An opening between the dunes attracts part of the sediment otherwise transported by the wind towards the adjacent dunes. Overall, the model underestimates the accretion.

The southern profiles 13–26 show alternating periods of accreting, stable and eroding dunes. Negative longshore sediment transport gradients in the southernmost profile 18–26 would result in dune erosion, if this effect wouldn't be counteracted by the numerous nourishments in this area. The dune growth as a result of these nourishments cause a pattern of stepwise evolution. Dune growth increases after nourishment and then stabilizes until the next nourishment.

The large storm on 11/9/2007 is visible in the simulated dune volume evolution. The southern profiles erode more than the northern profiles, because the beach is wider in the northern profiles, so that the travel distance of the waves over the beach is greater and there is less dune erosion for the same incoming wave height. These local differences in dune erosion are also observable in the data, therefore, storm erosion events are predicted satisfactory.
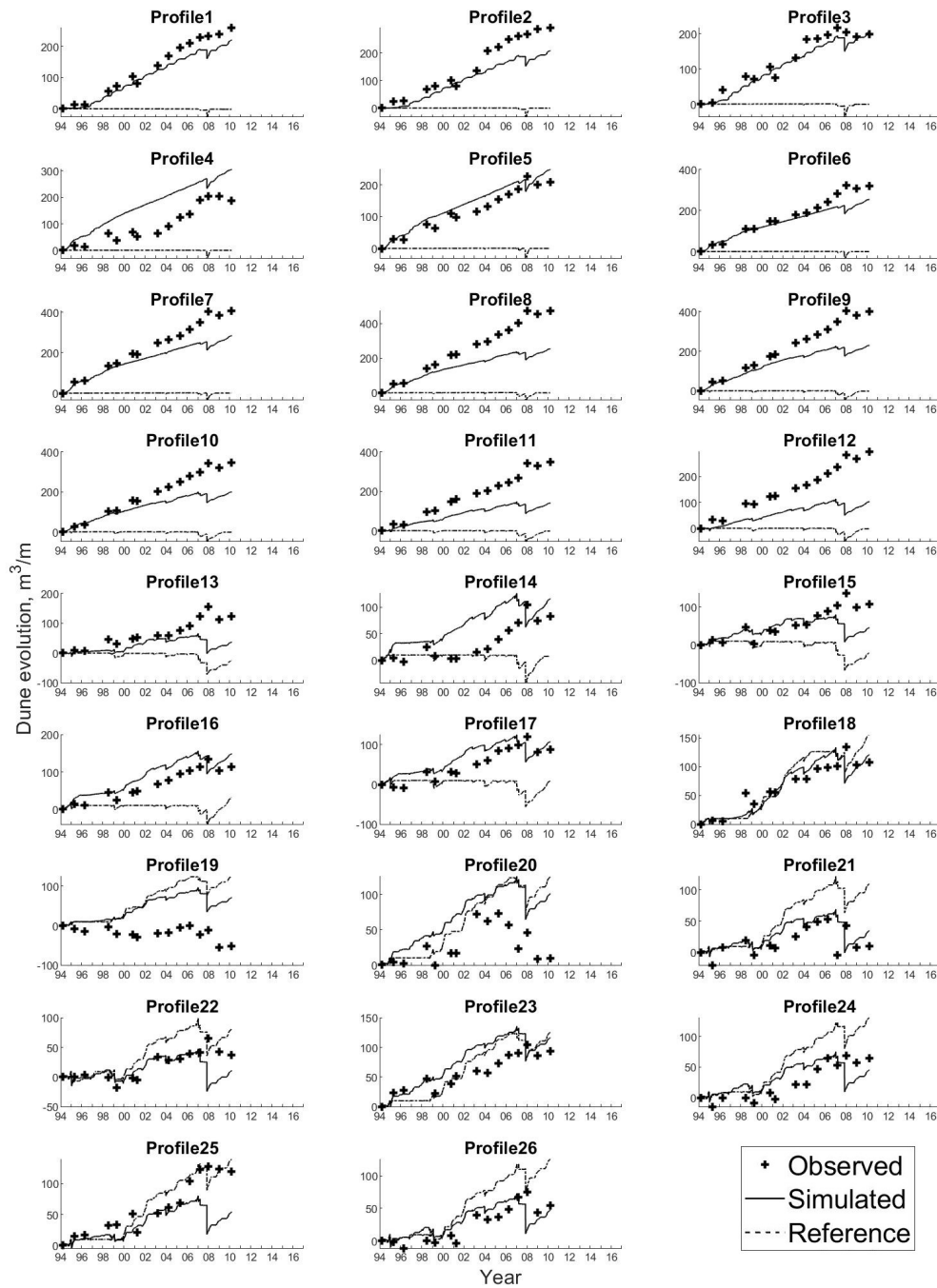
Figure 5.19: Evolution of the dune volume in cross-shore profiles 1-26, simulated with the calibrated coupled model for the period 1994-2010. The reference simulation is the CS-model simulation without longshore sediment transport gradients. Furthermore, the measured dune volume derived from the JARKUS-data evolution is depicted.

The by the coupled model simulated coastline evolution, the measured coastline evolution derived from the MKL-data and the coastline evolution simulated by the CL-model component are depicted for every

cross-shore profile location in Figure 5.20. Overall, the coupled model results show reasonable agreement with the data.

For profile 1–11, the simulated coastline evolution shows continuous accretion. In the linear accreting profiles 1–3, the coupled model under-predicts the accretion although the results of the simulation show the right trend. Because the CL-model simulates stronger accretion due to the lack of cross-shore spreading of sediment, the CL-model simulates the coastline evolution better at these profiles. Some initial erosion before continuous accretion are shown in the measured coastline evolution of profile 4 and 5. This erosion is not simulated by the coupled model and therefore the overall accretion within these profiles is predicted too strong. First, the coast accretes fast and then it slows down in profiles 6–10. This behaviour is simulated well by the coupled model. In profile 11, the model initially simulates erosion followed by accretion, though the data only shows accretion for this profile. Therefore, the accretion is underpredicted in this profile. Overall, the coastline is continuously accreting in profiles 1–11 and the coupled model simulates this behaviour well.

The alternating periods of erosion and accretion observed in profiles 12–26 are overall well simulated by the coupled model. For profiles 17–26 the simulated coastline evolution shows a strong accretion peak for 2002 onwards. After this peak, the predicted coastline evolution is still close to the observed evolution. However, the simulated accretion rate is higher than the observed. It is assumed that this peak is caused by the beach nourishment at Bloemendaal and Zandvoort in 2001. In the coupled model, the total volume of sand is added to the beach over a time period of one year. It is assumed that the nourishment took longer in reality resulting in a more gradual accretion in the observed coastline evolution.
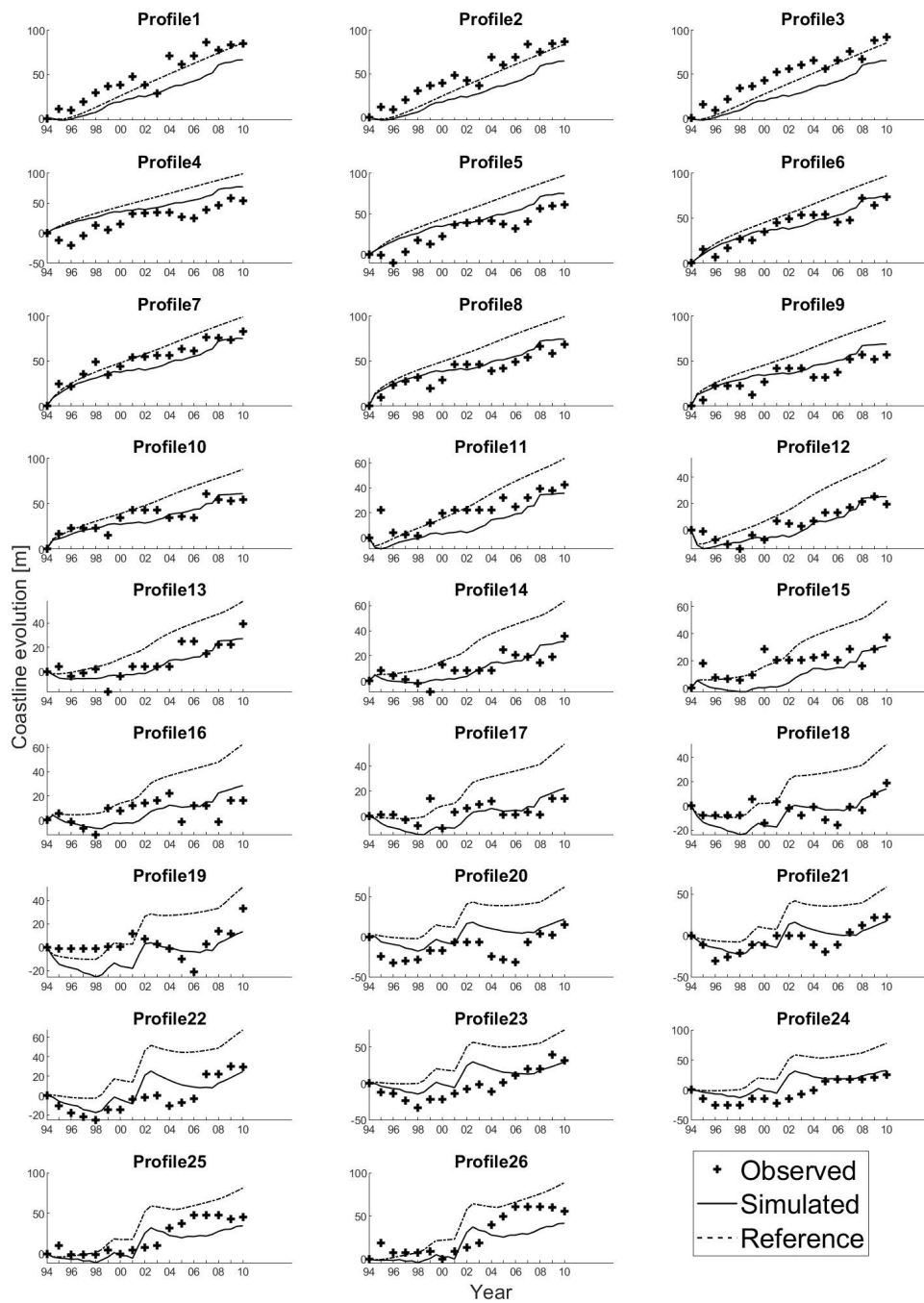
Figure 5.20: Evolution of the coastline at the location cross-shore profiles 1–26, simulated with the calibrated coupled model for the period of 1994-2010. The reference simulation is the CL-model simulation of the same case. Furthermore, the measured coastline evolution derived from MKL-data is depicted.

5.3. Model validation

In this section, the validation of the coupled model is described. The model is validated for the period of 03/12/2010 – 02/16/2016. The overall model performance is evaluated by comparing computed and measured values using the coefficient of determination, R^2 (Equation 5.1). The coefficient of determination describes the proportion of the measured variability that is explained by the model outcomes. An R^2 of 1 means that all variability in the data is described by the model and there is a perfect fit.

$$R^2 = 1 - \frac{\sum_{i=1}^{n}(m_i - c_i)^2}{\sum_{i=1}^{n}(m_i - \overline{m})^2} \tag{5.1}$$

In this equation, m is the measured value, n is the sample size, c is the computed value and $\overline{m}$ is the mean measured value.

It is shown in Figure 5.21 that the coefficient of determination of the dune volume evolution simulated by the coupled model during model calibration is 0.6. Simulations of the IJmuiden case with the CS-model resulted in a R^2 of 0 in case of no longshore sediment transport gradient, 0 in case of a constant longshore sediment transport gradient of 1×10^{-5} and 0.27 in case of a fixed longshore sediment transport gradient derived from observations respectively, as shown in Appendix A.8.
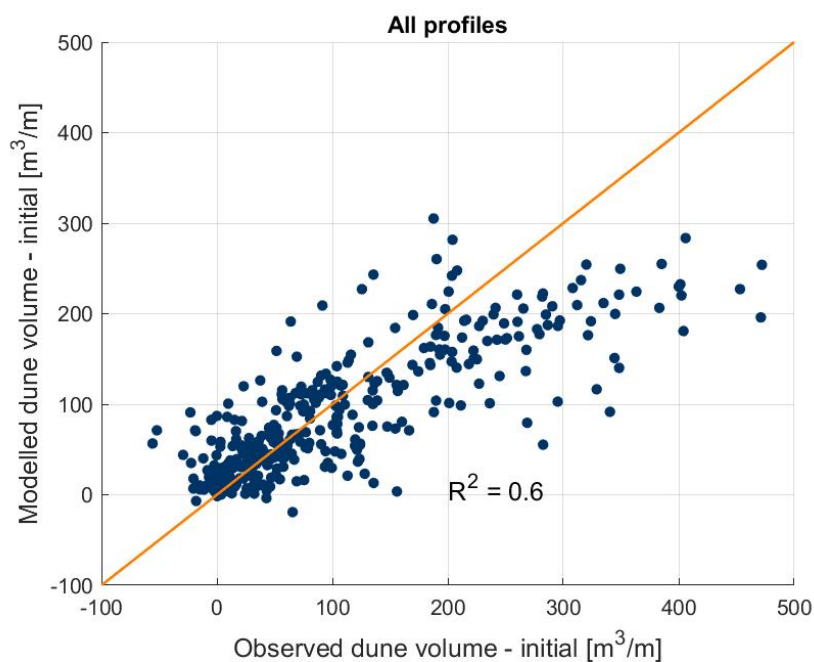
Figure 5.21: Scatterplot of the simulated and observed dune volume change from 1994-2010 with the coefficient of determination.

In Figure 5.22 the coefficient of determination of the coastline evolution simulated by the coupled model for the calibration period is depicted, which is 0.82.
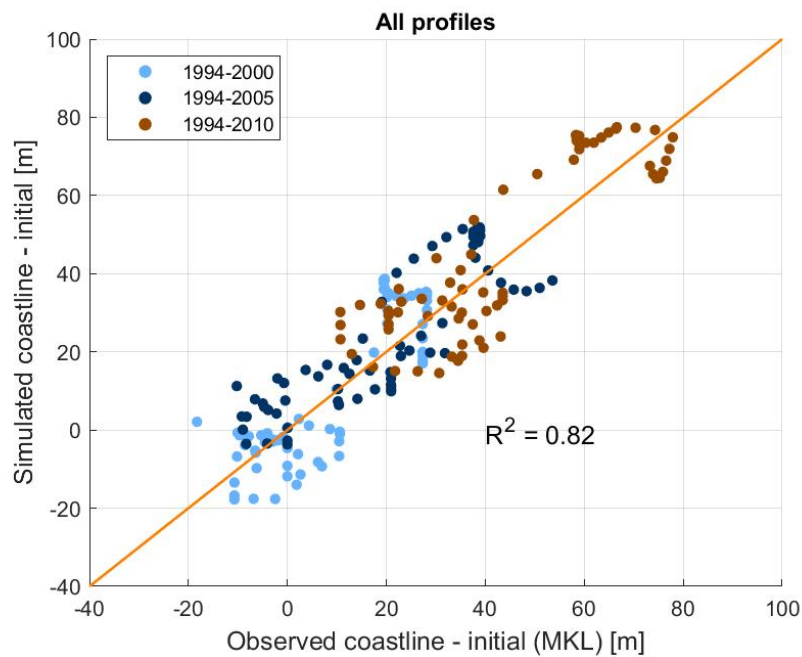
Figure 5.22: Scatterplot of the simulated and observed coastline change from 1994-2010 with the coefficient of determination.

For the validation period, the model coefficient of determination of the dune volume evolution is 0.13 (See Figure 5.23). In Appendix A.9, it is shown that the simulations with the CS-model resulted in a R^2 of the dune volume evolution of 0.13 in case of no longshore sediment transport gradient and zero for all other cases.
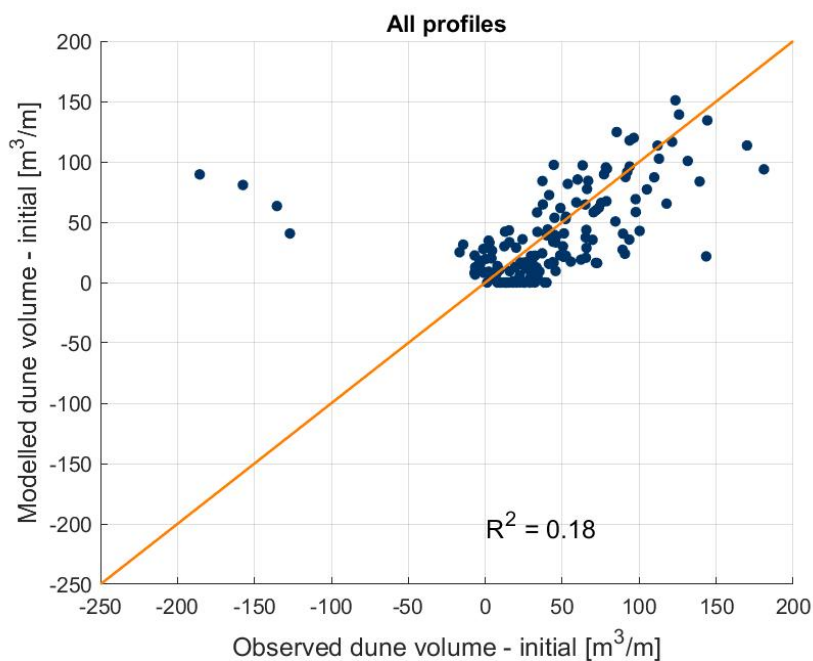
Figure 5.23: Scatterplot of the simulated and observed dune volume change from 2010-2016 with the coefficient of determination.

In Figure 5.24 the coefficient of determination of the coastline evolution simulated by the coupled model for the validation period only is depicted, which is 0.
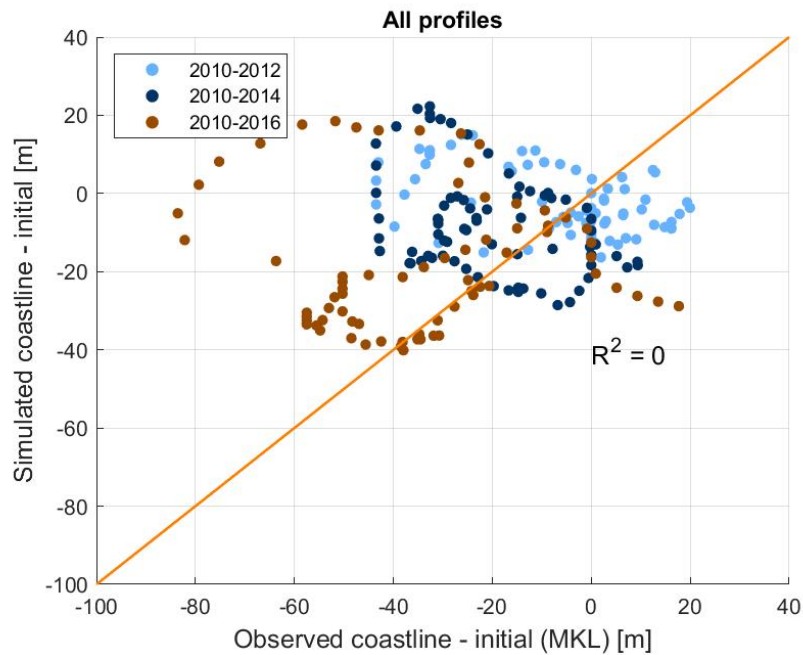
Figure 5.24: Scatterplot of the simulated and observed coastline change from 2010-2016 with the coefficient of determination.

5.3.1. Analysis of model validation

The coefficients of determination of the simulated dune volume evolution and coastline change from 2010-2016 are low. In order to distinguish possible explanations for these low values, some additional coefficients of determination are derived.

The coefficient of determination of the dune volume evolution between 2010 and 2016 is defined for every individual cross-shore profile. These results can be found in Appendix A.10. Comparing these results shows that the measured variability of the dune volume evolution within profiles 1–17 is explained by the model outcomes quite reasonably, but in profiles 18–26 the coefficient of determination is zero.

Considering the full period of 1994 – 2016, the coefficient of determination of the dune volume evolution is 0.69 (See Figure A.118 in Appendix A.11) and the R^2 of the coastline change is 0.7 as shown in Figure A.119 in Appendix A.11.

The effect of the length of the validation period is evaluated by determining the coefficient of determination of the coastline change and dune volume evolution for an alternative period of the same length. For simplicity reasons, the period of 1994 – 2000 is chosen, which equals the first 6 years of the calibration period. Because this alternative validation period is part of the calibrated period, the results cannot be considered actual validation results since the coupled model is calibrated for this period. The resulting R^2 of the dune volume evolution between 1994 and 2000 is 0.21 and the coefficient of determination of the coastline change is 0.48 (See Appendix A.12).

5.4. Conclusions of the IJmuiden case

The IJmuiden case consists of a naturally erosive coast that is accreting due to the combined effect of the harbour jetty and several beach and shoreface nourishments. These human interferences result in a dynamic coastal zone evolution over time, which is hindcasted using the coupled model.

In Section 5.2.1 the effect of the chosen schematization of the wave characteristics on the quality of the model performances is studied. It is concluded that although the dune and beach evolution show more fluctuations corresponding with the observed variation in the measured beach and dune volume in case wave characteristics are implemented in the model as a wave data timeseries, the gain of precision is

not in proportion to the increase in computational time. Therefore, the implementation of limited wave conditions in the form of a wave climate is recommended.

The effects of the tide- and wind-induced currents on the quality of the prediction of the coastline evolution in the IJmuiden case is studied in Section 5.2.2. Though the inclusion of tide-induced effects is smaller than the effects of the wind in this IJmuiden case, the combined effect of both phenomena is concluded to be most favourable. In Section 5.2.3, the effect of cross-shore processes on the simulated coastline evolution is studied, by comparing the coastline evolution simulated with the coupled model with the coastline evolution simulated with the CL-model. In this section, it is concluded that the cross-shore transport processes have a positive effect on the prediction of the coastline evolution by reducing the coastline accretion in the southern part. The combined effect of tide- and wind-induced longshore sediment transport and cross-shore transport processes enhance the curvature of the coastline that is otherwise not strong enough.

Nourishments and their spreading along the IJmuiden coast are evaluated in Section 5.2.4. Because the longshore interaction between cross-shore profiles is not included in the CS-model, the dune volume accretion of cross-shore profiles adjacent to nourishments was underestimated in previous simulations of the dune volume evolution along the IJmuiden coast using the CS-model. Furthermore, the exclusion of cross-shore spreading of the nourishments results in overestimation of the coastline change resulting from nourishments. The interaction between longshore and cross-shore transport processes is the key of the coupled model and the model results show that the coupled model is able to simulate the longshore and cross-shore redistribution of nourishments.

The coupled model simulates the longshore sediment transport rates using the CL-model component. It uses the gradients in the simulated longshore sediment transport rate to determine sediment availability for the various cross-shore processes included in the coupled model. Previous studies regarding the performance of the CS-model on itself, pointed out the importance of longshore sediment transport in long-term and large-scale dune evolution prediction.

For a previous study of the IJmuiden case, the constant longshore sediment transport gradients for all cross-shore profiles are derived from data (Hallin, Huisman, et al., 2019). Therefore, these rates are considered to be the optimum gradients, though they are not time-varying. The coupled model simulates longshore sediment transport gradients for every cross-shore profile and the mean of these time-varying gradients do differ from the previously found constant gradients. Overall, the time-varying gradients simulated by the coupled model are lower.

Comparing the coastline and dune volume evolution resulting from the simulations with the CS-model and the coupled model, it can be concluded that the dune volume evolution is better simulated by the coupled model. Time-varying longshore sediment transport gradients are therefore considered to be favourable over constant longshore sediment transport gradients. Furthermore, this part of the model application shows that it is possible to simulate the longshore sediment transport gradients using a schematized wave climate to predict dune evolution sufficiently rather than determine these gradients based on bathymetric data. Simulation of the gradients enlarges the possible model applications.

Looking at the overall results, the behaviour of the various cross-shore profiles along the coast is predicted reasonably. Considering the calibration period, the coupled model predicts the dune volume and coastline evolution satisfactory.

Considering the validation period only, the coupled model does not perform sufficiently. The coefficient of determination for the prediction of the dune volume is above zero, but low. For the coastline evolution, this R^2 is zero. The coefficient of determination of the simulated dune volume evolution is determined within every individual cross-shore profile (see Appendix A.10). It is shown, that the dune volume evolution is predicted reasonably for profiles 1–17 and poorly for profiles 18–26. Therefore, the volumetric change of the linearly evolving cross-shore profiles is predicted better than the evolution of the cross-shore profiles that show alternating periods of accreting, eroding and stable dunes.

Studying the full period (Figure A.118 and A.119), so the calibration and validation period combined, the model performs well. Because the coefficient of determination of the dune volume evolution for the full period is higher than that of the calibration period, the quality of the prediction of the dune volume evolution does improve with the simulation length. Although the coastline prediction shows a lower coefficient of determination for 1994 – 2016, with an R^2 of 0.7 the model performs satisfactory. Therefore, it is expected that the limited duration of the simulation and therewith the limited amount of data to compare model results and observations resulted in the unsatisfactory model performance during validation. In order to confirm the hypothesis that the disappointing model performance in the validation period is related to the length of this period, an alternative simulation was performed with the same duration.

As shown in Appendix A.12, the coefficient of determination of the dune volume evolution between 1994 and 2000 is 0.21. The R^2 of the coastline change within this same period is 0.48. The model performs better when simulating the period 1994 – 2000 with respect to the simulation of coastal evolution between 2010 and 2016. However, it should be taken into account that the coupled model is calibrated using the bathymetric data from 1994 to 2010. Therefore, the alternative validation period shows that the model performance on simulations of 6 years is unsatisfactory and this confirms the assumption that the chosen length of the validation period is not long enough. The interannual bar behaviour that is observed in the data but not included in the coupled model, as described in Section 5.1.1, may cause the poor model performance in the short-term simulations. With limited processes included in the coupled model, which focuses on long-term coastal development, longer simulations in the order of decadal to centennial timescales are needed to simulate the overall trends in bathymetric data.

6

Discussion

This study focuses on long-term beach and dune evolution with interacting longshore and cross-shore processes. The chosen approach is to develop a coupled surfzone-dune model to quantify the longshore and cross-shore processes, consisting of the model component Unibest-CL+ and the CS-model. The model was tested using academic cases and applied on the IJmuiden case. The conclusions drawn from model testing and application are presented in previous Sections 4.4 and 5.4. The meaning, importance and relevance of the results are discussed in the Discussion, using the results from Chapter 4 and 5. After this, recommendations on improvements of the coupled model and on future research enabled by the development of the coupled model are presented.

6.1. Interpretation of results and implications

It has been proven that the different cross-shore and longshore sediment transport equations and their interaction are implemented correctly in the coupled model, after testing the model. The sediment fluxes within the coupled model are balanced and no deviations from sediment conservation occurred in the interaction between the model components. By formulating two different accuracies, namely the Equivalent Sediment Flux Accuracy and the Equivalent Coastline Accuracy, it is further established with which theoretical precision the model can predict the sediment transports and the subsequent evolution of the coastal zone. In case one cross-shore profile is defined along every kilometer of coastline in this academic case, the Equivalent Sediment Flux Accuracy is 0.47% and the Equivalent Coastline Accuracy is 8 cm. Testing of the coupled model thus checked the construction of the coupled model on the one hand and quantitatively determined the possibilities of the coupled model on the other.

During the hindcast of the IJmuiden case, dune volume evolution and coastline evolution is predicted reasonably by the coupled model. The measurements (in Figure A.1 and A.2 in the Appendix) show significant dune growth of the northernmost dunes closest to the harbour jetties. At those locations, the corresponding coastline accretion is strong. The dune growth and coastline accretion is almost linear, whereas the profiles in the south show phases of dune erosion with coastal erosion, alternating with dune accretion and coastal accretion. This fluctuating evolution is the result of the nourishments along the IJmuiden coast. The different types of dune and coastline evolution along the IJmuiden coast are described by the coupled model, as one can see in Figures 5.19 and 5.20. Though the coefficient of determination, R^2, of the dune volume change is not significantly larger than the R^2 of the results of the simulation with the CS-model with longshore sediment transport gradients derived from observations, the achieved model performance is relevant. The coupled model does not need the data on coastline change, which is necessary for the CS-model. This makes it possible to perform forecasts of future scenarios that are not doable with the CS-model. Therefore, matching the predictive skill of the CS-model shows the potential of the coupled model. The coupled model is able to predict the long-term and large scale dune evolution sufficiently, including the simulation with interacting longshore and cross-shore processes, without the need for detailed bathymetric data.

The interaction of cross-shore and longshore sediment transport processes has a positive effect on the predictive skill of the coupled model with respect to the coastline evolution in the IJmuiden case. The coastline change is predicted more accurate when cross-shore sediment transport processes are taken into account. The coupled model consists of two model components that both attribute to uncertainties and errors in the predicted coastline and coastal profile evolution, and therefore the coupled model was expected to predict the volumetric evolution of beaches and dunes and the evolution of coastline position less accurate. However, when the coastline change predicted by the coupled model is compared to the change simulated by the CL-model, it can be observed that the effect of cross-shore sediment transport processes on the modeled coastline change is positive and the coastline position is better predicted by the coupled model.

The coupled model allows for the alongshore redistribution of nourished sediment. This is very relevant, because the CS-model underestimated dune growth in profiles adjacent to nourished areas in the previous study of the IJmuiden case conducted by Hallin, Huisman, et al. (2019). This was expected to be related to the absence of longshore redistribution of the nourished volumes in the model. The present coupled model represents this behaviour and the results in Figures 5.14, 5.15 and 5.19 show that the dune growth is not underestimated by the coupled model in these profiles. Furthermore, excluding the cross-shore transport of nourishments from the beach towards the dunes leads to an overestimation of the coastline change near the nourishments. The coupled model proved to simulate the coastline evolution more accurately along nourished parts of the coastline compared to the CL-model, presumably due to the inclusion of cross-shore redistribution of nourishments. The model results show that the coupled model is able to simulate the longshore and cross-shore redistribution of nourishments and that the coupling improves the predictive skill of both model components regarding the simulation of the effect of nourishments.

6.2. Recommendations

6.2.1. Recommendations on improvements of the model

In the CS-model component, deep-water wave conditions are used to obtain the amount of dune erosion. For the CL-model component, shallow-water wave conditions are determined by using a built-in random wave propagation and decay model, which transforms offshore wave data to the coast taking the principal processes of linear refraction and non-linear dissipation by wave breaking and bottom friction into account (Deltares, 2011). It should be studied whether it is possible to rewrite the dune erosion formulation to shallow-water wave condition forcing, because this would reduce the amount of different wave data the coupled model demands.

Furthermore, the CS-model component requires a time series of wind, wave and water level conditions, whereas the CL-model component enables the use of climates. Implementing climates instead of time-series as forcing in the CS-model component will result in a more trend-like simulation of the beach and dune volume evolution when compared with the evolution under timeseries of forcing. Enabling the definition of climates instead of timeseries makes it easier to change the forcing (i.e. in case of climate change) and it will make the coupling between the model components more robust since they will consequently use the same input data. It is likely that the computational time will decrease as well. In conclusion, it is recommended to study whether the CS-model can be modified in such a way that it is possible to use the wind, wave and water level climates – defined in the CL-model component– in the CS-model component.

For the nourishments, site specific data on the decay rates is used in the present study. To improve the model and enlarge its applicability, an empirical formulation should be implemented. Initially, the linear decay rates found in the research of Huisman et al. (2019) could be used. Besides the decay rates, losses in shoreface nourishments are supposed to be formulated as well.

6.2.2. Recommendations on future application and research

For future research it is recommended to use the coupled model to look into nourishment strategies and their effectiveness on the long-term, because the model includes the effect of longshore spreading of shoreface and beach nourishments and it could therefore be used to evaluate the effectiveness of various nourishment strategies, especially when the impact on dune growth and resilience is a relevant aspect.

Furthermore, the coupled model is useful for the simulation of various climate change scenarios and their effect on decadal to centennial scale dune and beach evolution. Because climate change consists of the combination of various effects (e.g. mean sea level rise, increased storm intensity, longer periods of draught and precipitation), the relative impact of these effects on the larger scale dune and beach evolution should be examined with models that can deal with these processes. Climate change related effects induce cross-shore and longshore transport processes, the coupled model is applicable for this kind of research. This study would provide insight into the consequences of climate change on the coastal zone, but also enables the design of targeted adaptation measures.

Lastly, the importance of the various longshore and cross-shore transport mechanisms on the large scale dune and beach evolution can be studied using the coupled model, by including and excluding their effect for several cases. The effect of still not well-known processes (e.g. wind-driven) can also be better researched with the coupled model. Especially combined with the effects of nourishments and climate change, one could use the coupled model to determine the relative impact of the various transport mechanisms on the long-term dune and beach development and therewith improve humans capability to predict future developments and adapt to the changing climate.

<div align="right">

7

</div>

<div align="right">

Conclusion

</div>

In the conclusion, the research questions presented in Section 1.3 are answered in order to conclude this thesis. Thereafter, the present research is summarized and the method and process are reflected on. Next, limitations of the coupled model are discussed.

7.1. Answers to research questions

SQ1 - "Does the coupled model simulate the effect of longshore sediment transport, dune erosion, aeolian transport, nourishments and sea level rise on the shoreline and dune volume evolution in accordance with the sediment balance?"

The results of the model testing for a simplified model with only two grid cells in the longshore beach component (referred to as the CL-model component) and only one profile in the cross-shore dune component (referred to as the CS-model), which are presented in Chapter 4, show that for all test cases the sediment fluxes between the model components are balanced. The coupled model is simulating the relevant processes – i.e. longshore sediment transport and the effect of gradients on coastline and dune evolution, dune build-up by aeolian transport, dune erosion during storms and the associated deposition of sediment on the beach, nourishments and their distribution over the beach and dunes and sea level rise with its subsequent erosion of sediment from beach and dune – in accordance with the sediment balance.

Sediment is completely conserved in the simple cases. The cases with multiple cross-shore profiles and 26 grid cells in the CL-model component do, however, show results which differ depending on the number of cross-shore (CS-model) profiles that are used. For these test cases, the linear interpolation that the coupled model uses to obtain the volume changes in the grid cells between the cross-shore profile locations has an effect on the accuracy of the outcome of the models, especially in case of non-linear behaviour. It is therefore important to define a sufficient number of cross-shore profiles close to each other on most dynamic parts of the coastal stretch under consideration. Furthermore, the processes of longshore sediment transport gradients causing coastline erosion or accretion and dune build-up may give rise to inaccuracies, even though the found deviations from sediment conservation are small. If a minimum of one cross-shore profile is defined along every kilometer of coastline in an academic case, the maximum sediment deficit between the theoretical and the simulated sediment fluxes including all processes mentioned is 0.5% and the precision of simulated coastline position is 8 cm. Therefore, the inaccuracies found during model testing are small enough to assess the coupled model to be sediment conserving.

SQ2 - "How well does the coupled model perform when compared to field data?"

The coupled model is used to hindcast the 22-year long dune and beach evolution along the coast of IJmuiden. The description and results of the application of the coupled model on the IJmuiden case can be found in Chapter 5. The model performance is evaluated using the coefficient of determination

R^2, which describes the proportion of the measured variability that is explained by the model outcomes. An R^2 of 1 means that all variability in the data is described by the model and there is a perfect fit.

For the model calibration period from 1994 – 2010, the R^2 of the dune volume evolution is 0.6 and of the coastline evolution 0.82. Therefore, it can be concluded that the model performs well during the simulation of coastal behavior in this period. However, the coefficients of determination are 0.18 (for the dune volume evolution) and 0 (for the coastline evolution) in case the simulation covers the validation period of 2010 – 2016 only. These low coefficients of determination are analysed by deriving the coefficient of determination for the evolution of individual cross-shore profiles, the full 22-year long dune and coastline evolution and the coastal evolution during an alternative validation period.

The R^2 of the evolution of individual cross-shore profiles shows that the model performs reasonably when simulating linearly accreting cross-shore profiles. However, it predicts the behaviour of profiles that show alternating periods of accreting, eroding and stable dunes poorly. For the full 22-year long simulation, the coefficient of determination of the dune volume evolution is 0.69 and the R^2 of the coastline evolution is 0.7, illustrating the sufficient model performance. The alternative validation period (1994 – 2000) shows the expected effect of the length of the simulation, whereas the R^2 of both dune and coastline evolution are smaller when compared to the results of the simulation of the calibration period. Thus, the model performs unsatisfactory during model validation but it is expected that this is caused by the limited length of the validation period. With limited processes included in the coupled model, which focuses on long-term coastal development, longer simulations in the order of decadal to centennial timescales are needed to simulate the overall trends in bathymetric data. Therewith, it is concluded that the coastline evolution is not predicted very accurately, albeit with the right trend of coastline change, but the coupled model predicts the dune volume evolution satisfactory.

MQ - *"What are the forecasting capabilities of the coupled model for decadal to centennial scale coastline and dune evolution?"*

With the answer on both subquestions, the forecasting capabilities can be determined. Simulation of academic cases shows that the coupled model simulates cross-shore and longshore sediment transport processes and their interaction in accordance with the sediment balance, thus the implementation of the different sediment transport equations and their interaction in the coupled is technically correct. Hence, it is concluded that the coupled model has the capability to predict the decadal to centennial dune volume and coastline evolution under the effects of storm impact, aeolian transport, gradients in longshore sediment transport, nourishments and sea level rise. Application of the coupled model shows that the model components reinforce each other, since the inclusion of cross-shore effects positively affects the simulated coastline change and simulated longshore sediment transport gradients result in an adequate prediction of the evolution of the dune volume. Furthermore, the model is able to predict the longshore and cross-shore spreading of nourishments. In general, the expected trends in the coastal evolution can be captured with the coupled model.

7.2. Summary and reflection

The aim of this thesis was to develop a coupled surfzone-dune model, which is needed to quantify the long-term beach and dune evolution with interacting longshore and cross-shore processes. The present research consisted of the model coupling and description of the included processes and formulations, the model testing and model application including model calibration and validation. Relevant processes for the decadal to centennial scale beach and dune evolution are the combined effects of longshore sediment transport gradients, aeolian transport, dune erosion as a result of storm impact, nourishments and sea level rise. During model testing, these processes and their interaction were found to be simulated in accordance with the sediment balance.

After this model testing, the model was applied on the IJmuiden case. During model application, the prediction of the coastline evolution is found to improve by the coupling of the model components, because of the positive effect of the inclusion of cross-shore distribution of nourishments. Furthermore,

dune volume evolution is predicted satisfactory when longshore sediment transport gradients are simulated instead of derived from data. The beach and dune evolution vary strongly, also in the data, and therefore the model performance illustrates the reasonable forecasting capabilities of the coupled model.

Reflecting on the process, the model is found to quantitatively and qualitatively perform satisfactory and therefore is considered a useful means to quantify long-term beach and dune evolution with interacting longshore and cross-shore processes.

7.3. Limitations of the coupled model

The main limitation of the coupled model is the CS-model components dependency on data. The model specific parameters need to be calibrated for every case, which is only possible with sufficient quantative and qualitative data. In the model testing phase of this study, it is found that the coupled model is performing best if at least one cross-shore profile is defined along every kilometer of coastline simulated with the model in order to limit the negative effect of the linear interpolation of volume exchanges between the defined cross-shore profiles. This recommended minimum number of cross-shore profiles amplifies the need for data.

Bibliography

Bagnold, R. A. (2012). *The physics of blown sand and desert dunes*. Courier Corporation.

Bakker, M. A., van Heteren, S., Vonhögen, L. M., van der Spek, A. J., & Van der Valk, B. (2012). Recent coastal dune development: Effects of sand nourishments. *Journal of Coastal Research*, *28*(3), 587–601.

Battjes, J. A., & Janssen, J. (1978). Energy loss and set-up due to breaking of random waves. In *Coastal engineering 1978* (pp. 569–587).

Booij, N., Ris, R. C., & Holthuijsen, L. H. (1999). A third-generation wave model for coastal regions: 1. model description and validation. *Journal of geophysical research: Oceans*, *104*(C4), 7649–7666.

Bosboom, J., & Stive, M. J. F. (2011). *Coastal dynamics*. Lecture Notes CT4305. VSSD.

Bruun, P. (1954). *Coast erosion and the development of beach profiles*. US Beach Erosion Board.

Bruun, P. (1962). Sea-level rise as a cause of shore erosion. *Journal of the Waterways and Harbors division*, *88*(1), 117–132.

Christiansen, M. B., & Davidson-Arnott, R. (2004). Rates of landward sand transport over the foredune at skallingen, denmark and the role of dune ramps. *Geografisk Tidsskrift-Danish Journal of Geography*, *104*(1), 31–43.

Crossland, C. J., Kremer, H. H., Lindeboom, H., Crossland, J. I. M., & Tissier, M. D. A. L. (2005). *Coastal Fluxes in the Anthropocene - The Land-Ocean Interactions in the Coastal Zone Project of the International Geosphere-Biosphere Programme*. doi:10.1007/3-540-27851-6

De Ruig, J. H. (1998). Coastline management in the netherlands: Human use versus natural dynamics. *Journal of Coastal Conservation*, *4*(2), 127–134.

Deltares. (2011). Unibest-cl+ manual: Manual for version 7.1 of the shoreline model unibest-cl. Deltares Delft, The Netherlands.

Fryslān, P., Noord-Holland, P., Zeeland, P., & Zuid-Holland, P. (2011). Ruimte voor recreatie op het strand.

Guillén, J., Stive, M., & Capobianco, M. (1999). Shoreline evolution of the holland coast on a decadal scale. *Earth Surface Processes and Landforms: The Journal of the British Geomorphological Research Group*, *24*(6), 517–536.

Hallin, C., Huisman, B. J., Larson, M., Walstra, D. J. R., & Hanson, H. (2019). Impact of sediment supply on decadal-scale dune evolution — Analysis and modelling of the Kennemer dunes in the Netherlands. *Geomorphology*, *337*, 94–110. doi:10.1016/j.geomorph.2019.04.003

Hallin, C., Larson, M., & Hanson, H. (2019). Simulating beach and dune evolution at decadal to centennial scale under rising sea levels. *PLoS ONE*, *14*(4), 1–30. doi:10.1371/journal.pone.0215651

Hanson, H., Larson, M., & Kraus, N. C. (2010). Calculation of beach change under interacting cross-shore and longshore processes. *Coastal Engineering*, *57*(6), 610–619.

Hesp, P. (2002). Foredunes and blowouts: Initiation, geomorphology and dynamics. *Geomorphology*, *48*, 245–268. doi:10.1016/S0169-555X(02)00184-8

Huisman, B., Walstra, D.-J., Radermacher, M., De Schipper, M., & Ruessink, G. (2019). Observations and modelling of shoreface nourishment behaviour. *Journal of Marine Science and Engineering*, *7*, 59. doi:10.3390/jmse7030059

KNMI. (2021). Klimaatviewer. https://www.knmi.nl/klimaat-viewer/kaarten/wind/gemiddelde-windsnelheid/jaar/Periode_1981-2010.

Kraus, N. C., Larson, M., & Wise, R. A. (1998). *Depth of closure in beach-fill design*. Army Engineer Waterways Experiment Station Vicksburg MS.

Larson, M., Donnelly, C., Jiménez, J. A., & Hanson, H. (2009). Analytical model of beach erosion and overwash during storms. In *Proceedings of the institution of civil engineers-maritime engineering* (Vol. 162, *3*, pp. 115–125). Thomas Telford Ltd.

Larson, M., Erikson, L., & Hanson, H. (2004). An analytical model to predict dune erosion due to wave impact. *Coastal Engineering*, *51*(8-9), 675–696.

Lettau, K., & Lettau, H. (1978). Experimental and micrometeorological field studies of dune migration. *Exploring in the World's driest climate*, 110–147.

Luijendijk, A., De Vroeg, H., Swinkels, C., & Walstra, D.-J. (2011). Coastal response on multiple scales: A pilot study on the ijmuiden port. In *The proceedings of the coastal sediments 2011: In 3 volumes* (pp. 602–615). World Scientific.

Luijendijk, A., Hagenaars, G., Ranasinghe, R., Baart, F., Donchyts, G., & Aarninkhof, S. (2018). The State of the World's Beaches. *Scientific Reports*, *8*(1), 1–11. doi:10.1038/s41598-018-24630-6

Mulder, J. (2000). Zandverliezen in het nederlandse kustsysteem: Advies voor dynamisch handhaven in de 21e eeuw. *rapport RIKZ/2000.36*.

Neumann, B., Vafeidis, A. T., Zimmermann, J., & Nicholls, R. J. (2015). Future coastal population growth and exposure to sea-level rise and coastal flooding - A global assessment. *PLoS ONE*, *10*(3). doi:10.1371/journal.pone.0118571

Nicholls, R. J., Wong, P. P., Burkett, V., Codignotto, J., Hay, J., McLean, R., … Arblaster, J., et al. (2007). Coastal systems and low-lying areas.

Overton, M., Fisher, J., & Young, M. (1988). Laboratory investigation of dune erosion. *Journal of Waterway, Port, Coastal, and Ocean Engineering*, *114*(3), 367–373.

Pelnard-Considère, R. (1957). Essai de theorie de l'evolution des formes de rivage en plages de sable et de galets. *Journées de l'hydraulique*, *4*(1), 289–298.

Prandtl, L. (1933). Neuere ergebnisse der turbulenzforschung. *Z. vdi*, *77*(5), 105–114.

Provincie Noord-Holland. (2012). Atlas van de Natura 2000 duingebieden van Noord-Holland., 126.

Psuty, N. P. (1988). Sediment budget and dune/beach interaction. *Journal of coastal research*.

Rijkswaterstaat. (2017). De jaarlijkse kustmetingen.

Roelvink, D. J., & Reniers, A. (2011). *A guide to modeling coastal morphology*. doi:10.1142/9789814304269_0006

Rosati, J. D., Dean, R. G., & Walton, T. L. (2013). The modified bruun rule extended for landward transport. *Marine Geology*, *340*, 71–81.

Sallenger Jr, A. H. (2000). Storm impact scale for barrier islands. *Journal of Coastal Research*, 890–895.

Sauermann, G., Kroy, K., & Herrmann, H. J. (2001). Continuum saltation model for sand dunes. *Physical Review E*, *64*(3), 031305.

Smith, S., & Banke, E. (1975). Variation of the sea surface drag coefficient with wind speed. *Quarterly Journal of the Royal Meteorological Society*, *101*(429), 665–673.

Spanhoff, R., & van de Graaff, J. (2007). Towards a better understanding and design of shoreface nourishments. In *Coastal engineering 2006: (in 5 volumes)* (pp. 4141–4153). World Scientific.

Stolk, A. (1989). *Zandsysteem kust: Een morfologische karakterisering*. Rijkswaterstaat (RWS), Ministerie van Verkeer en Waterstaat.

TAW. (1984). Leidraad voor de beoordeling van de veiligheid van duinenals waterkering.

Van Der Spek, A., & Lodder, Q. J. (2015). A new sediment budget for the netherlands; the effects of 15 years of nourishing (1991-2005). In *The proceedings of the coastal sediments 2015*. World Scientific.

Van Rijn, L. C. (1997). Sediment transport and budget of the central coastal zone of holland. *Coastal Engineering*, *32*(1), 61–90.

van Thiel de Vries, J. (2009). *Dune erosion during storm surges*. Deltares select series. IOS Press. Retrieved from https://books.google.nl/books?id=0RVctfkjE4wC

van Verkeer en Waterstaat, M. (2021). Kustlijnkaarten 2020. www.kustlijnkaarten.nl. Rijkswaterstaat (RWS).

Vitousek, S., Barnard, P. L., Limber, P., Erikson, L., & Cole, B. (2017). A model integrating longshore and cross-shore processes for predicting long-term shoreline response to climate change. *Journal of Geophysical Research: Earth Surface*, *122*(4), 782–806. doi:10.1002/2016JF004065

Wijnberg, K. M. (2002). Environmental controls on decadal morphologic behaviour of the Holland coast. *Marine Geology*, *189*(3-4), 227–247. doi:10.1016/S0025-3227(02)00480-2

Williams, A. T., Rangel-Buitrago, N., Pranzini, E., & Anfuso, G. (2018). The management of coastal erosion. *Ocean and Coastal Management*, *156*, 4–20. doi:10.1016/j.ocecoaman.2017.03.022

Wright, L., & Short, A. (1984). Morphodynamic variability of beaches and surf zones, a synthesis. *Marine Geology*, *56*, 92–118.

Zingg, A. (1953). Wind tunnel studies of the movement of sedimentary material. In *Proceedings of the 5th hydraulic conference bulletin* (Vol. 34, pp. 111–135). Inst. of Hydraulics Iowa City.

A
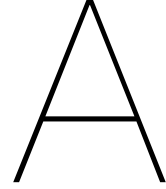
Appendix

A.1. Longshore sediment transport gradients for the CS-model simulation of the IJmuiden case

Longshore sediment transport gradients		
Profile	LST gradient [m^3/s/m]	LST gradient corrected for nourishments [m^3/s/m]
1	2.0424×10^{-6}	2.0424×10^{-6}
2	2.2257×10^{-6}	2.2257×10^{-6}
3	1.887×10^{-6}	1.887×10^{-6}
4	2.0812×10^{-6}	2.0812×10^{-6}
5	1.6941×10^{-6}	1.6941×10^{-6}
6	1.9341×10^{-6}	1.9341×10^{-6}
7	1.7461×10^{-6}	1.7461×10^{-6}
8	1.8954×10^{-6}	1.8954×10^{-6}
9	1.6881×10^{-6}	1.6881×10^{-6}
10	1.3048×10^{-6}	1.3048×10^{-6}
11	1.0581×10^{-6}	1.0581×10^{-6}
12	1.0891×10^{-6}	1.0891×10^{-6}
13	7.0328×10^{-7}	7.0328×10^{-7}
14	6.6727×10^{-7}	6.6727×10^{-7}
15	7.7934×10^{-7}	7.7934×10^{-7}
16	7.3293×10^{-7}	9.8642×10^{-9}
17	7.4895×10^{-7}	2.589×10^{-8}
18	7.2926×10^{-7}	-4.2304×10^{-7}
19	5.3813×10^{-7}	-6.1416×10^{-7}
20	5.6085×10^{-7}	-5.9144×10^{-7}
21	5.3962×10^{-7}	-6.1268×10^{-7}
22	6.9664×10^{-7}	-4.5566×10^{-7}
23	6.5571×10^{-7}	-4.9659×10^{-7}
24	6.6003×10^{-7}	-1.0699×10^{-6}
25	5.4674×10^{-7}	-4.6008×10^{-7}
26	7.0739×10^{-7}	-2.9943×10^{-7}

Table A.1: Longshore sediment transport gradients for the IJmuiden case derived from observations, used by the CS-model in (previous) IJmuiden case studies (Hallin, Huisman, Larson, Walstra, & Hanson, 2019)

A.2. IJmuiden beach and dune evolution data
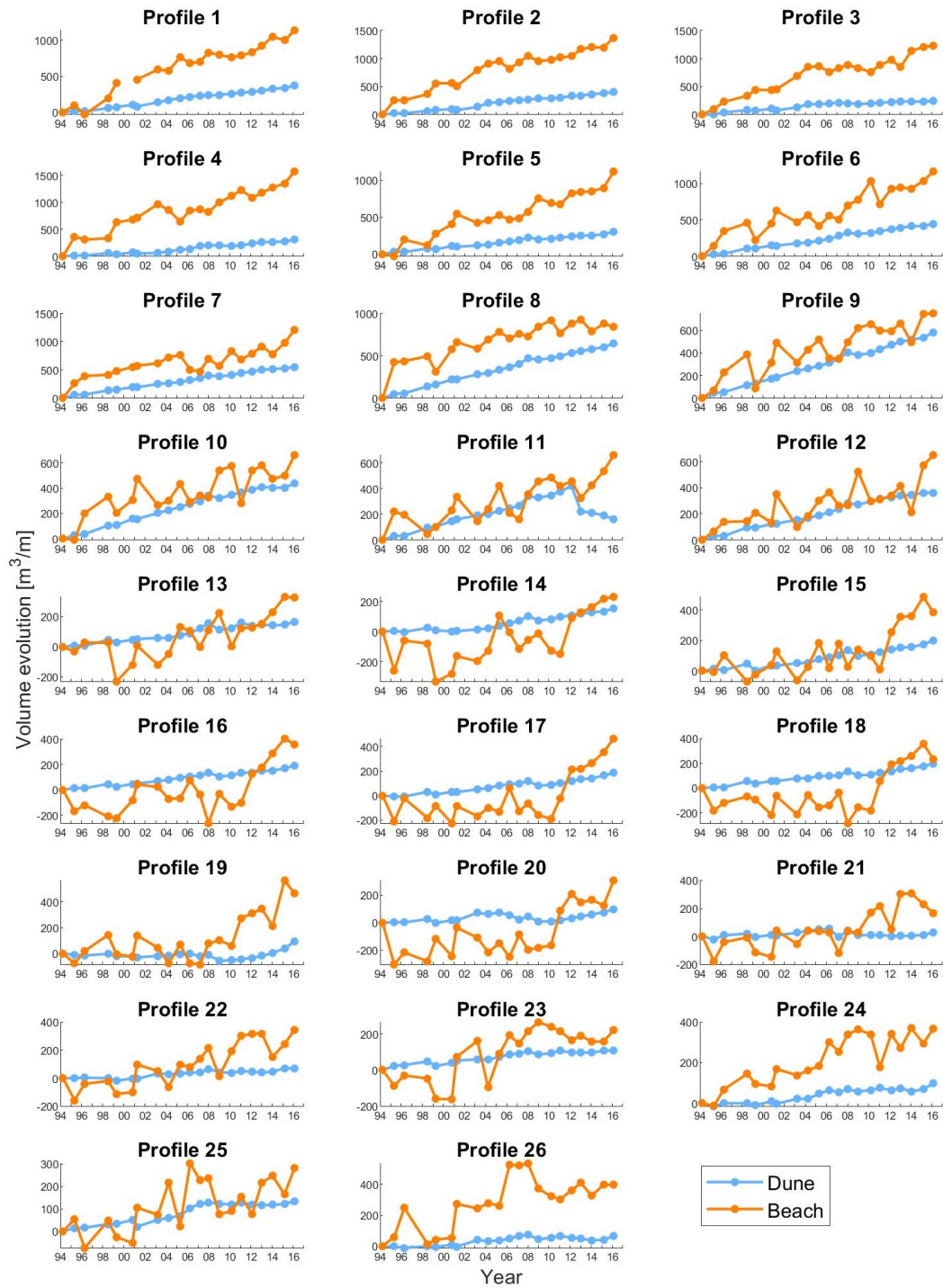
Figure A.1: Measured beach and dune evolution at the IJmuiden coast for the period of 1994 - 2016, derived from JARKUS data.

A.3. IJmuiden coastline evolution data
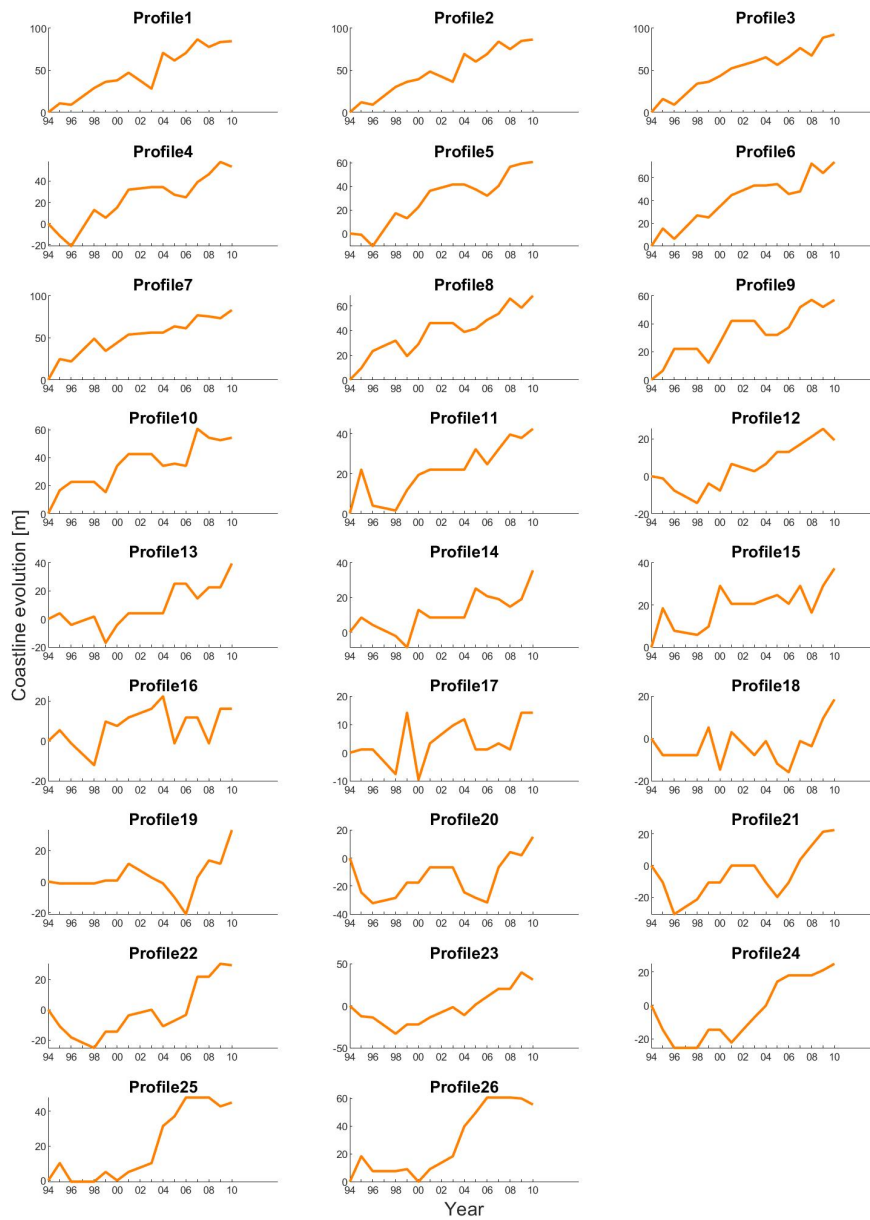
Figure A.2: Measured coastline evolution at cross-shore profiles 1–26 along the IJmuiden coast for the period of 1994 - 2016, derived from MKL-data
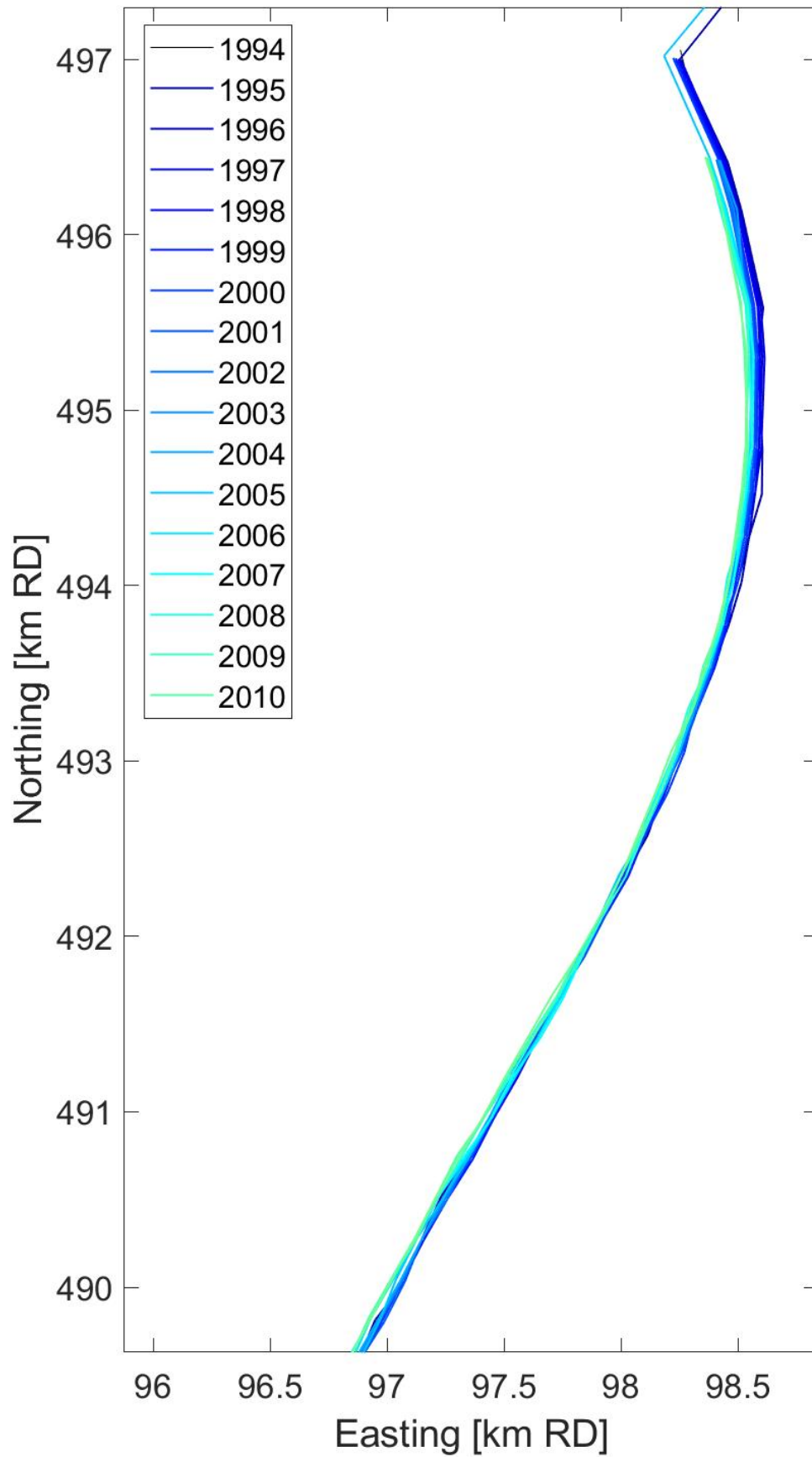
Figure A.3: Measured coastline evolution at the IJmuiden coast for the period of 1994 - 2016, derived from MKL-data

A.4. Simulated coastline position, effect of wind and tide
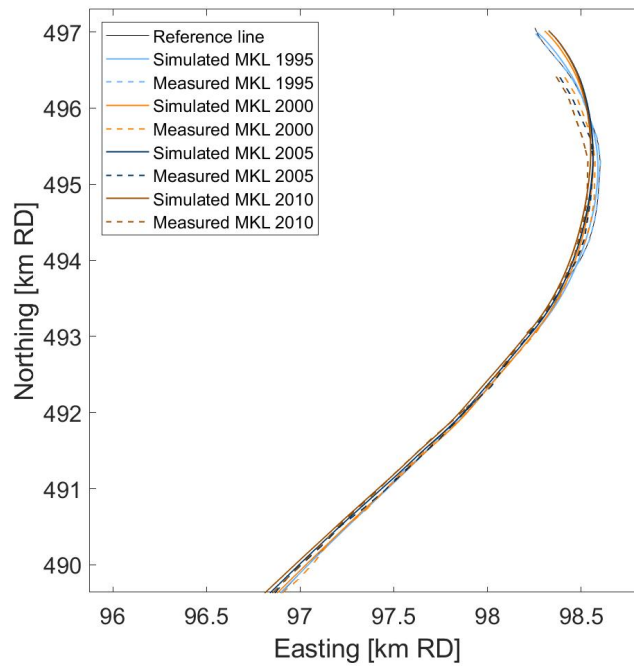
Figure A.4: Simulated and measured coastline change between 1994 and 2010; simulated coastline evolution under the effect of wave-induced longshore sediment transport only; measurements derived from MKL-data
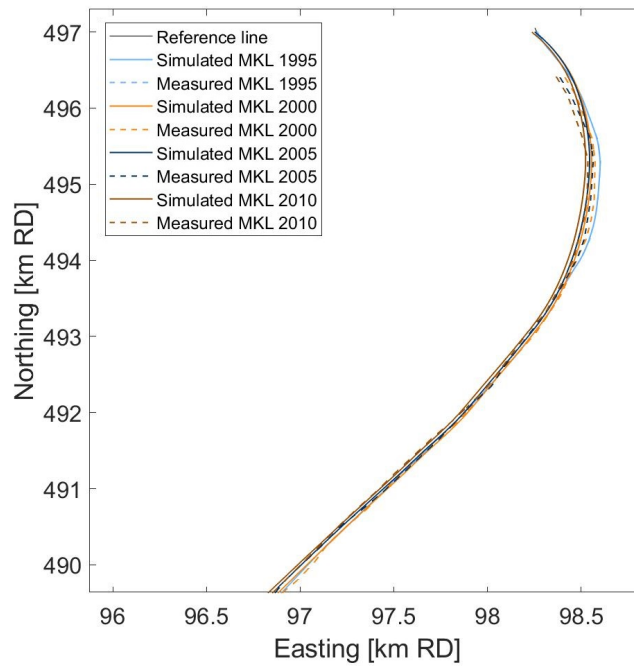
Figure A.5: Simulated and measured coastline change between 1994 and 2010; simulated coastline evolution under the effect of wind- and wave-induced longshore sediment transport; measurements derived from MKL-data
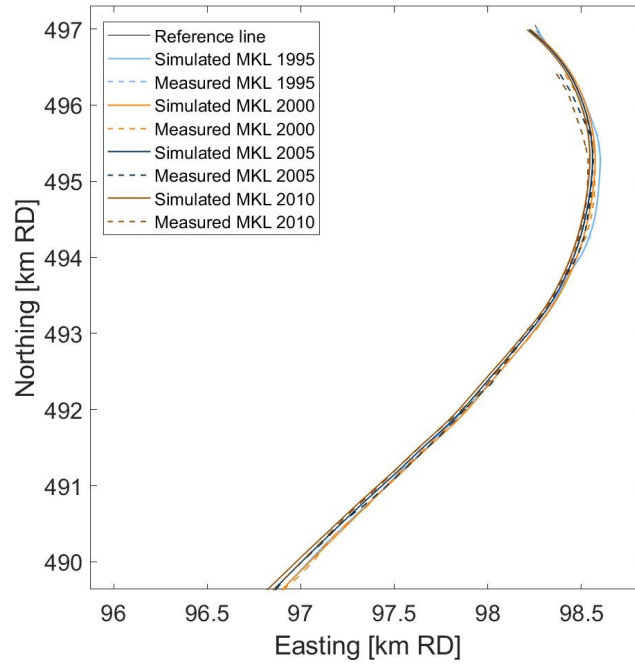
Figure A.6: Simulated and measured coastline change between 1994 and 2010; simulated coastline evolution under the effect of tidal- and wave-induced longshore sediment transport; measurements derived from MKL-data
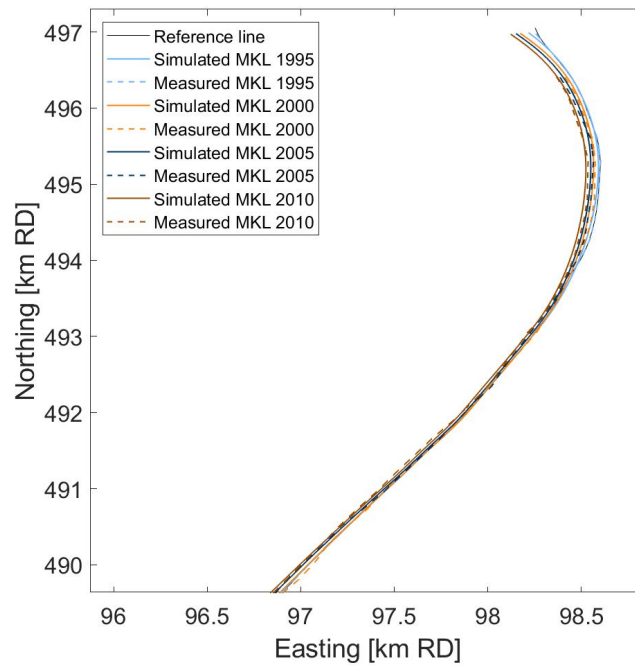
Figure A.7: Simulated and measured coastline change between 1994 and 2010; simulated coastline evolution under the effect of tidal-, wind- and wave-induced longshore sediment transport; measurements derived from MKL-data

A.5. Model results of simulation using wave data timeseries and static wave climate

In this Appendix the beach and dune volume change of the IJmuiden case are shown, simulated by the coupled model. The difference between the definition of a full timeseries of wave data and a static wave climate is illustrated by depicting the simulated dune and beach volume evolution simulated in both cases.
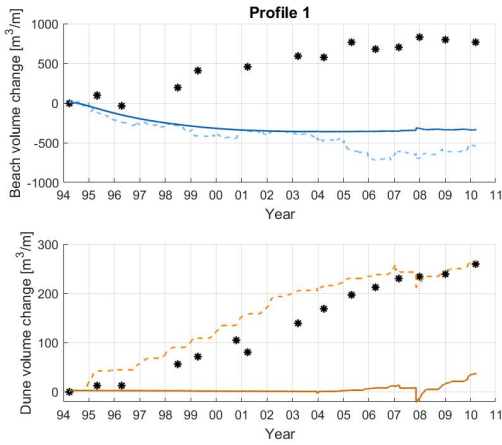
Figure A.8: Simulated and observed dune and beach volume evolution in cross-shore profile 1 for 1994-2010
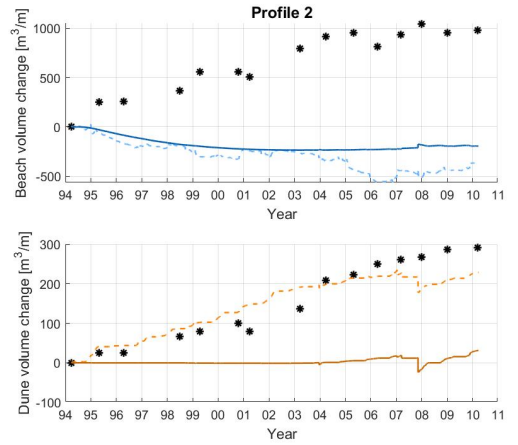
Figure A.9: Simulated and observed dune and beach volume evolution in cross-shore profile 2 for 1994-2010
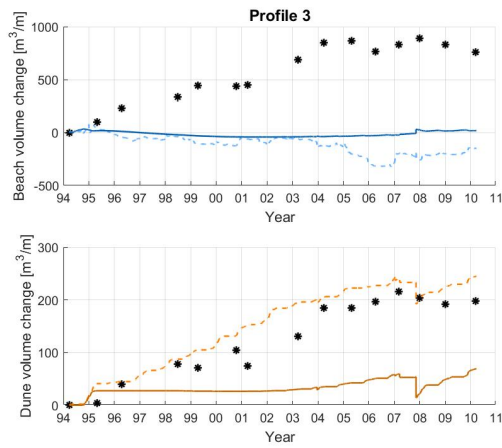
Figure A.10: Simulated and observed dune and beach volume evolution in cross-shore profile 3 for 1994-2010
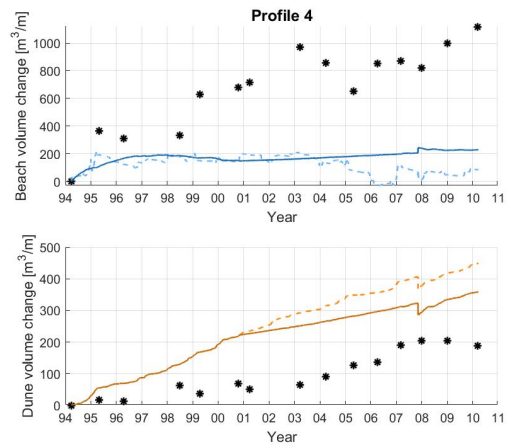
Figure A.11: Simulated and observed dune and beach volume evolution in cross-shore profile 4 for 1994-2010
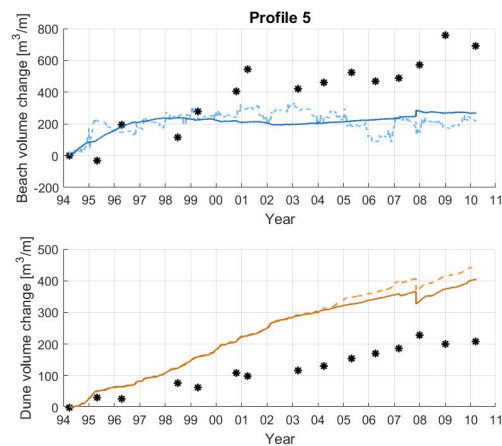
Figure A.12: Simulated and observed dune and beach volume evolution in cross-shore profile 5 for 1994-2010
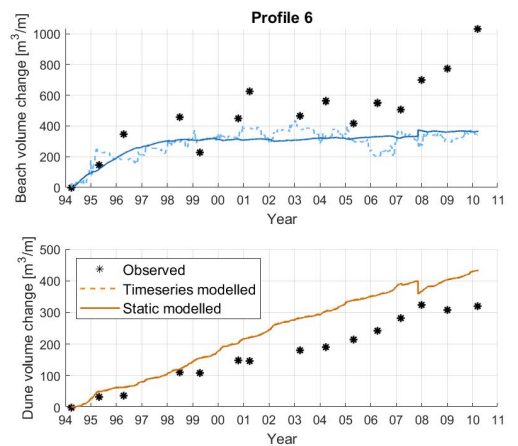
Figure A.13: Simulated and observed dune and beach volume evolution in cross-shore profile 6 for 1994-2010
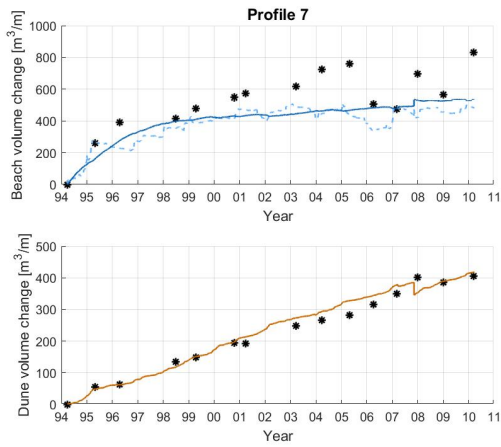
Figure A.14: Simulated and observed dune and beach volume evolution in cross-shore profile 7 for 1994-2010
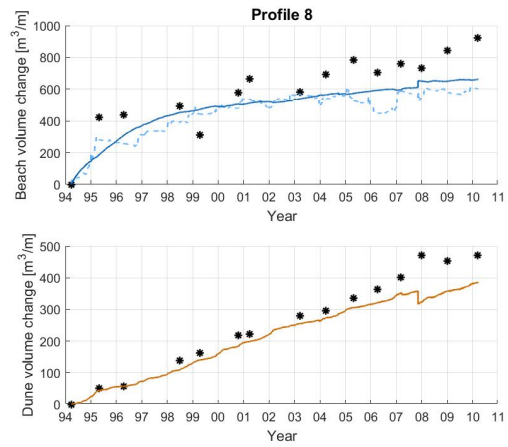
Figure A.15: Simulated and observed dune and beach volume evolution in cross-shore profile 8 for 1994-2010
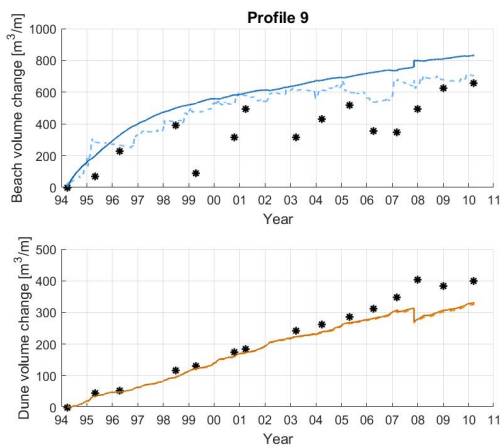
Figure A.16: Simulated and observed dune and beach volume evolution in cross-shore profile 9 for 1994-2010
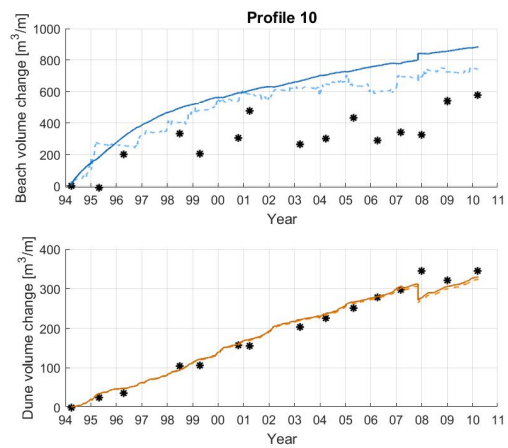
Figure A.17: Simulated and observed dune and beach volume evolution in cross-shore profile 10 for 1994-2010
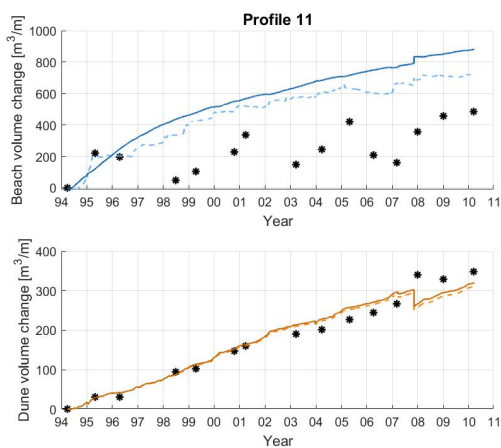
Figure A.18: Simulated and observed dune and beach volume evolution in cross-shore profile 11 for 1994-2010
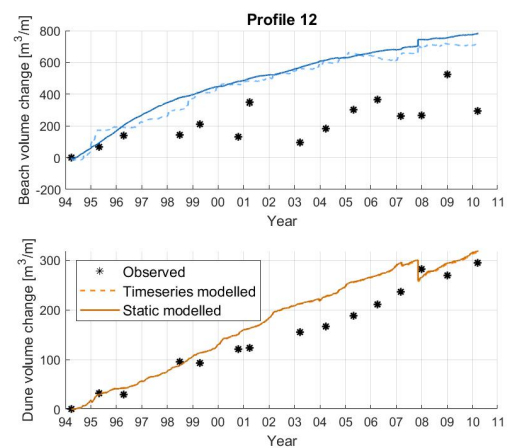
Figure A.19: Simulated and observed dune and beach volume evolution in cross-shore profile 12 for 1994-2010
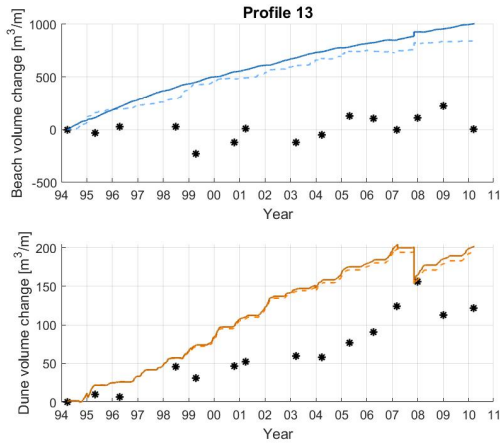
Figure A.20: Simulated and observed dune and beach volume evolution in cross-shore profile 13 for 1994-2010
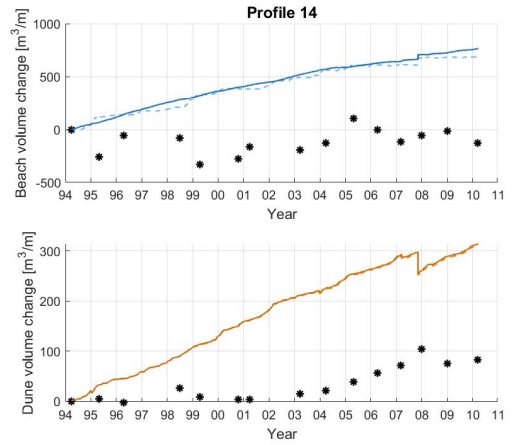
Figure A.21: Simulated and observed dune and beach volume evolution in cross-shore profile 14 for 1994-2010
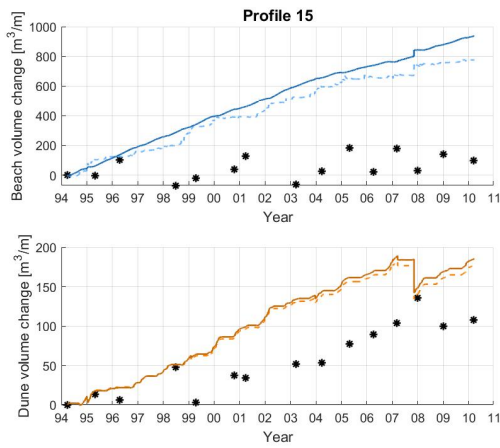
Figure A.22: Simulated and observed dune and beach volume evolution in cross-shore profile 15 for 1994-2010
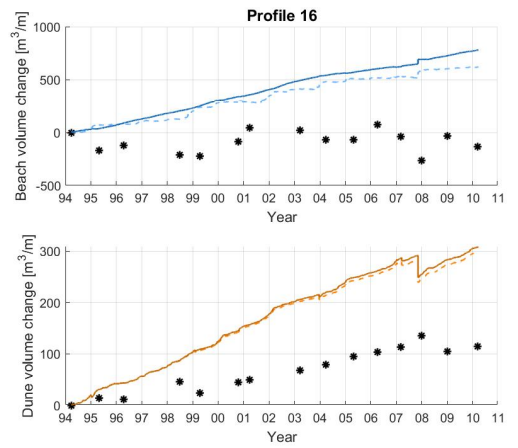
Figure A.23: Simulated and observed dune and beach volume evolution in cross-shore profile 16 for 1994-2010
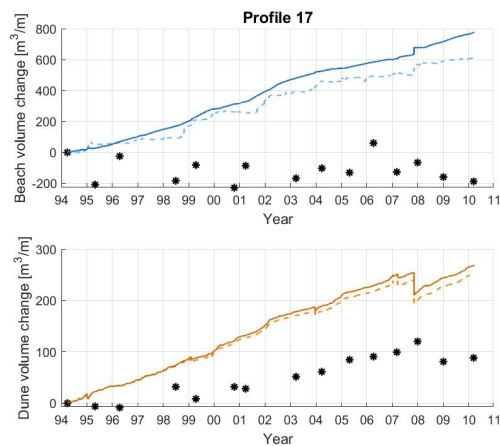
Figure A.24: Simulated and observed dune and beach volume evolution in cross-shore profile 17 for 1994-2010
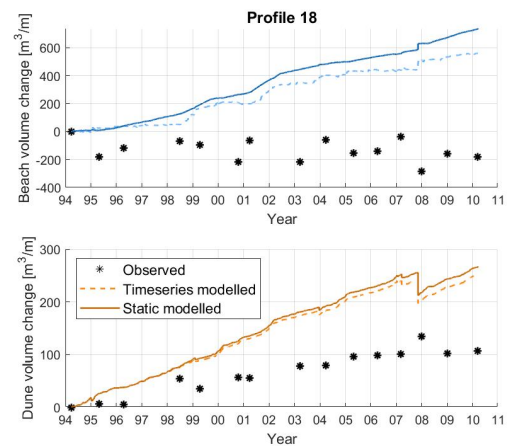
Figure A.25: Simulated and observed dune and beach volume evolution in cross-shore profile 18 for 1994-2010
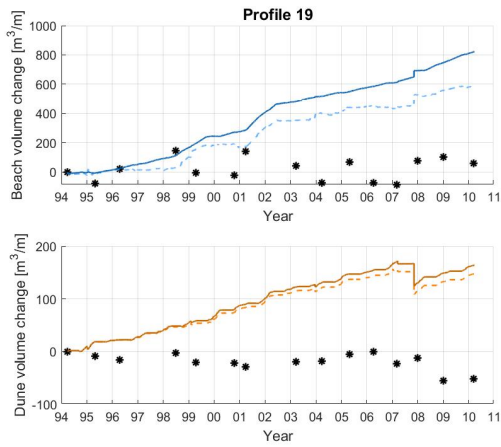
Figure A.26: Simulated and observed dune and beach volume evolution in cross-shore profile 19 for 1994-2010
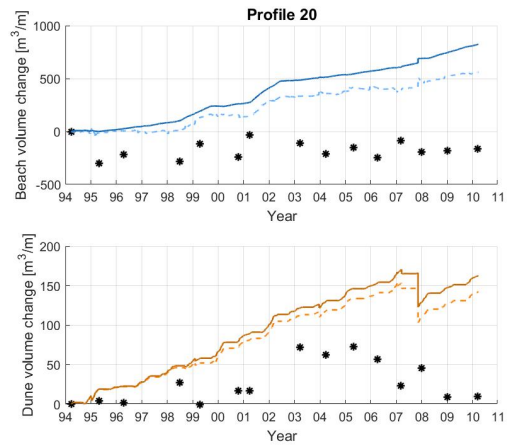
Figure A.27: Simulated and observed dune and beach volume evolution in cross-shore profile 20 for 1994-2010
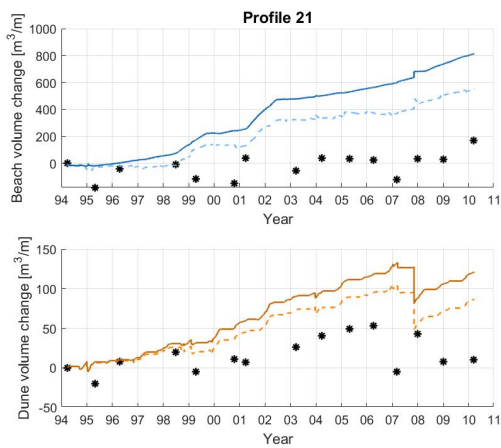
Figure A.28: Simulated and observed dune and beach volume evolution in cross-shore profile 21 for 1994-2010
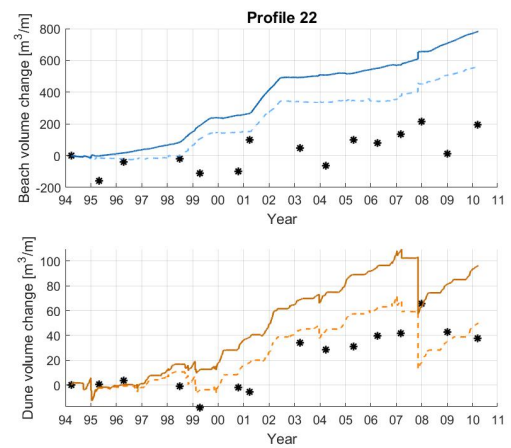
Figure A.29: Simulated and observed dune and beach volume evolution in cross-shore profile 22 for 1994-2010
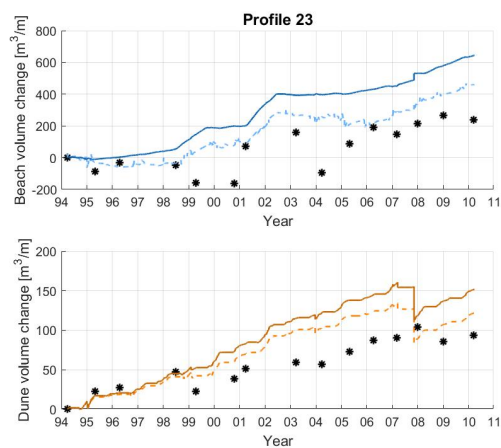
Figure A.30: Simulated and observed dune and beach volume evolution in cross-shore profile 23 for 1994-2010
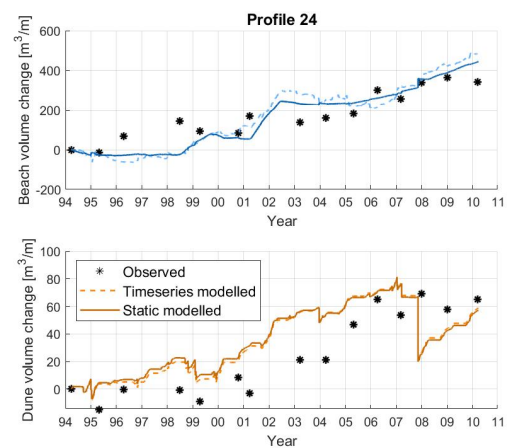
Figure A.31: Simulated and observed dune and beach volume evolution in cross-shore profile 24 for 1994-2010
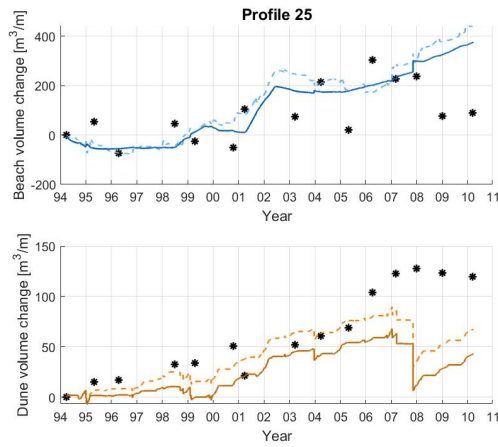
Figure A.32: Simulated and observed dune and beach volume evolution in cross-shore profile 25 for 1994-2010
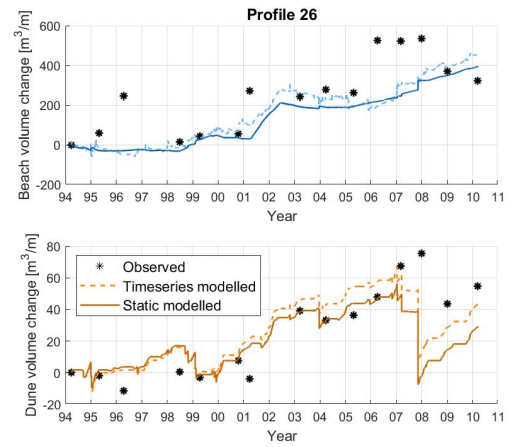
Figure A.33: Simulated and observed dune and beach volume evolution in cross-shore profile 26 for 1994-2010

A.6. Dune evolution of coupled model calibration

In this Appendix the dune volume change of the IJmuiden case are shown, simulated by the coupled model after model calibration. For referential purposes, the results of the CS-model and the data are depicted as well. The CS-model is used to simulate the IJmuiden case without longshore sediment transport gradients, with a constant longshore sediment transport gradient of 1×10^{-5} in every profile and with observed longshore sediment transport gradients.
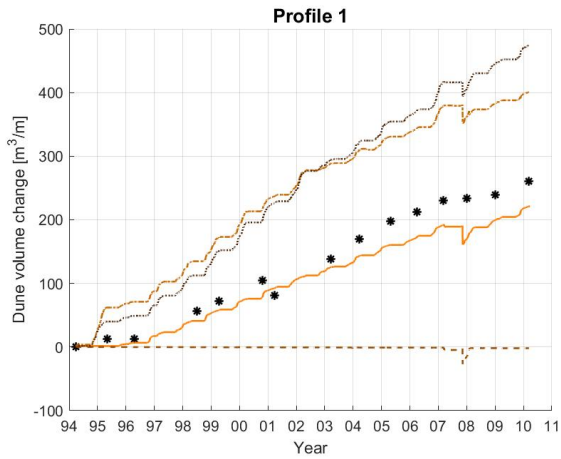
Figure A.34: Simulated and observed dune volume evolution in cross-shore profile 1 for 1994-2010
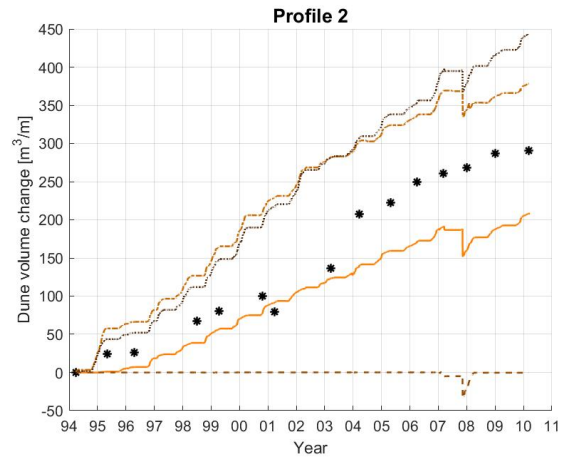
Figure A.35: Simulated and observed dune volume evolution in cross-shore profile 2 for 1994-2010
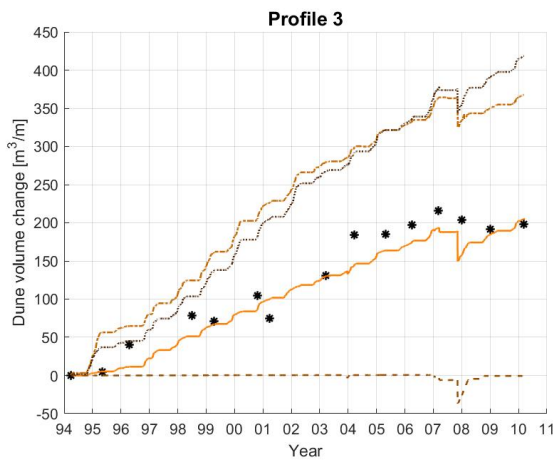
Figure A.36: Simulated and observed dune volume evolution in cross-shore profile 3 for 1994-2010
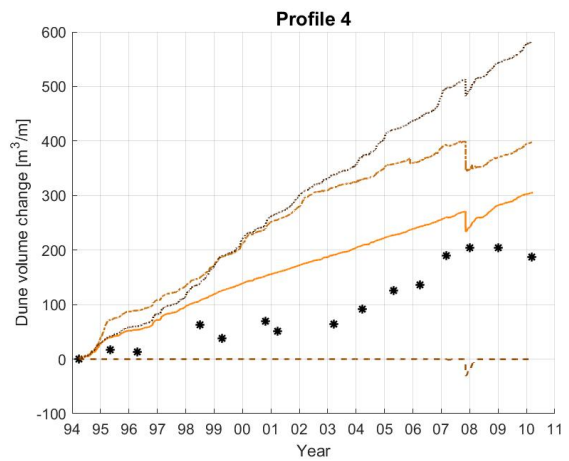
Figure A.37: Simulated and observed dune volume evolution in cross-shore profile 4 for 1994-2010
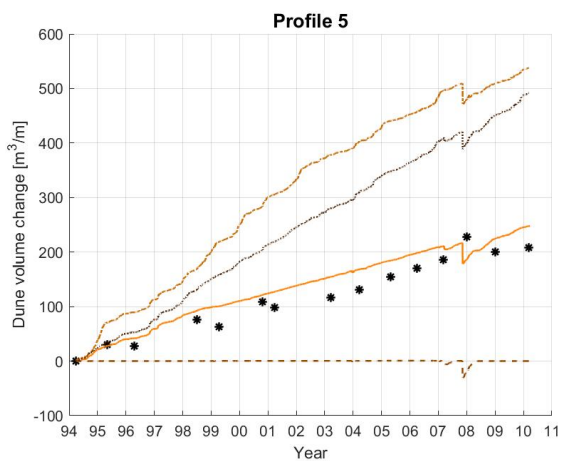
Figure A.38: Simulated and observed dune volume evolution in cross-shore profile 5 for 1994-2010
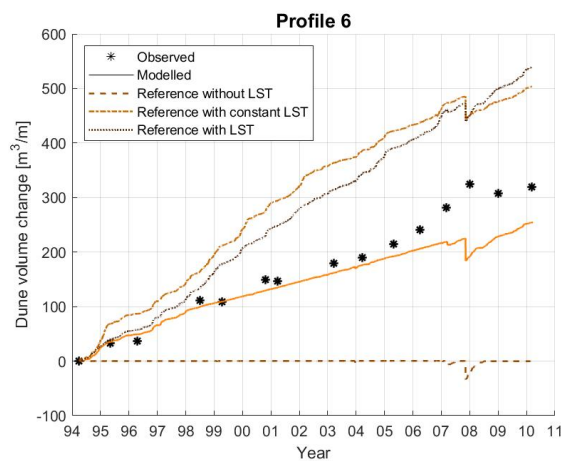
Figure A.39: Simulated and observed dune volume evolution in cross-shore profile 6 for 1994-2010
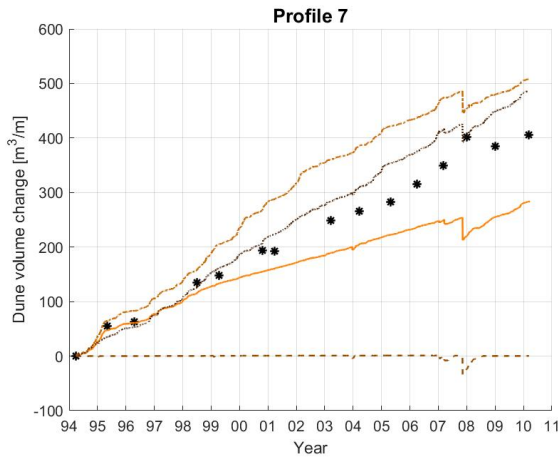
Figure A.40: Simulated and observed dune volume evolution in cross-shore profile 7 for 1994-2010
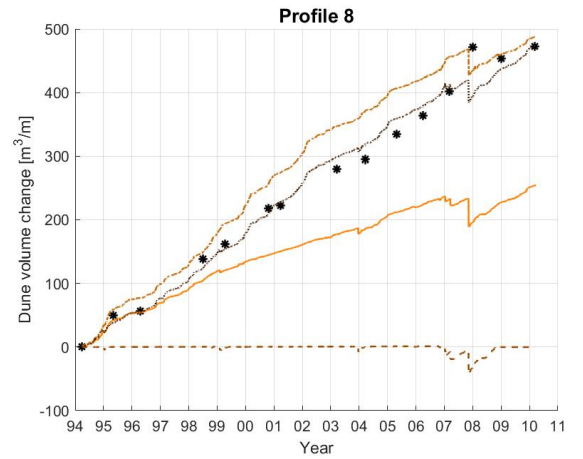
Figure A.41: Simulated and observed dune volume evolution in cross-shore profile 8 for 1994-2010
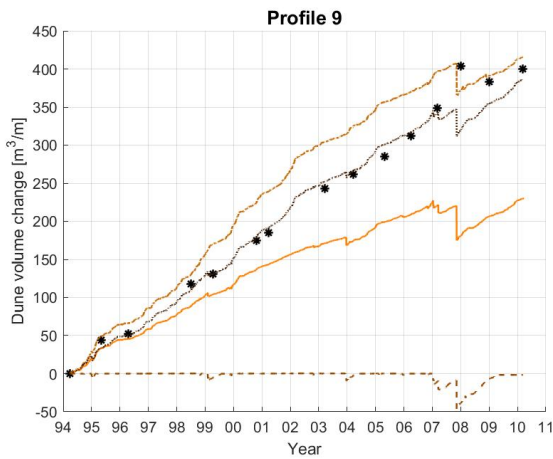
Figure A.42: Simulated and observed dune volume evolution in cross-shore profile 9 for 1994-2010
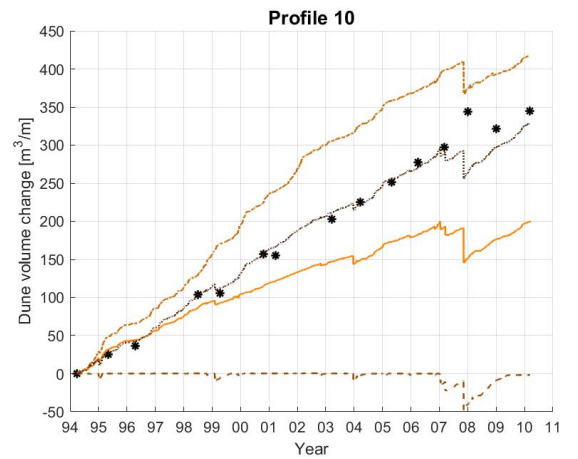
Figure A.43: Simulated and observed dune volume evolution in cross-shore profile 10 for 1994-2010
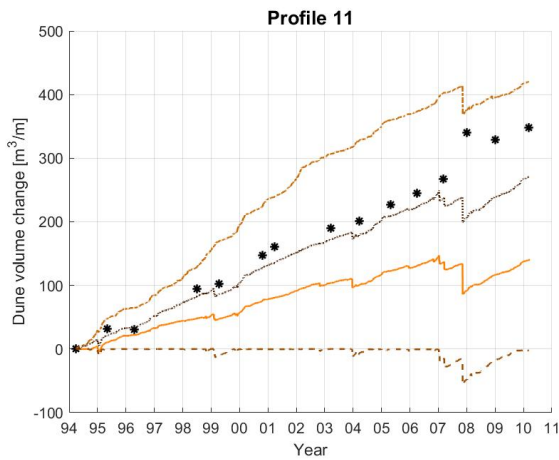
Figure A.44: Simulated and observed dune volume evolution in cross-shore profile 11 for 1994-2010
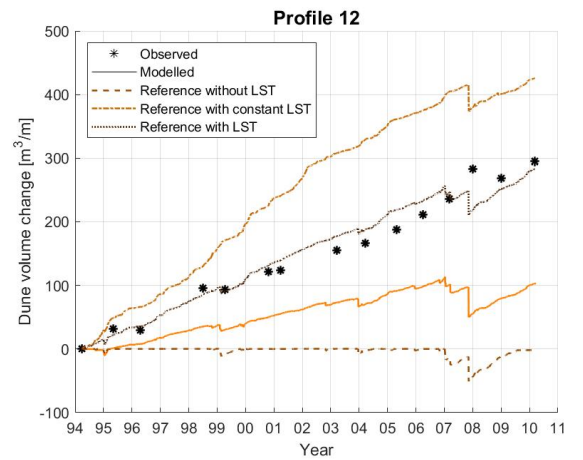
Figure A.45: Simulated and observed dune volume evolution in cross-shore profile 12 for 1994-2010
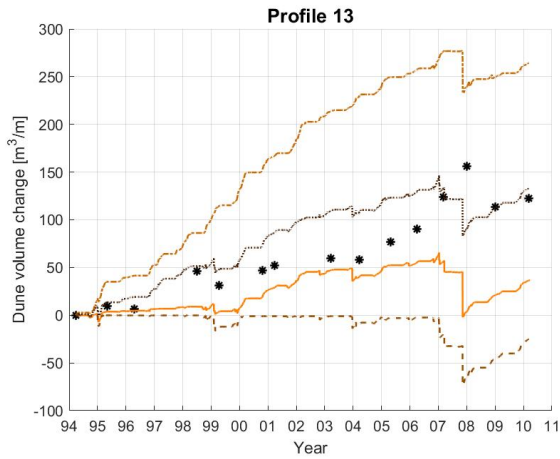
Figure A.46: Simulated and observed dune volume evolution in cross-shore profile 13 for 1994-2010
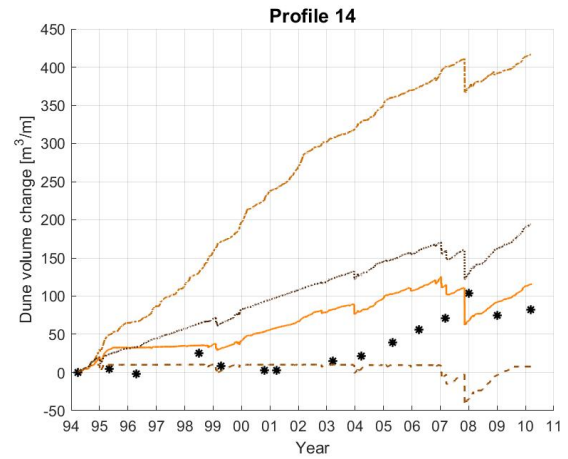
Figure A.47: Simulated and observed dune volume evolution in cross-shore profile 14 for 1994-2010
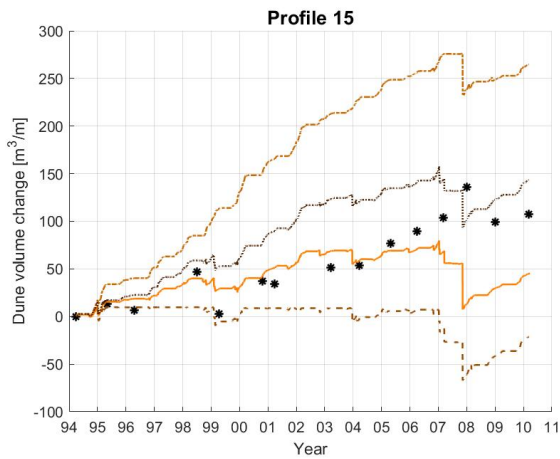
Figure A.48: Simulated and observed dune volume evolution in cross-shore profile 15 for 1994-2010
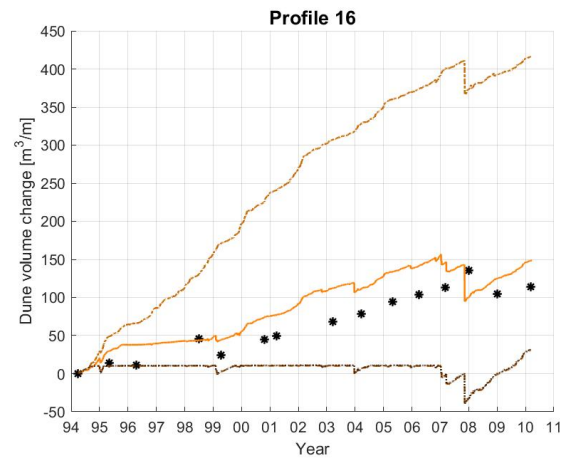
Figure A.49: Simulated and observed dune volume evolution in cross-shore profile 16 for 1994-2010
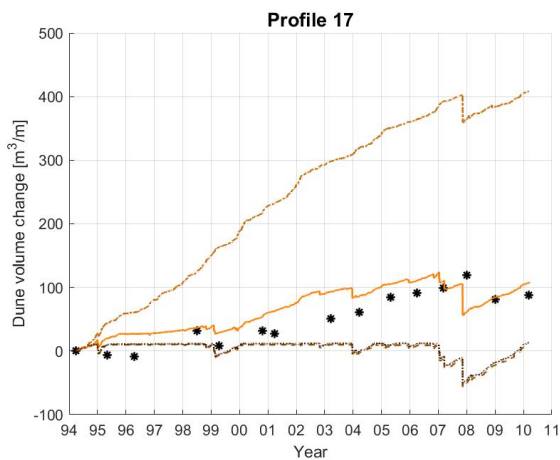
Figure A.50: Simulated and observed dune volume evolution in cross-shore profile 17 for 1994-2010
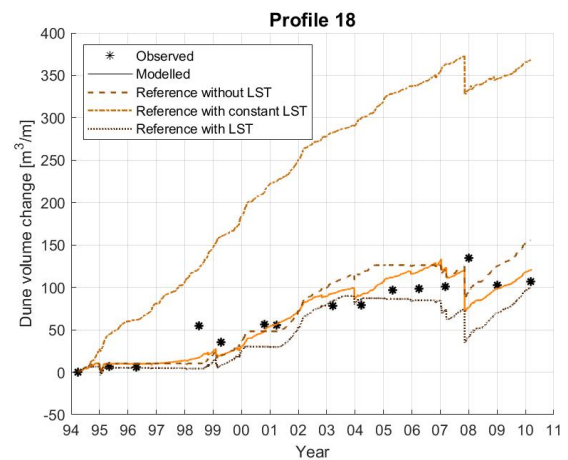
Figure A.51: Simulated and observed dune volume evolution in cross-shore profile 18 for 1994-2010
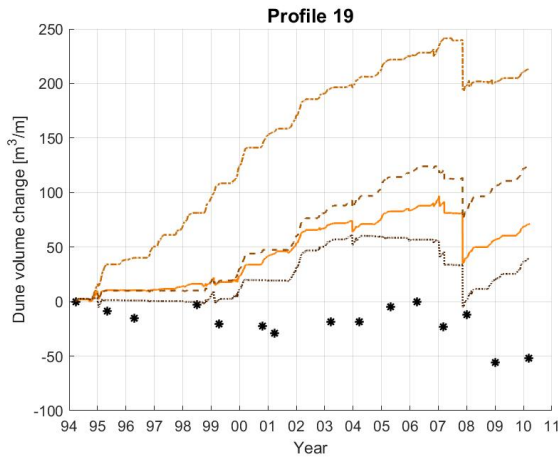
Figure A.52: Simulated and observed dune volume evolution in cross-shore profile 19 for 1994-2010
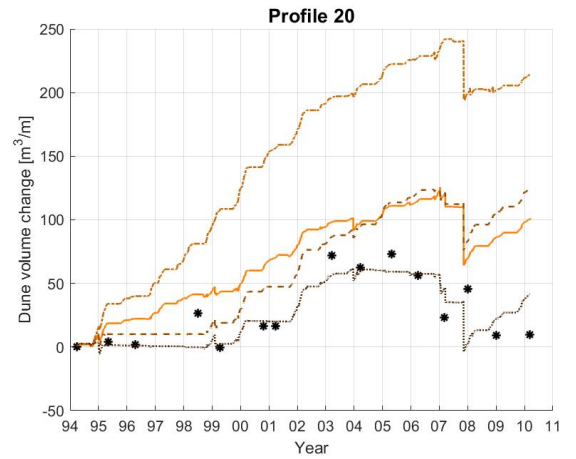
Figure A.53: Simulated and observed dune volume evolution in cross-shore profile 20 for 1994-2010
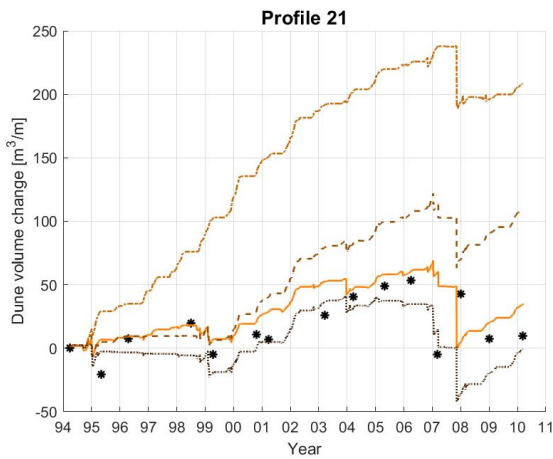
Figure A.54: Simulated and observed dune volume evolution in cross-shore profile 21 for 1994-2010
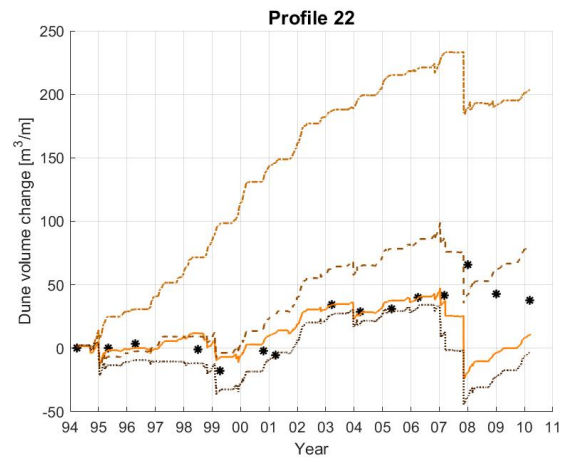
Figure A.55: Simulated and observed dune volume evolution in cross-shore profile 22 for 1994-2010
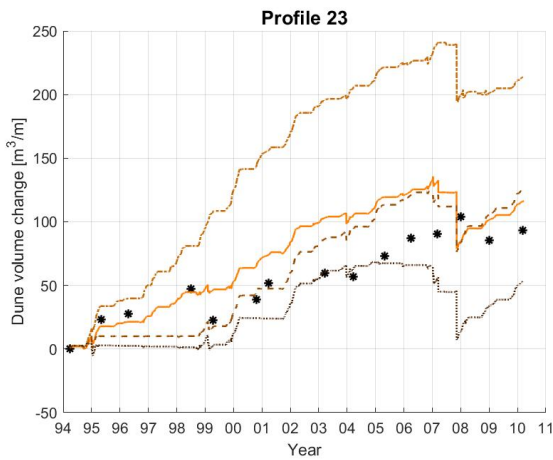
Figure A.56: Simulated and observed dune volume evolution in cross-shore profile 23 for 1994-2010
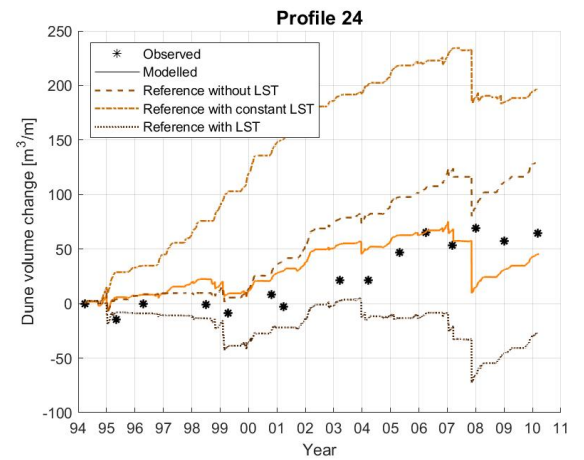
Figure A.57: Simulated and observed dune volume evolution in cross-shore profile 24 for 1994-2010
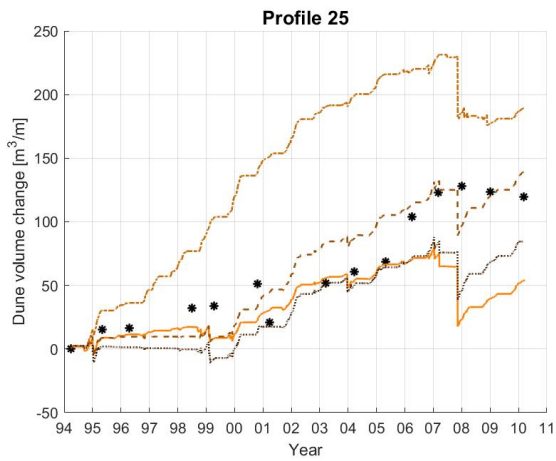
Figure A.58: Simulated and observed dune volume evolution in cross-shore profile 25 for 1994-2010
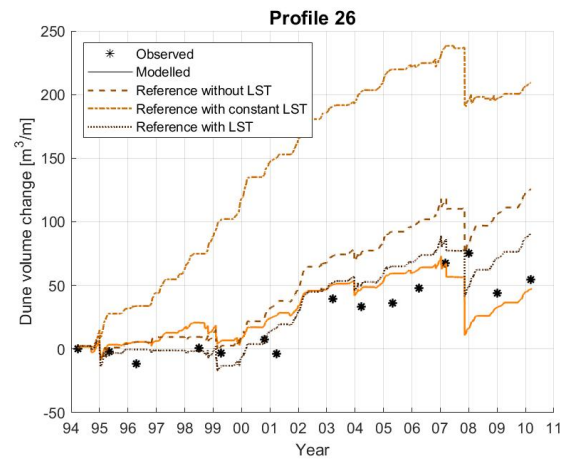
Figure A.59: Simulated and observed dune volume evolution in cross-shore profile 26 for 1994-2010

A.7. Coastline evolution of coupled model calibration

In this Appendix the coastline change of the IJmuiden case are shown, simulated by the coupled model after model calibration. For referential purposes, the results of the CL-model and the data are depicted as well.
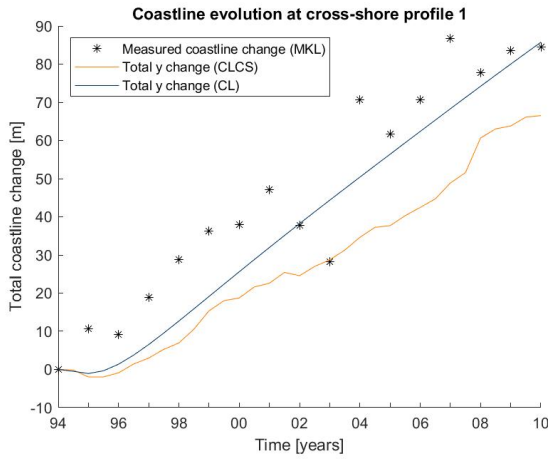
Figure A.60: Simulated and observed coastline evolution at cross-shore profile 1 between 1994-2010
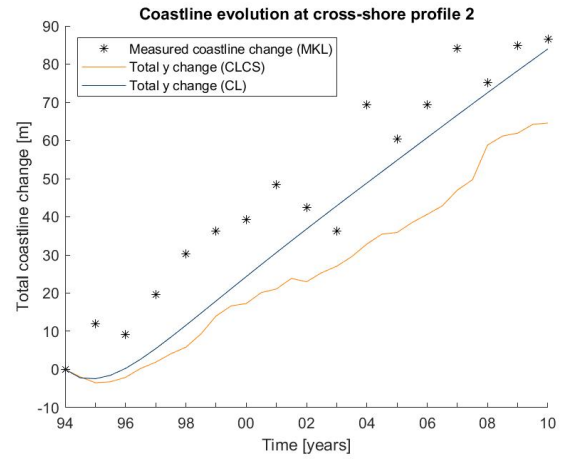
Figure A.61: Simulated and observed coastline evolution at cross-shore profile 2 between 1994-2010
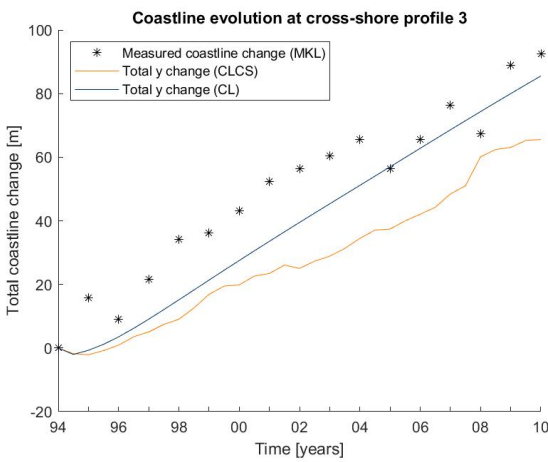
Figure A.62: Simulated and observed coastline evolution at cross-shore profile 3 between 1994-2010
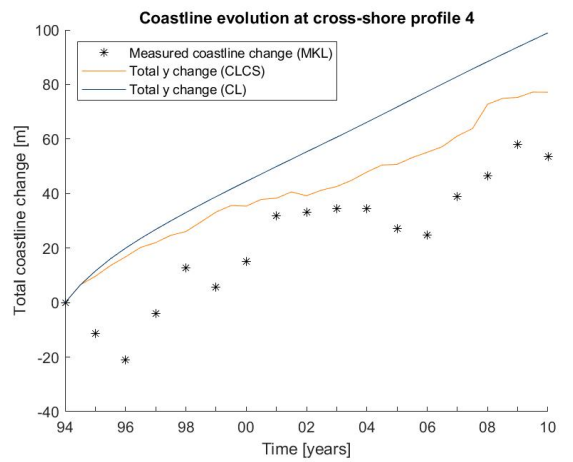
Figure A.63: Simulated and observed coastline evolution at cross-shore profile 4 between 1994-2010
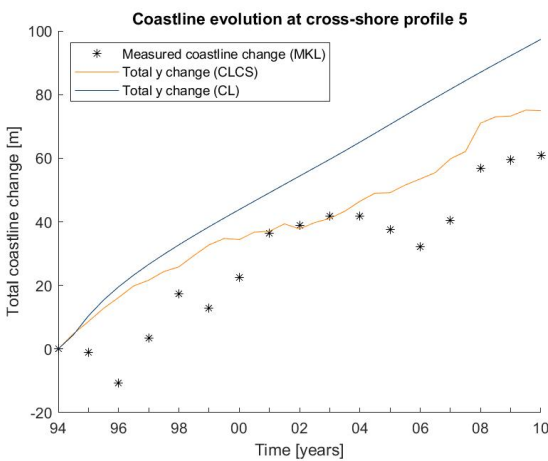
Figure A.64: Simulated and observed coastline evolution at cross-shore profile 5 between 1994-2010
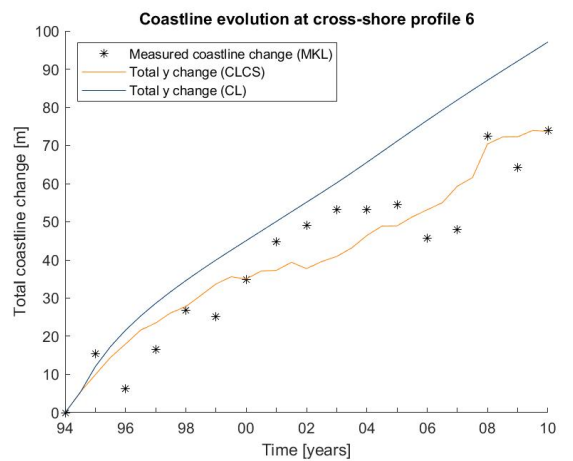
Figure A.65: Simulated and observed coastline evolution at cross-shore profile 6 between 1994-2010
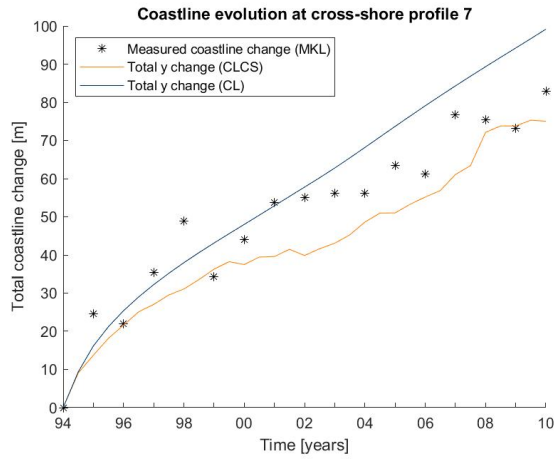
Figure A.66: Simulated and observed coastline evolution at cross-shore profile 7 between 1994-2010
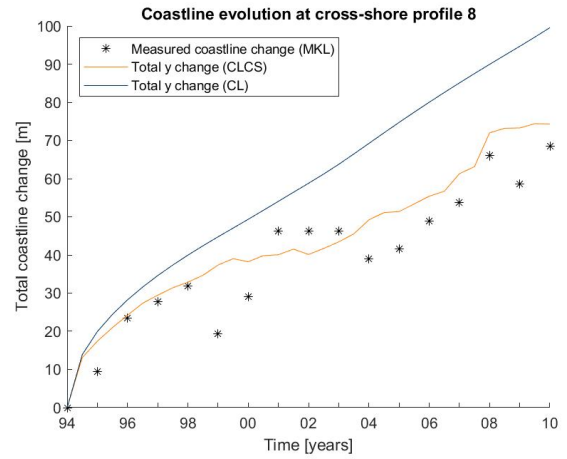
Figure A.67: Simulated and observed coastline evolution at cross-shore profile 8 between 1994-2010
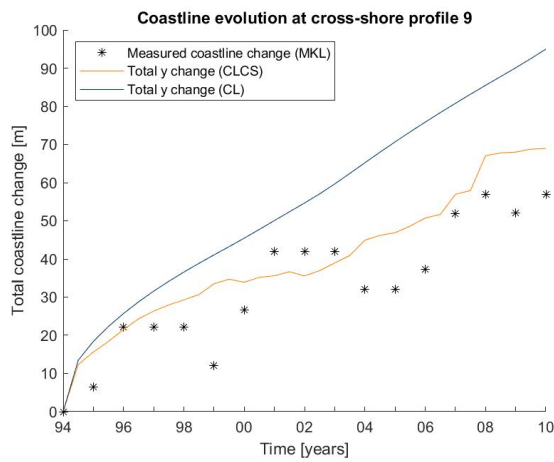
Figure A.68: Simulated and observed coastline evolution at cross-shore profile 9 between 1994-2010
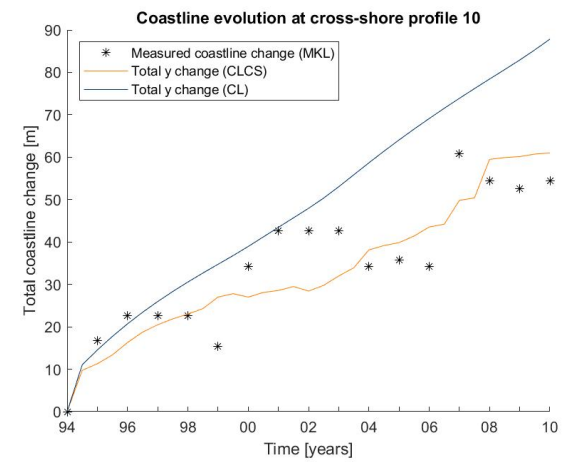
Figure A.69: Simulated and observed coastline evolution at cross-shore profile 10 between 1994-2010
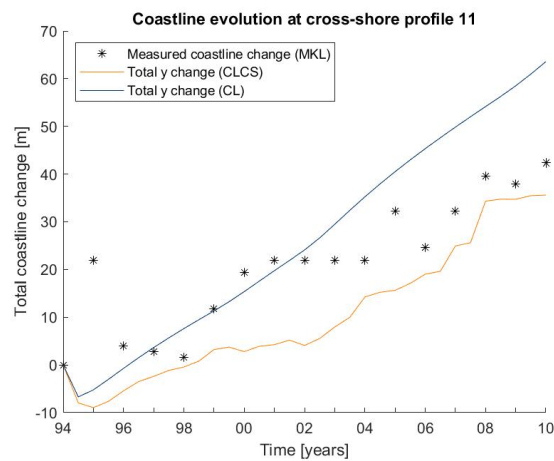
Figure A.70: Simulated and observed coastline evolution at cross-shore profile 11 between 1994-2010
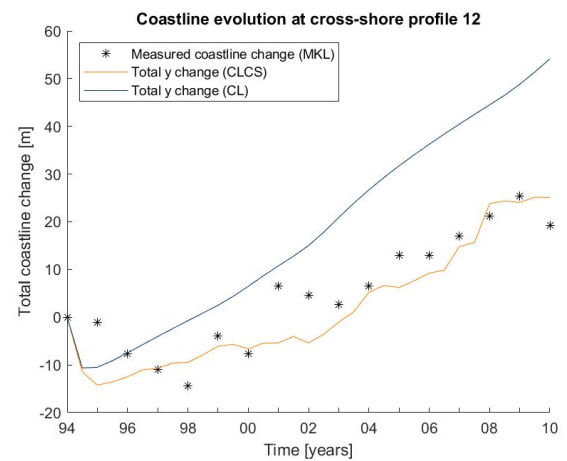
Figure A.71: Simulated and observed coastline evolution at cross-shore profile 12 between 1994-2010
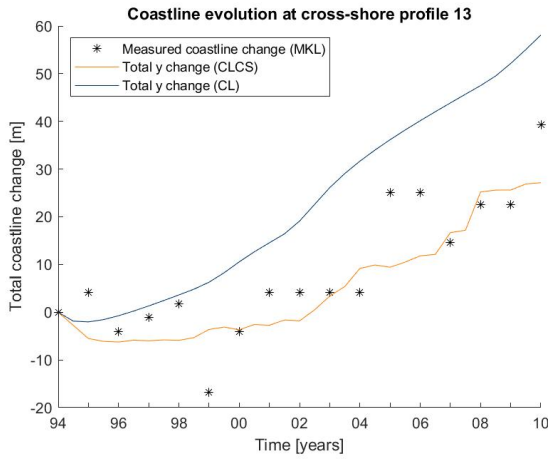
Figure A.72: Simulated and observed coastline evolution at cross-shore profile 13 between 1994-2010
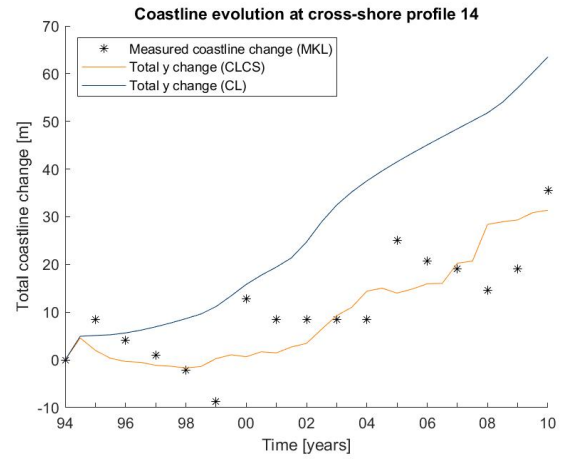
Figure A.73: Simulated and observed coastline evolution at cross-shore profile 14 between 1994-2010
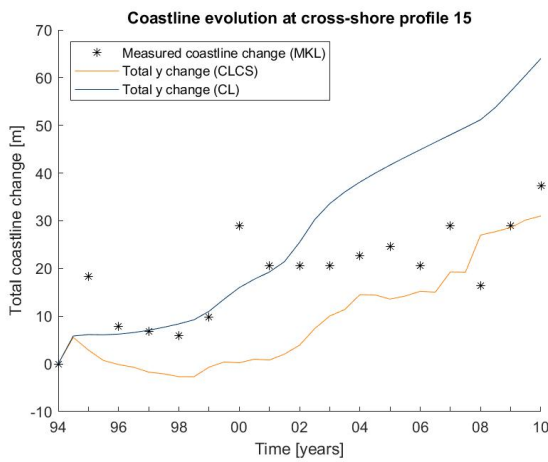
Figure A.74: Simulated and observed coastline evolution at cross-shore profile 15 between 1994-2010
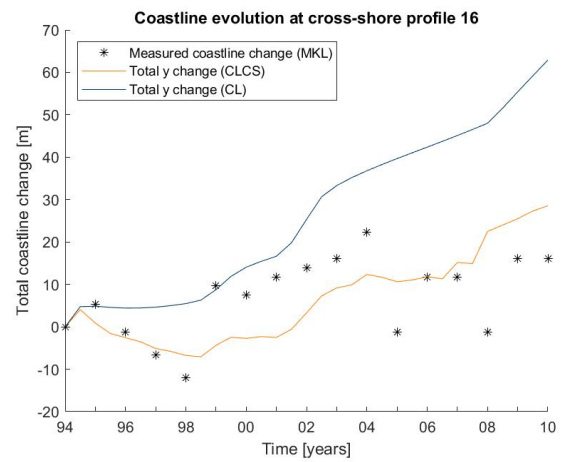
Figure A.75: Simulated and observed coastline evolution at cross-shore profile 16 between 1994-2010
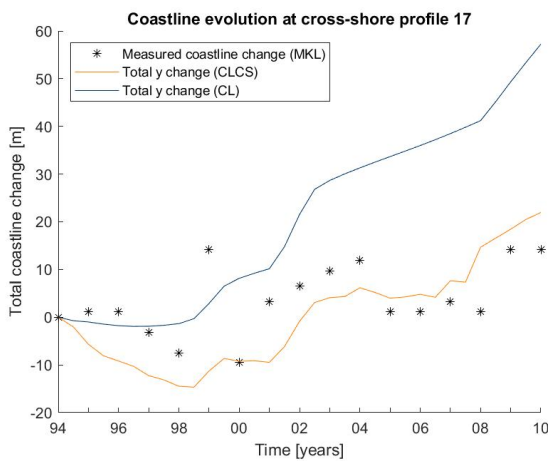
Figure A.76: Simulated and observed coastline evolution at cross-shore profile 17 between 1994-2010
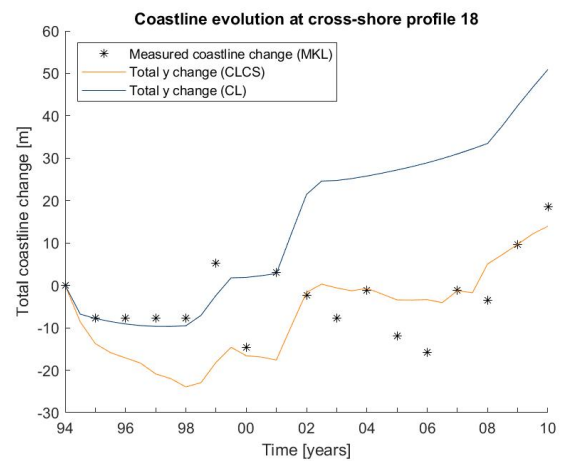
Figure A.77: Simulated and observed coastline evolution at cross-shore profile 18 between 1994-2010
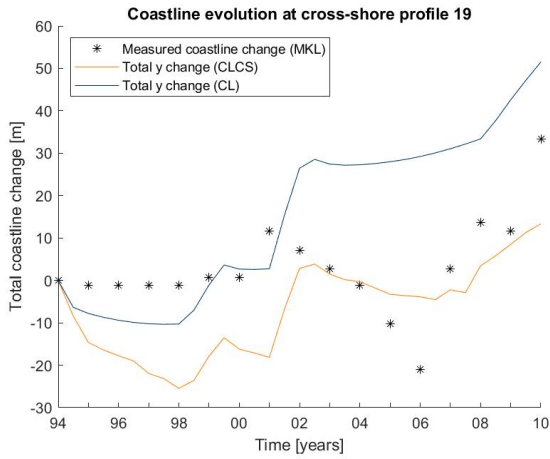
Figure A.78: Simulated and observed coastline evolution at cross-shore profile 19 between 1994-2010
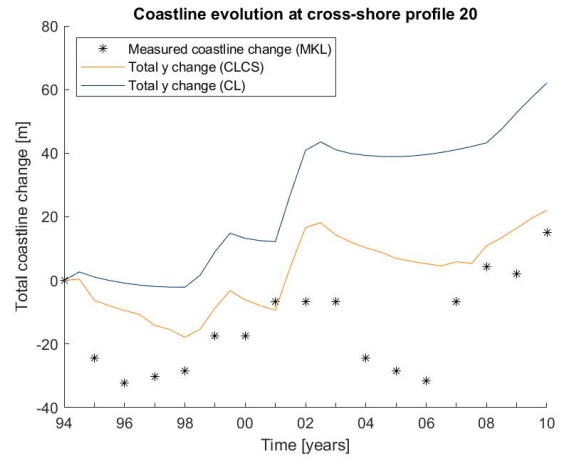
Figure A.79: Simulated and observed coastline evolution at cross-shore profile 20 between 1994-2010
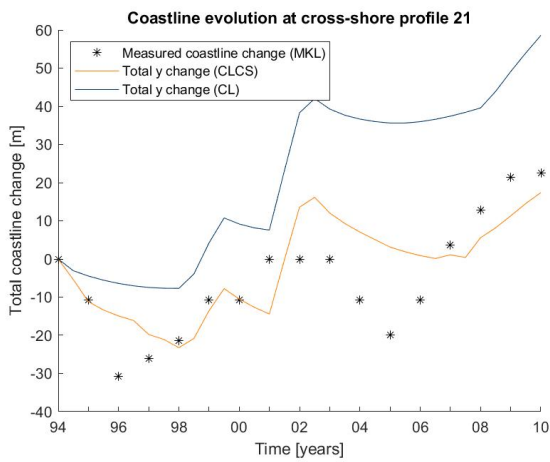
Figure A.80: Simulated and observed coastline evolution at cross-shore profile 21 between 1994-2010
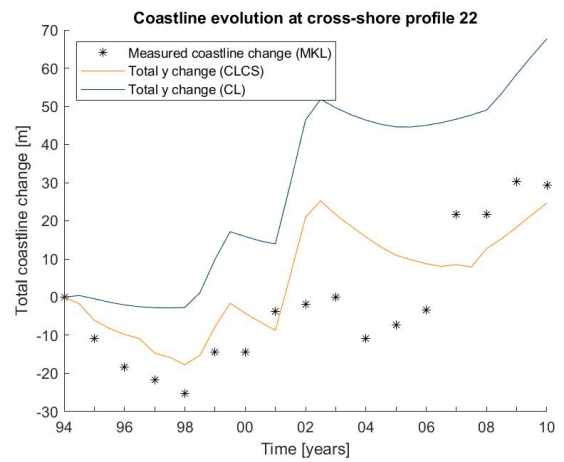
Figure A.81: Simulated and observed coastline evolution at cross-shore profile 22 between 1994-2010
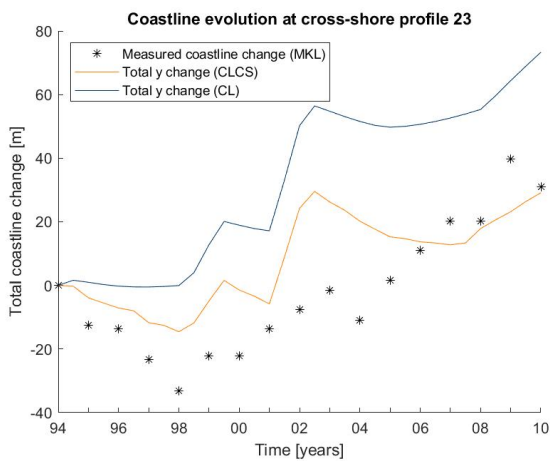
Figure A.82: Simulated and observed coastline evolution at cross-shore profile 23 between 1994-2010
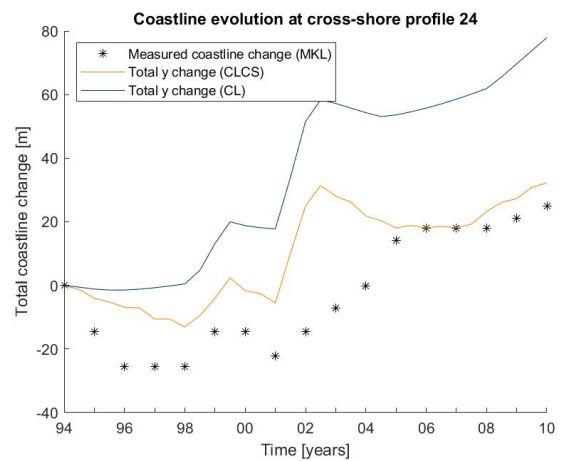
Figure A.83: Simulated and observed coastline evolution at cross-shore profile 24 between 1994-2010
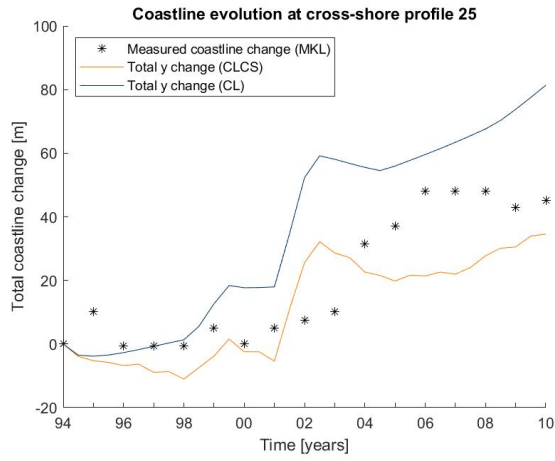
Figure A.84: Simulated and observed coastline evolution at cross-shore profile 25 between 1994-2010
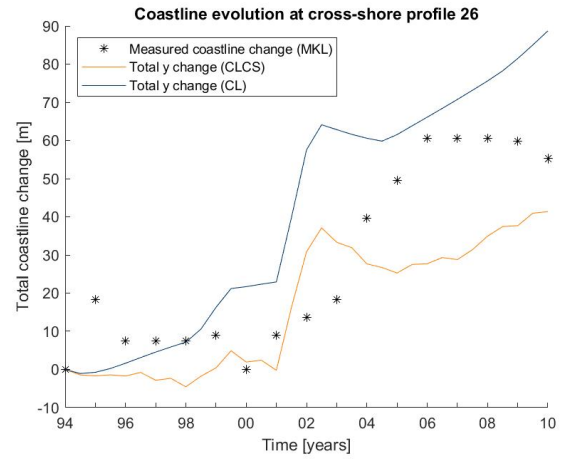
Figure A.85: Simulated and observed coastline evolution at cross-shore profile 26 between 1994-2010

A.8. Coefficient of determination of CS-model reference simulations of calibration period
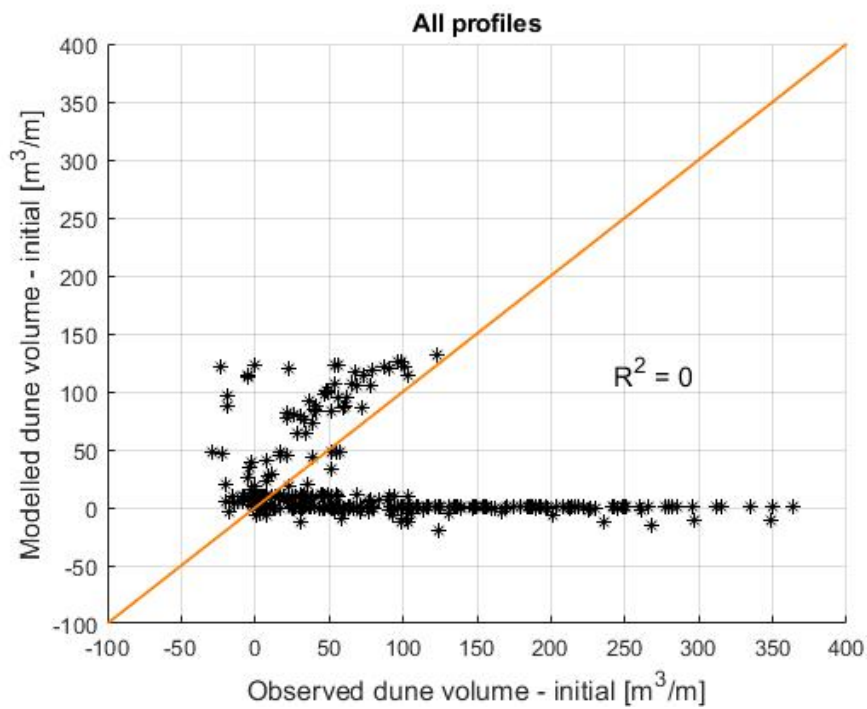
Figure A.86: Coefficient of determination of the dune volume evolution simulated for 1994-2010 with the CS-model, without longshore sediment transport gradients
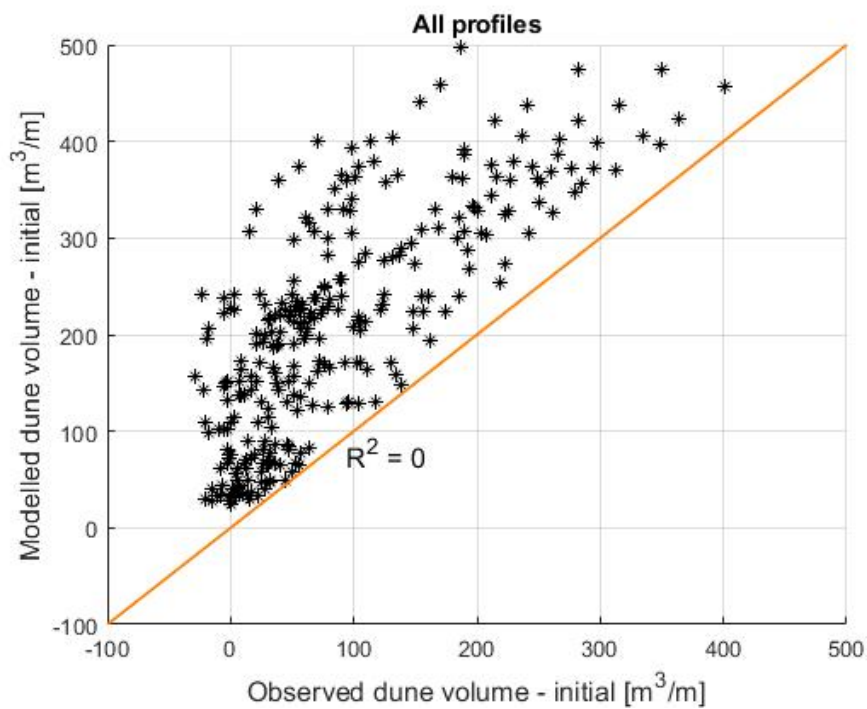
Figure A.87: Coefficient of determination of the dune volume evolution simulated for 1994-2010 with the CS-model, with a constant longshore sediment transport gradient of 1×10^{-5} m^3/s/m in every cross-shore profile
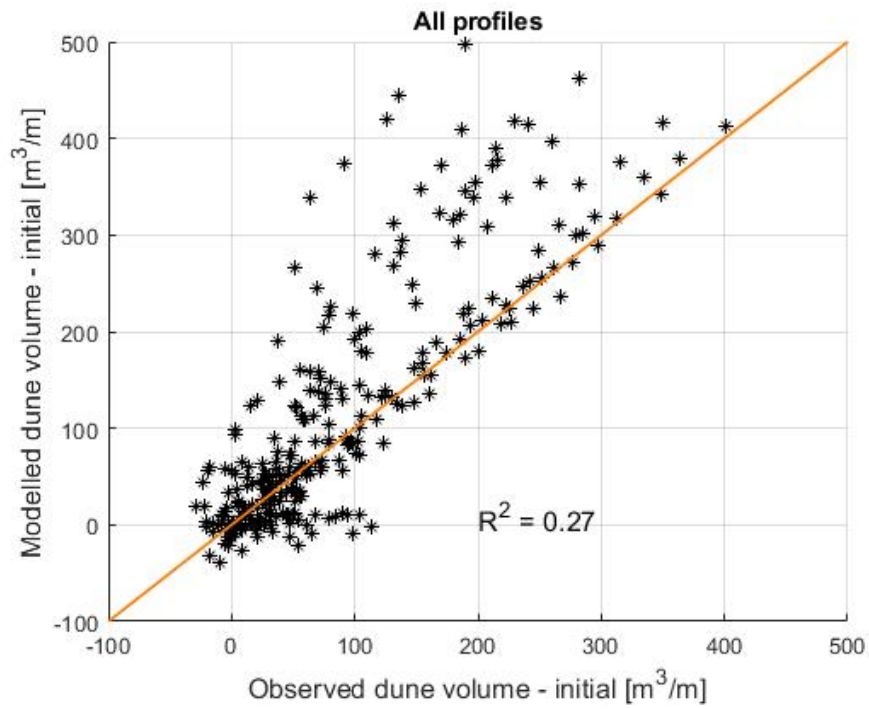
Figure A.88: Coefficient of determination of the dune volume evolution simulated for 1994-2010 with the CS-model, with observed longshore sediment transport gradients

A.9. Coefficient of determination of CS-model reference simulations of validation period
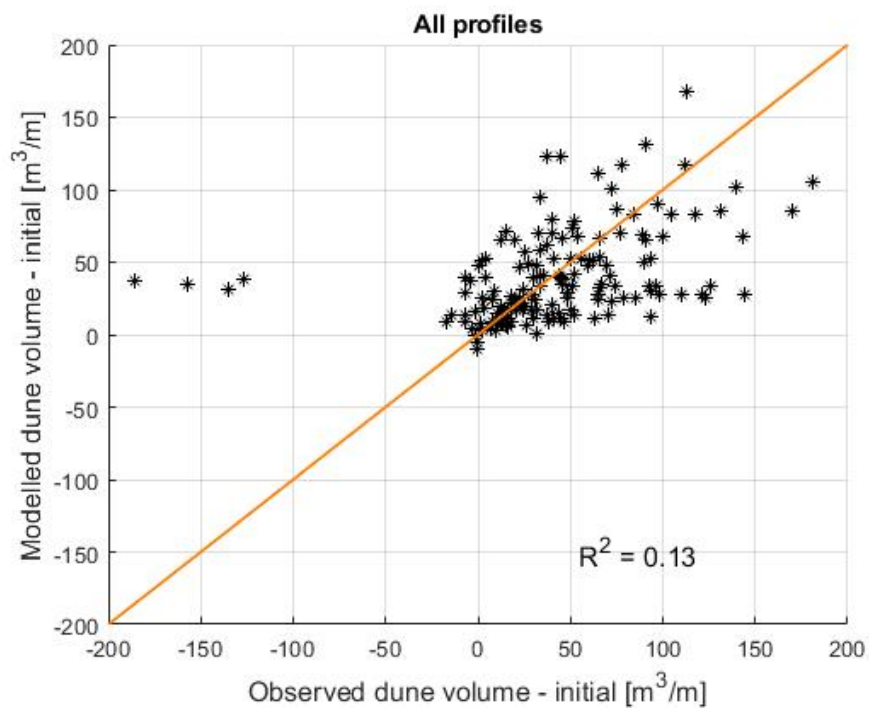
Figure A.89: Coefficient of determination of the dune volume evolution simulated for 2010-2016 with the CS-model, without longshore sediment transport gradients
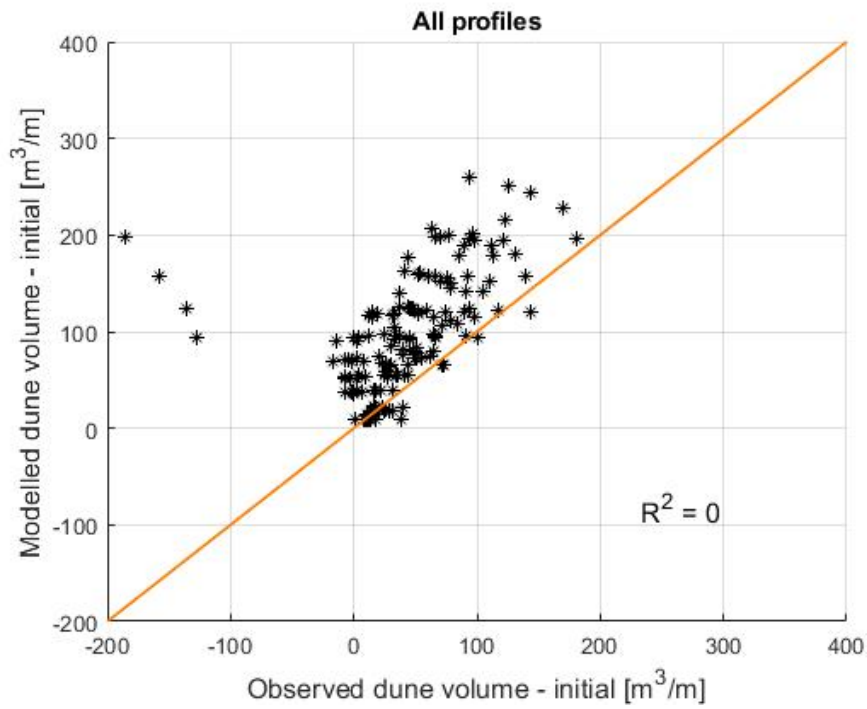
Figure A.90: Coefficient of determination of the dune volume evolution simulated for 2010-2016 with the CS-model, with a constant longshore sediment transport gradient of 1×10^{-5} m^3/s/m in every cross-shore profile
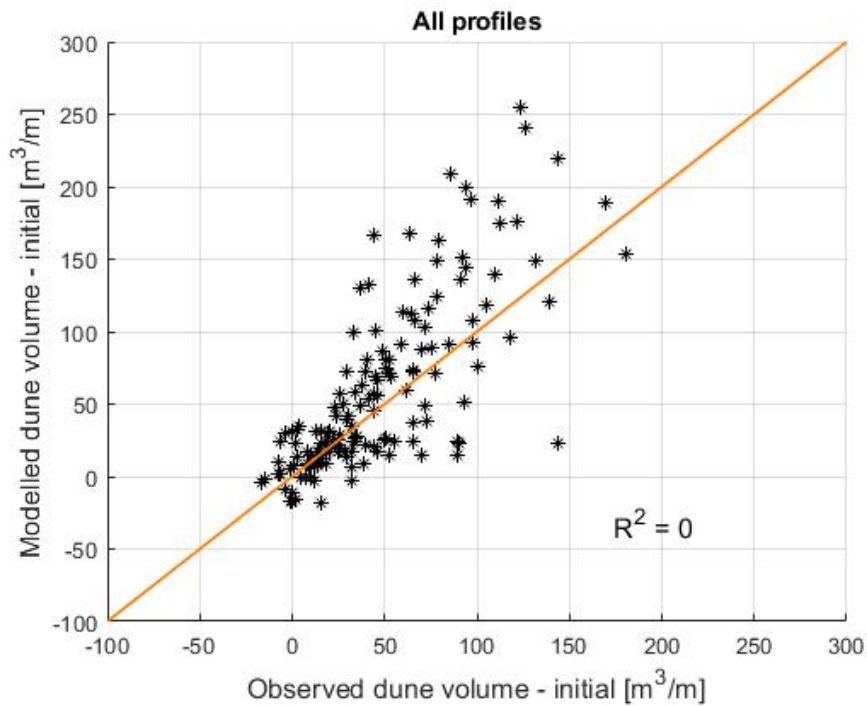
Figure A.91: Coefficient of determination of the dune volume evolution simulated for 2010-2016 with the CS-model, with observed longshore sediment transport gradients

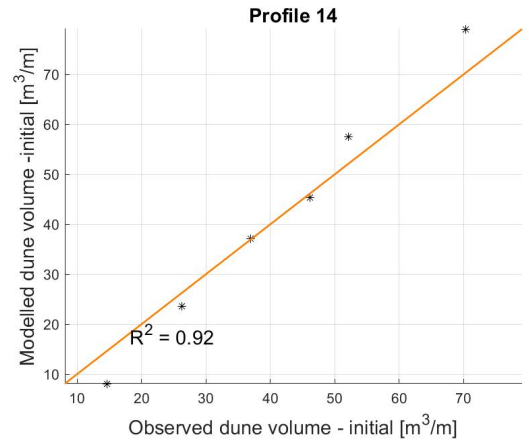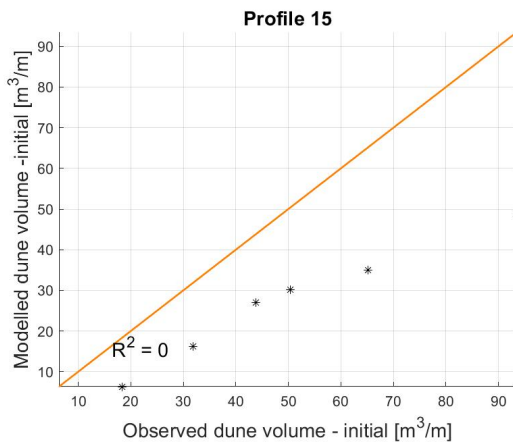# A.10. Coefficient of determination dune volume evolution between 2010 and 2016 in every cross-shore profile
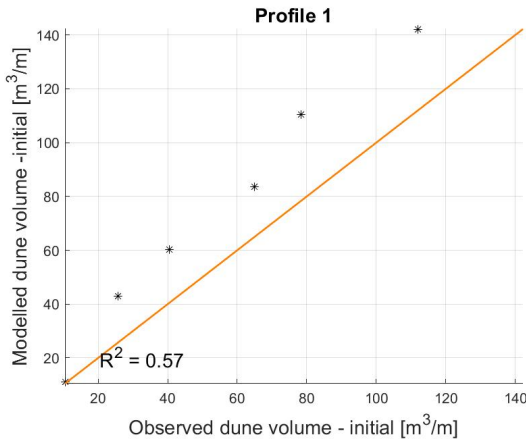
Figure A.92: Coefficient of determination of the dune volume evolution between 2010-2016 in cross-shore profile 1 simulated with the coupled model
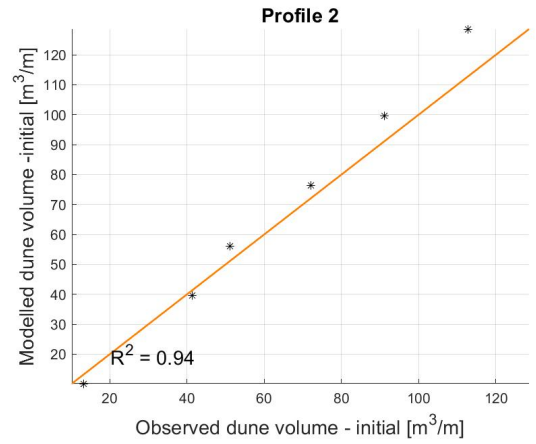
Figure A.93: Coefficient of determination of the dune volume evolution between 2010-2016 in cross-shore profile 2 simulated with the coupled model
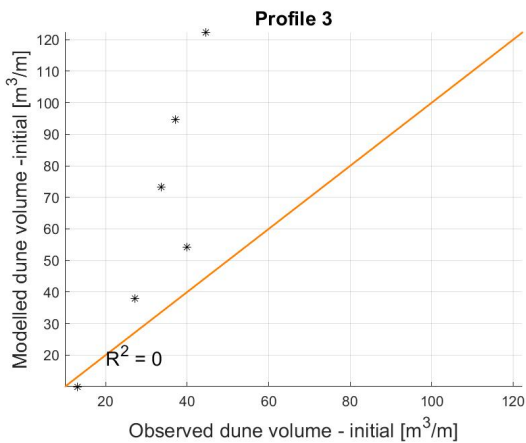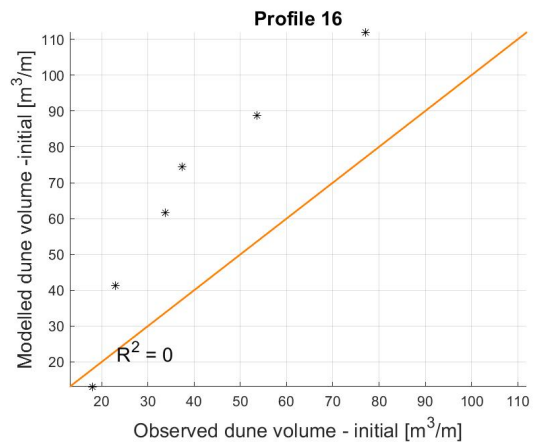

Figure A.94: Coefficient of determination of the dune volume evolution between 2010-2016 in cross-shore profile 3 simulated with the coupled model
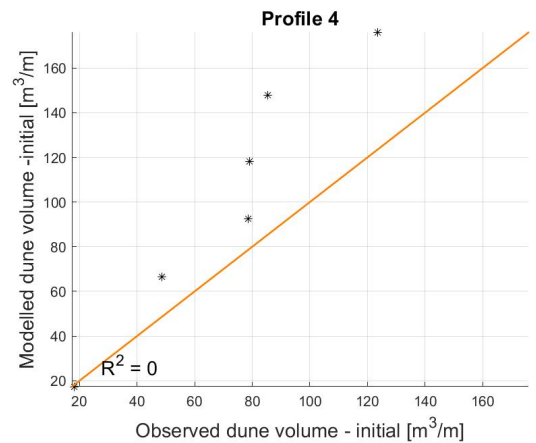
Figure A.95: Coefficient of determination of the dune volume evolution between 2010-2016 in cross-shore profile 4 simulated with the coupled model
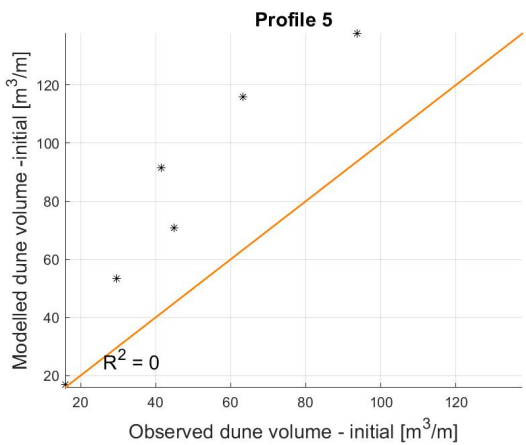
Figure A.96: Coefficient of determination of the dune volume evolution between 2010-2016 in cross-shore profile 5 simulated with the coupled model
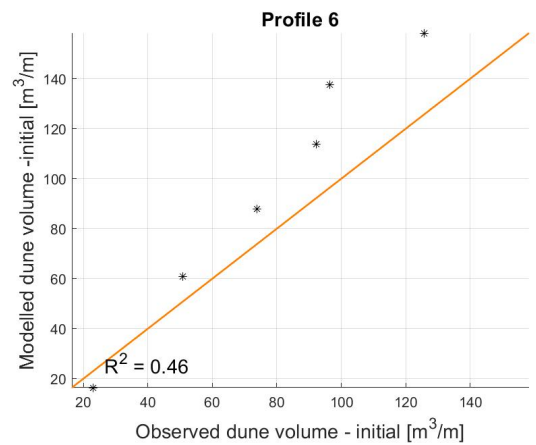
Figure A.97: Coefficient of determination of the dune volume evolution between 2010-2016 in cross-shore profile 6 simulated with the coupled model
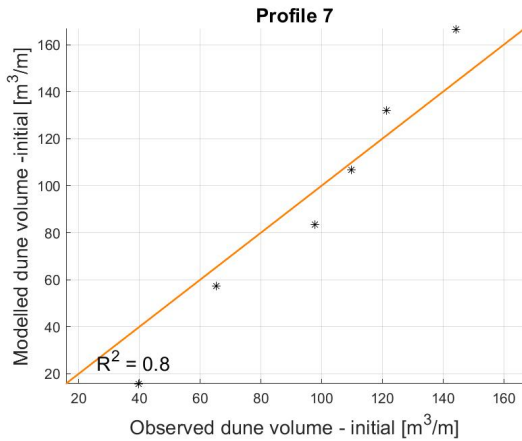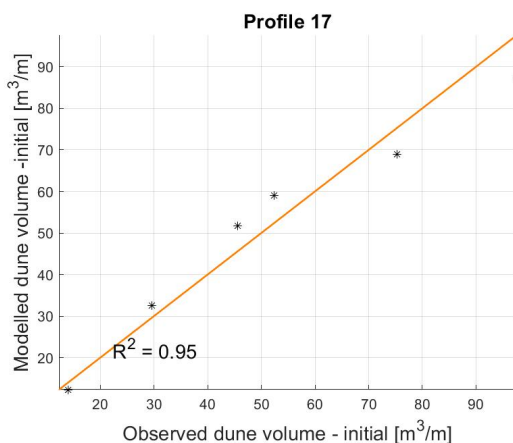
Figure A.98: Coefficient of determination of the dune volume evolution between 2010-2016 in cross-shore profile 7 simulated with the coupled model
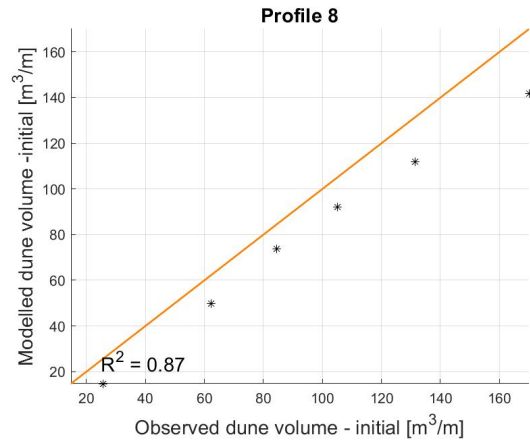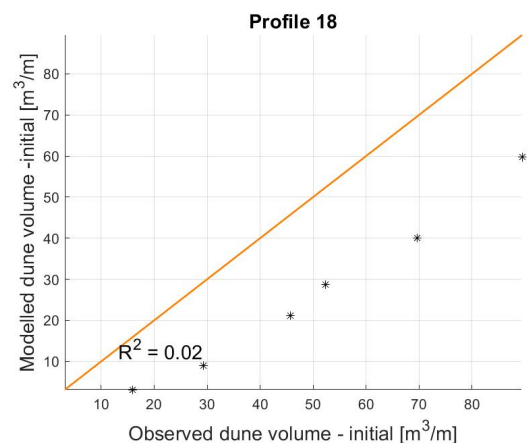
Figure A.99: Coefficient of determination of the dune volume evolution between 2010-2016 in cross-shore profile 8 simulated with the coupled model
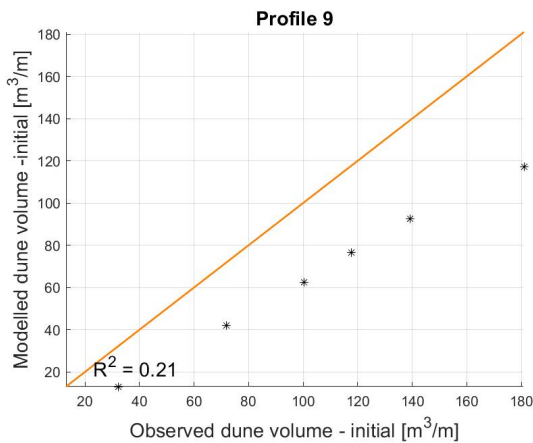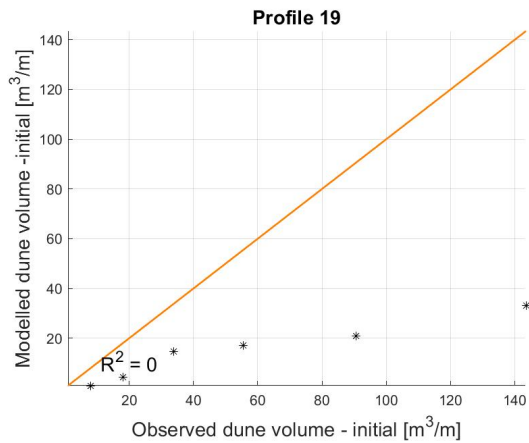
Figure A.100: Coefficient of determination of the dune volume evolution between 2010-2016 in cross-shore profile 9 simulated with the coupled model
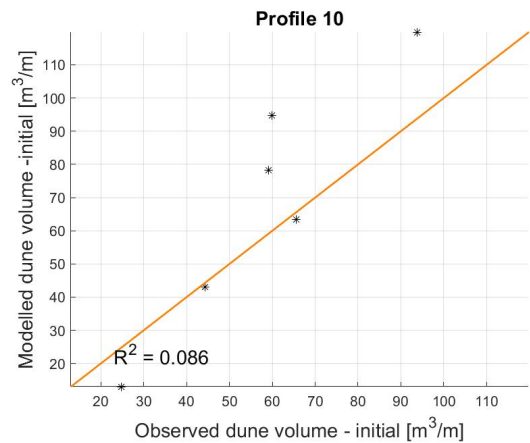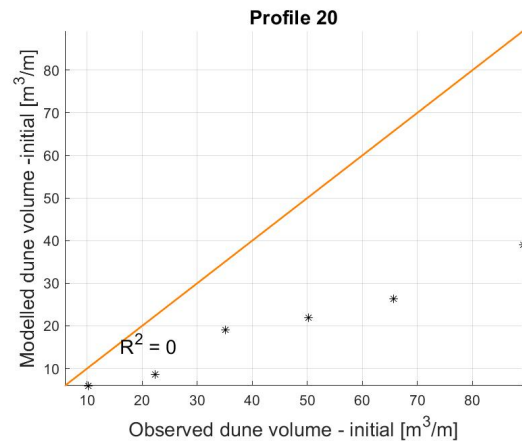
Figure A.101: Coefficient of determination of the dune volume evolution between 2010-2016 in cross-shore profile 10 simulated with the coupled model
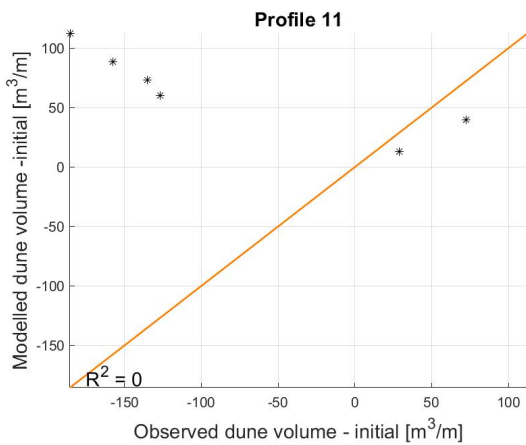
Figure A.102: Coefficient of determination of the dune volume evolution between 2010-2016 in cross-shore profile 11 simulated with the coupled model
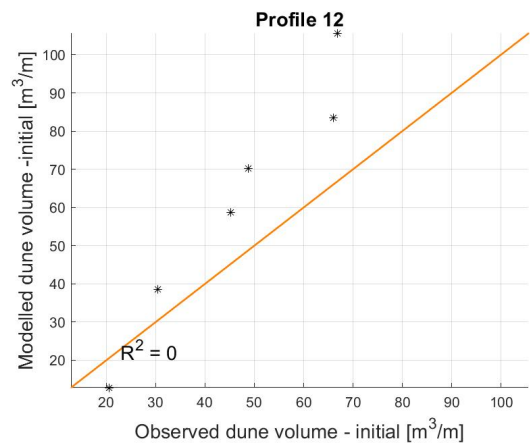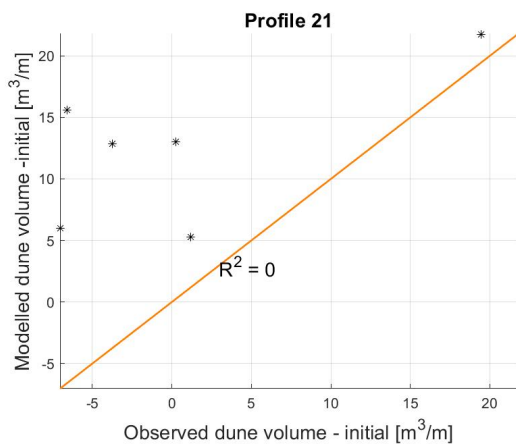
Figure A.103: Coefficient of determination of the dune volume evolution between 2010-2016 in cross-shore profile 12 simulated with the coupled model
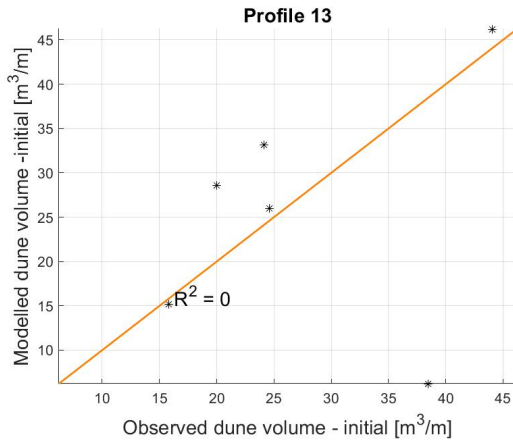
Figure A.104: Coefficient of determination of the dune volume evolution between 2010-2016 in cross-shore profile 13 simulated with the coupled model

Figure A.105: Coefficient of determination of the dune volume evolution between 2010-2016 in cross-shore profile 14 simulated with the coupled model

Figure A.106: Coefficient of determination of the dune volume evolution between 2010-2016 in cross-shore profile 15 simulated with the coupled model
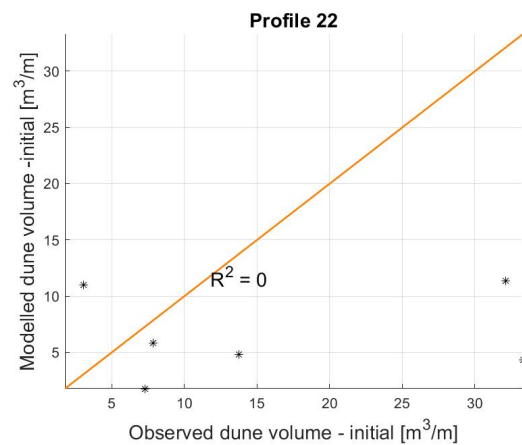
Figure A.107: Coefficient of determination of the dune volume evolution between 2010-2016 in cross-shore profile 16 simulated with the coupled model
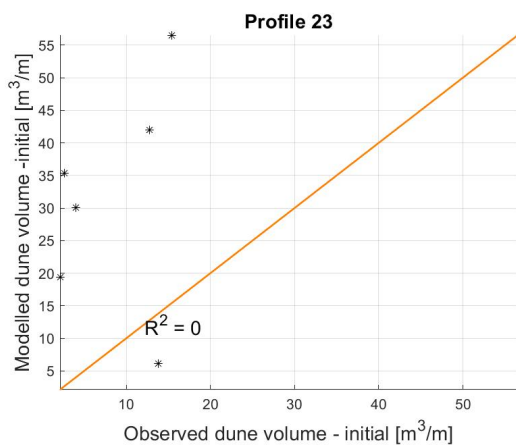
Figure A.108: Coefficient of determination of the dune volume evolution between 2010-2016 in cross-shore profile 17 simulated with the coupled model

Figure A.109: Coefficient of determination of the dune volume evolution between 2010-2016 in cross-shore profile 18 simulated with the coupled model

Figure A.110: Coefficient of determination of the dune volume evolution between 2010-2016 in cross-shore profile 19 simulated with the coupled model
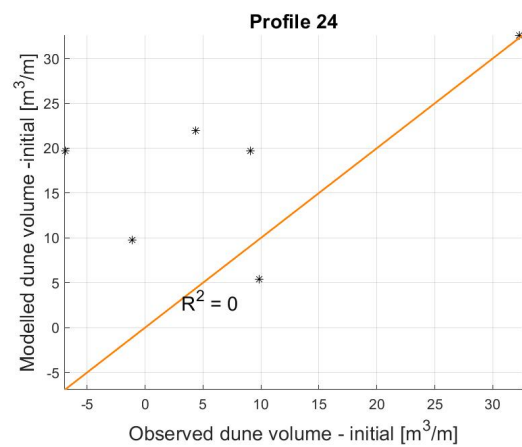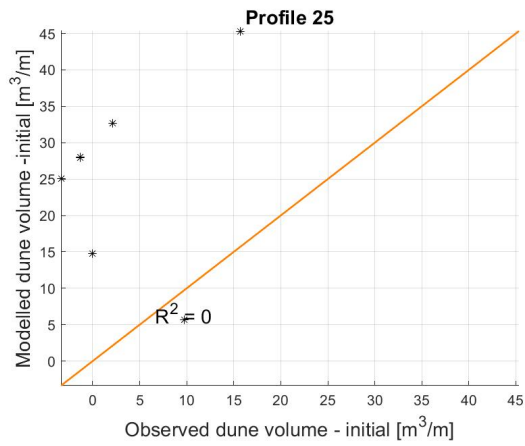
Figure A.111: Coefficient of determination of the dune volume evolution between 2010-2016 in cross-shore profile 20 simulated with the coupled model

Figure A.112: Coefficient of determination of the dune volume evolution between 2010-2016 in cross-shore profile 21 simulated with the coupled model

Figure A.113: Coefficient of determination of the dune volume evolution between 2010-2016 in cross-shore profile 22 simulated with the coupled model
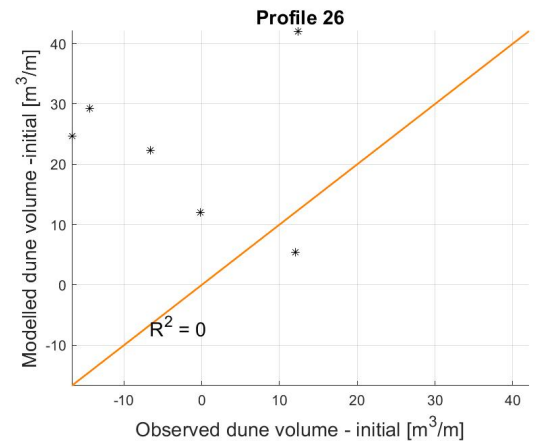
Figure A.114: Coefficient of determination of the dune volume evolution between 2010-2016 in cross-shore profile 23 simulated with the coupled model

Figure A.115: Coefficient of determination of the dune volume evolution between 2010-2016 in cross-shore profile 24 simulated with the coupled model

Figure A.116: Coefficient of determination of the dune volume evolution between 2010-2016 in cross-shore profile 25 simulated with the coupled model

Figure A.117: Coefficient of determination of the dune volume evolution between 2010-2016 in cross-shore profile 26 simulated with the coupled model

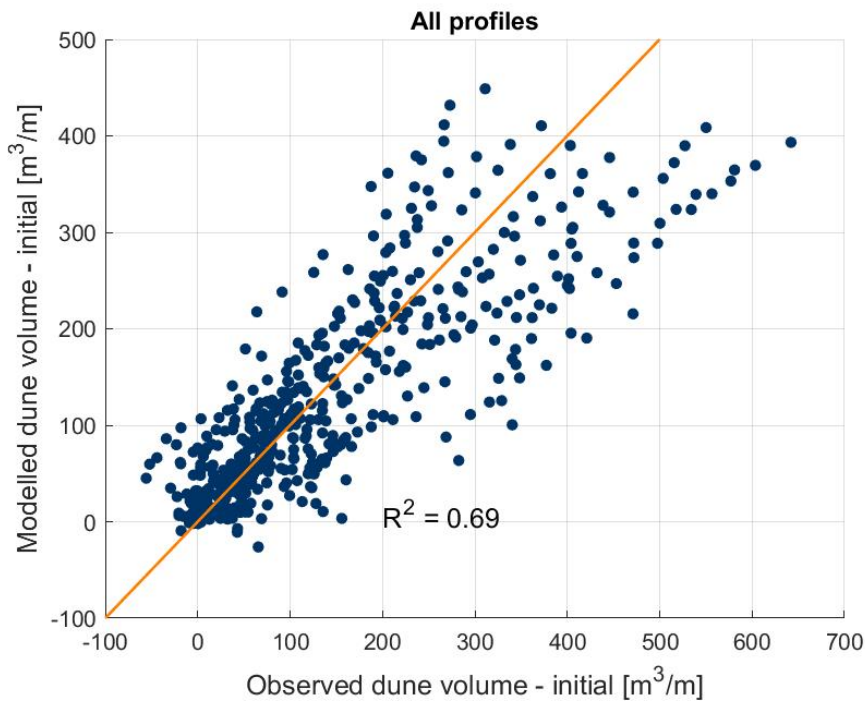## A.11. Coefficient of determination of dune volume evolution and coastline change 1994-2016

Figure A.118: Scatterplot of the simulated and observed dune volume change between 1994-2016 with the coefficient of determination
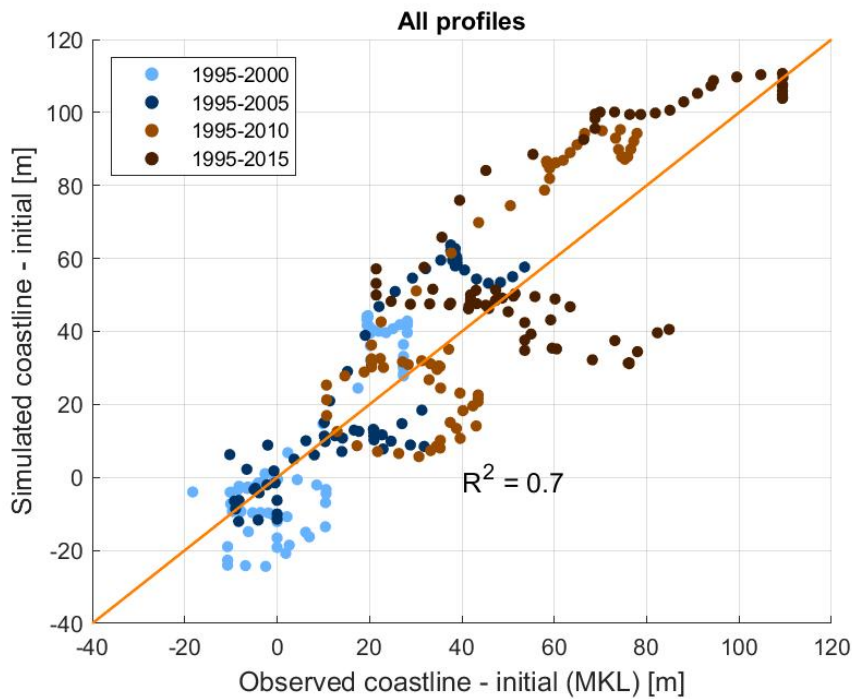

Figure A.119: Scatterplot of the simulated and observed coastline change between 1994-2016 with the coefficient of determination.

A.12. Coefficient of determination of dune volume evolution and coastline change 1994-2000
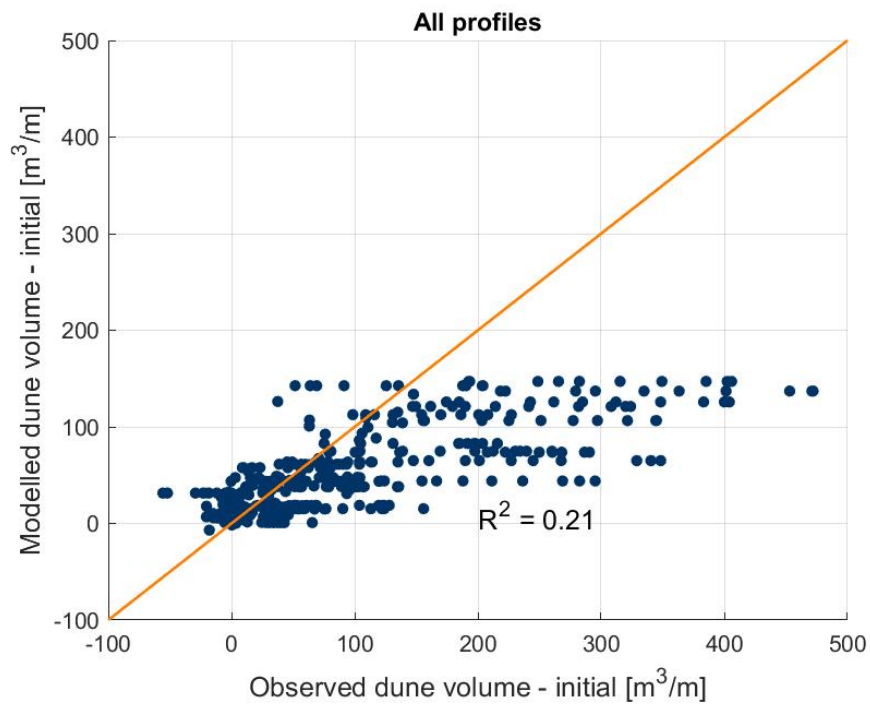

Figure A.120: Coefficient of determination of the dune volume evolution simulated for 1994-2000 with the coupled model
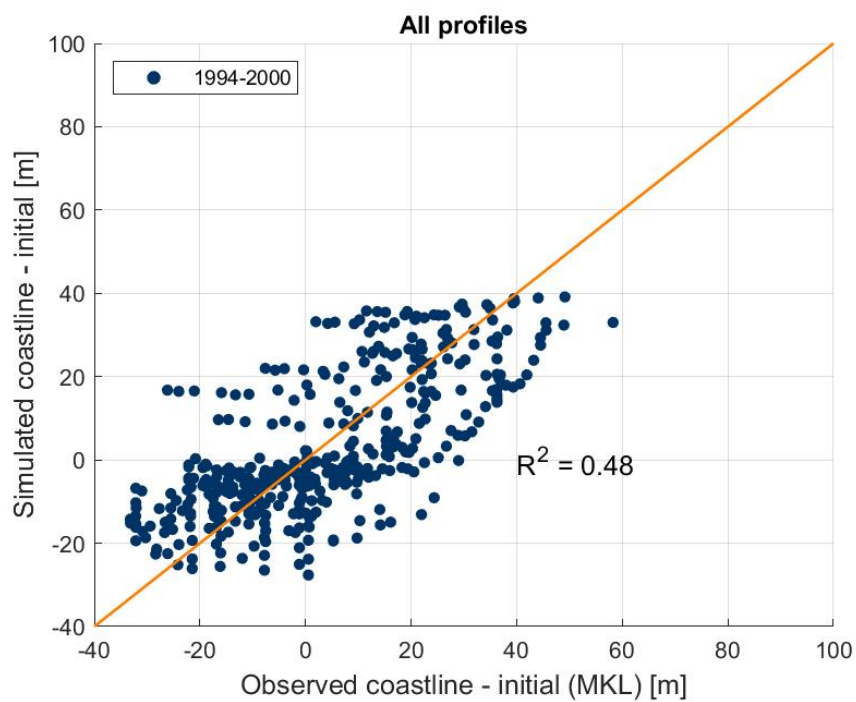

Figure A.121: Coefficient of determination of the coastline change simulated for 1994-2000 with the coupled model